

# **PREDICTING FUTURE LANDSLIDE SUSCEPTIBILITY USING ESTIMATED FUTURE LAND COVER SCENARIO IN IDUKKI, KERALA**

MD. SUDMAN KABIR ISHMAM

June, 2021

SUPERVISORS:

Dr. Luigi Lombardo  
Ir. Bart Krol

Advisor:

Prof. Dr. Cees Van Westen



# **PREDICTING FUTURE LANDSLIDE SUSCEPTIBILITY USING ESTIMATED FUTURE LAND COVER SCENARIO IN IDUKKI, KERALA**

MD. SUDMAN KABIR ISHMAM

Enschede, The Netherlands, [June, 2021]

Thesis submitted to the Faculty of Geo-Information Science and Earth Observation of the University of Twente in partial fulfilment of the requirements for the degree of Master of Science in Geo-information Science and Earth Observation.

Specialization: Natural Hazards and Disaster Risk Reduction (NHR)

SUPERVISORS:

Dr. Luigi Lombardo  
Ir. Bart Krol

Advisor:

Prof. Dr. Cees Van Westen

THESIS ASSESSMENT BOARD:

Prof. Dr. Victor Jetten (Chair)

Dr. A.C. (Harry) Seijmonsbergen (External Examiner, University of Amsterdam)

#### DISCLAIMER

This document describes work undertaken as part of a programme of study at the Faculty of Geo-Information Science and Earth Observation of the University of Twente. All views and opinions expressed therein remain the sole responsibility of the author, and do not necessarily represent those of the Faculty.

## ABSTRACT

---

The interrelationship between landslide susceptibility and land cover is not a very well explored area of science. This study thrives to investigate the way future land cover scenarios characterize future landslide susceptibility and vice versa. The modelling approach involves two different scenarios, one where land cover can change without any consideration to landslide susceptibility and the other where land cover changes in a manner that the landslide susceptibility is well-accounted for a duration of forty years (2010-2050). For an inventory of 2018, landslide susceptibility modelling was conducted through a Bayesian version of GAMM (Generalized Additive Mixed Model) built in R-INLA, whereas land cover prediction was conducted using the DynaCLUE model for 2010's land cover data. In the scenario where landslide susceptibility is accounted for, the outputs of both the models were considered as inputs in each other.

Results show interesting differences in land cover and landslide dynamics. Changes in land cover with landslide susceptibility mitigation measures resulted in low landslide susceptibility as opposed to the one where no mitigation measures were in place. Landslide susceptibility dynamics also characterized the propagation of different land cover classes over space as directed by the scenario rulesets.

This modelling approach can set the basis of a further research as well as help policy makers and legislators for pre-informed decision making. High resolution and recent datasets can significantly improve the model performances while iteration of different scenarios may provide vital insights.

## ACKNOWLEDGEMENTS

---

I would like to express my deepest gratitude to the Faculty of Geo-information Science and Earth Observation (ITC) for the ITC Excellence Scholarship that provided financial support during my MSc tenure.

I extend my earnest gratitude to my supervisors, Dr. Luigi Lombardo and Ir. Bart Krol for their relentless support and sheer patience. Their amicable yet critical approach helped me grow as a researcher as well as individual. It has been a privilege to be able to work under their supervision.

I am highly indebted to my advisor Prof. Dr. Cees Van Westen, for his immense support and sharing his wisdom. The study would have been impossible without his support in all phases of the study.

I am also indebted to Dr. Ziga Malek (IVM, Vrije Universiteit Amsterdam) for supervising me as an intern and also for his extended guidance during different aspects of this thesis.

Finally, I want to thank my beautiful family – my loving parents, ‘apun’ (sister), brother-in-law and my darling niece ‘Tahia’, for believing in me and providing unconditional support throughout my life.

I express my gratitude to my Creator Almighty, who gave me a second chance to live, love and make things happen.

Ishmam Kabir

June, 2021

Enschede

# TABLE OF CONTENTS

---

List Of Figures .....	iii
List Of Tables .....	iv
List Of Equations .....	iv
1. Introduction And Research Problem .....	1
1.1 General Introduction.....	1
1.2 Land Cover Prediction.....	1
1.3 Landslide Susceptibility.....	2
1.4 Link Between Landslides And Land Cover.....	2
1.5 Research Problem .....	3
1.6 Study Area .....	3
1.7 Background And State-Of-Art .....	4
2. Research Objectives And Research Questions .....	4
2.1 Overall Objective .....	5
2.2 Sub-Objectives.....	5
2.3 Research Questions .....	5
3. Research Design And Methods .....	5
3.1 Beginning Phase .....	5
3.1.1 Scenario Development And Setting Boundary Conditions.....	5
3.2 Input Data .....	8
3.2.1 DEM (Digital Elevation Model) .....	8
3.2.2 Landslide Point Data.....	9
3.2.3 Soil Data .....	9
3.2.4 Land Cover Data.....	9
3.2.5 Rainfall Data .....	9
3.2.6 Road Network Data .....	9
3.2.7 Protected Area Data.....	9
3.3 Preparation Phase .....	9
3.3.1 Masking Out Landslides .....	9
3.3.2 Correction Of Resolution And Clipping .....	9
3.3.3 Computing Location Factors / Covariates .....	10
3.4 Mapping Unit Definition.....	10
3.5 Susceptibility Modelling Phase .....	11
3.6 Land Cover Prediction Phase .....	12
3.6.1 Dynaclue Modelling.....	12
3.6.2 Analyzing Historical Data.....	13
3.6.3 Extracting Regression Coefficients And Calibrating The Model.....	13
3.6.4 Aggregating To Mapping Unit Level.....	15

3.7	Validation And Simulation Phase.....	15
3.7.1	Multi-Fold Cross Validation .....	15
3.7.2	Statistical Simulation.....	15
4.	Results And Discussions.....	17
4.1	Land Cover Modelling .....	17
4.1.1	Regression Outputs .....	17
4.1.2	Predictive Performance.....	18
4.1.3	Land Cover Model Outputs .....	19
4.2	Landslide Susceptibility.....	24
4.2.1	Covariates' Effects.....	24
4.2.2	Predictive Performance.....	25
4.2.3	Susceptibility Model Outputs .....	26
4.3	Overall Discussion.....	28
4.4	Novelty In Modelling Approach .....	29
4.5	Uncertainties And Limitations Of The Study.....	29
4.6	Implications Of The Study.....	30
5.	Concluding Remarks.....	30
	List Of References.....	33
	Appendices .....	42

# LIST OF FIGURES

---

Figure 1: Study area extent.....	4
Figure 2: Methodology process flow.....	7
Figure 3: Process flow of statistical simulation (modified from Luo et al., 2020) .....	16
Figure 4: ROC curves of cropland (left panel) and agricultural plantation (right panel).....	18
Figure 5: Probability maps of cropland (left panel) and agricultural plantation (right panel).....	19
Figure 6: Land cover of year 2010 (Starting year).....	20
Figure 7: Estimated future land cover of 2050 (Left panel: 'No landslide mitigation' scenario, Right panel: 'With landslide mitigation' scenario) .....	21
Figure 8: Difference between scenarios in 2050 .....	22
Figure 9: Land cover difference between the first (2010) and final (2050) year; TL : NL scenario, TR: WL scenario, Bottom: Difference between scenarios (TL vs. TR) .....	23
Figure 10: Top: Significant fixed effects (blue dots depict the posterior mean and black dots depict 95% CI); Bottom: Random ordinal effect of slope steepness (blue line highlights the mean and black lines highlight 95% CI) .....	24
Figure 11: Left: Ten cross validated ROC curves of the reference landslide susceptibility model; Right: Associated AUC distribution.....	25
Figure 12: Calculated landslide susceptibility (left panel) and uncertainty (right panel) of year 2010 .....	26
Figure 13: Simulated landslide susceptibility (top and bottom left) and uncertainty (top and bottom right) of 2050; Top panels: NL scenario, Bottom panels: WL scenario .....	27
Figure 14: Difference of landslide susceptibility in 2050 .....	28
Figure 15: Protected Areas of Idukki.....	42
Figure 16: DynaCLUE system files (TL: Alloc1 file, TR: Main file, Middle: Demand file, Bottom: Allow file) .....	43
Figure 17: ROC curves of villages (top left), grassland (top right), forests (bottom left) and forest plantation (bottom right).....	44
Figure 18: Probability maps of villages (TL), grassland (TR), forest (BL) and forest plantation (BR) .....	45
Figure 19: Probability maps of waterbodies (L) and Rocks & others (R) .....	46
Figure 20: Estimated future land cover (NL scenario) (2025, 2030, 2035, 2040) .....	47
Figure 21: Estimated future land cover (NL scenario) of 2045 .....	48
Figure 22: Estimated future land cover (WL scenario) (2015 & 2020).....	48
Figure 23: Estimated future land cover (WL scenario) (2025, 2030, 2035, 2040).....	49
Figure 24: Estimated future land cover (WL scenario) of 2045.....	50
Figure 25: Estimated future land cover (WL scenario) (2015 and 2020).....	50
Figure 26: Difference between land cover scenarios (2015, 2020, 2025 and 2030).....	51
Figure 27: Difference between land cover scenarios (2035, 2040 and 2045) .....	52
Figure 28: Simulated landslide susceptibility (2015, 2020, 2025 & 2030) – Scenario NL.....	53
Figure 29: Simulated landslide susceptibility (2035, 2040 and 2045) - Scenario NL.....	54
Figure 30: Simulated landslide susceptibility (2015, 2020, 2025, 2030) - Scenario WL .....	55
Figure 31: Simulated landslide susceptibility (2035, 2040 and 2045) - Scenario WL.....	56
Figure 32: Simulated uncertainty (2015, 2020, 2025, 2030) - NL scenario .....	57
Figure 33: Simulated uncertainty (2035, 2040 and 2045) - NL scenario.....	58
Figure 34: Simulated uncertainty (2015, 2020, 2025 and 2030) - WL scenario .....	59
Figure 35: Simulated uncertainty (2035, 2040 and 2045) - WL scenario .....	60
Figure 36: Landslide susceptibility differences (2015, 2020, 2025 and 2030).....	61
Figure 37: Landslide susceptibility differences (2035, 2040 and 2045).....	62

## LIST OF TABLES

---

Table 1: Source and details of input datasets.....	8
Table 2: List of location factors / covariates.....	11
Table 3: List of land cover classes .....	13
Table 4: Location factors and their significance as per regression .....	17
Table 5: AUCs (Area under the curves) of land cover prediction model.....	18
Table 6: Pixel differences of land cover scenario difference maps.....	20
Table 7: Difference between 2010 & 2050 (Scenario NL, WL and scenario difference).....	21

## LIST OF EQUATIONS

---

3.1.....	12
3.2.....	13
3.3.....	13
3.4.....	15

# 1. INTRODUCTION AND RESEARCH PROBLEM

## 1.1 General introduction

The landscape of the earth's surface is characterized by natural and anthropogenic processes. Changes in land use can have direct or indirect causes possibly consisting of human actions or a complex human-environment relationship (Contreras-Hermosilla, 2000; Geist & Lambin, 2002; Ojima et al., 1994). These changes in land use can eventually lead to changes in land cover (Lambin et al., 2003). Changes in land use and land cover is a rapid driver of global change and might emerge from natural or anthropogenic causes as well as from the interaction of both (Promper et al., 2014; P. Reichenbach et al., 2014; Rindfuss et al., 2004; Slaymaker et al., 2009). Landslides are rapid natural processes involving complex mass movements of rock, debris or soil from upslope to deposition areas (Cruden, 1991; Cruden & Varnes, 1996; Restrepo & Alvarez, 2006). They can be triggered by rainfall and/or earthquake, loss of vegetation, etc. (Cendrero & Dramis, 1996; Sidle et al., 1985; Solonenko, 1977; Thomas, 1994). The way in which landslides are distributed spatially is characterized by the climatic and environmental conditions, of which land use/cover is an important aspect (P. Reichenbach et al., 2014).

## 1.2 Land cover prediction

Many researchers across the world have used several techniques to predict land use and land cover changes in the future. The models commonly used for such purposes can be classified into four broad categories, namely:

- Empirical and statistical models e.g. Markov Chain (MC), regression models, etc. (Bell, 1974; Clark, 1965).
- Dynamic models e.g. cellular automata (CA) (Mohmand et al., 2011), agent-based models (ABM) (R. B. Matthews et al., 2007), artificial neural network (ANN) (Dai et al., 2005), system dynamic (SD) models (Shen et al., 2007), etc.
- Integrated models e.g. CLUE (Conversion of Land Use and its Effects) (P. H. Verburg et al., 2002), DynaCLUE model (P. H. Verburg & Overmars, 2009), etc.
- Hybrid models e.g. MC, CA and regression (Arsanjani et al., 2012), CLUE and SD (G. Luo et al., 2010) etc.

CLUE model (Veldkamp & Fresco, 1996) is a popular modelling approach for predicting land use and/or land cover changes and different versions (some modified) of the model e.g. Dyna-CLUE (P. H. Verburg & Overmars, 2009), CLUE-S (P. H. Verburg et al., 2002), have been applied in different parts of the world. For instance, Kucsicsa et al., (2019) predicted the future land use/cover changes in Romania using a CLUE-S model, Oh, Choi, Bae, Yoo and Lee, predicted land cover change in Korea using the CLUE model (Oh et al., 2010), studies focused on the impact of land-use change on groundwater system using different versions of the CLUE model, i.e. Dyna-CLUE (Lima et al., 2015) and CLUE-S (Dams et al., 2008), Cai et al., used the CLUE-S model to simulate land use change in Shenzhen, China (Cai et al., 2004), Oh et al. predicted the land cover change based on climate change in Korea using Dyna-CLUE model (Oh et al., 2011) etc.

Among other models used to predict land use and/or land cover, LSTM (Long Short Term Memory) model (Jia et al., 2017) and the Hopfield Neural Network model (Tatem et al., 2002) can be mentioned.

Because of the limitations of solo modelling approaches, some researchers find integrated modelling approaches more appropriate for modelling such processes (Guan et al., 2011). Some also opt for hybrid modelling approaches; for instance, Markov-CA (Cellular Automata) model is a popular integrated approach adopted by many researchers across the world to predict land use and land cover (Corner et al., 2014; P. Ghosh et al., 2017; Guan et al., 2011; Halmy et al., 2015; Hyandye & Martz, 2017; Karimi et al., 2018); the

combined approach of Markov and CLUE-S model has also been tested (Han et al., 2015); CA-ANN model is another example of such integrated approach (Rahman et al., 2017), etc.

### **1.3 Landslide susceptibility**

Landslide susceptibility is the probability of landslide occurrence triggered by some influencing factors over the space (Brabb, 1984). Efforts have been made to evaluate the landslide susceptibility throughout the world; many researchers have adopted probabilistic methods (Jibson et al., 2000; S. Lee & Talib, 2005; Luzi et al., 2000; Ohlmacher & Davis, 2003; Parise & Jibson, 2000). Some researchers followed the combined approach of GIS and data mining techniques e.g. artificial neural network, fuzzy logic, etc. to evaluate landslides (Ercanoglu & Gokceoglu, 2002; S. Lee et al., 2003, 2004; Pistocchi et al., 2002); whereas some others used the geotechnical and safety factor method (Carro et al., 2003; Gokceoglu et al., 2000; Refice & Capolongo, 2002; Romeo, 2000; Shou & Wang, 2003; Zhou et al., 2003).

Using predictive models to assess landslide susceptibility has been in practice since the early 1990s (Carrara et al., 1991). Specifically, landslide predictive models are used to discriminate between locations where landslides occurred with respect to the locations where landslides are absent (Atkinson & Massari, 1998; Erener & Düzgün, 2012; Luigi Lombardo, Opitz, et al., 2018; Pourghasemi & Rossi, 2017). More recently this binary susceptibility paradigm has been extended to the landslide intensity (Luigi Lombardo et al., 2019; Luigi Lombardo, Opitz, et al., 2018) where one aims at modelling the full spectrum of landslide count.

Landslide susceptibility modelling can be estimated on the basis of historical/geomorphological inventories and event-specific inventories (Luigi Lombardo & Tanyas, 2020). The former case usually produces landslide predictive models which are useful in a relatively long timespan, and specifically for land management planning. This is achieved because a historical inventory is not tied to a specific trigger but is rather the image of where landslides are distributed in a given landscape across a long period of observation. Therefore, the validity of such susceptibility is also spread over a long time. Conversely, event-based inventories are specifically induced by a single trigger of known date and time. Therefore, susceptibility models generated in such cases are typically used in near-real-time or post-disaster phases.

In both cases, the available validation routines are similar in nature. It is always possible to split a single inventory into two parts, one used for calibration and one used for validation. However, this situation is not ideal because one should validate the predictive power of a given susceptibility model on the basis of future landslide occurrences. This is rarely done as it is particularly difficult to consistently map landslides in space and time (Paola Reichenbach et al., 2018).

Additionally, a class of susceptibility models chiefly deal with transferring the predictive equations over unknown datasets. This is primarily the case for transferability models in space, where one may want to train a model to predict landslide occurrences in one geographic area and predict over a different area (L. Lombardo et al., 2014).

As for the process of validation - the foremost requirement of such a model (Begueria, 2006), varies from historical to event-specific inventories (Camilo et al., 2017; C. T. Lee et al., 2008). Statistical simulation can also be an efficient validation process where a random number of generated predictive functions can be used to test the predictive capabilities of a fitted model on anonymous datasets (Luigi Lombardo & Tanyas, 2020). Much more rarely, this is done involving the very same geographic area but transferring the predictive equation in time (P. Reichenbach et al., 2014).

### **1.4 Link between landslides and land cover**

Landslides and the changes of land cover are interrelated, though establishing a direct relationship might be complicated (Glade, 2003). Changes in land cover is recognized throughout the world to impact landslide occurrence (Glade, 2003). Since historical times many researchers have been focusing on landslide occurrence in response to changes in land use and land cover in different parts of the world, for instance during the Holocene in Europe and adjacent regions (J. Matthews, 1997), in Canada (Goff, 1997; GOFF &

HICOCK, 1995), in New Zealand (Page et al., 1994), in Japan (Tomomi Marutani et al., 1999), etc. Moreover, landslides are also known to be the significant and in some parts of the world the main reason behind the evolution of the landscape, though they vary in different geological and geomorphological environments (Cendrero & Dramis, 1996; González Díez et al., 1996; Restrepo & Alvarez, 2006).

Different measures have been adopted in different environments within different timescales to establish the link between the changes of land use & land cover and the occurrences of landslides (Glade, 2003). For instance, Glade (2003) in New Zealand analyzed historical data from newspapers, report, scientific articles, and other sources, Marutani et al. studied the sediment generation from landslides resulting from clear-cutting in Japan (T Marutani et al., 2000), Chen and Huang (2013) evaluated a frequency-area distribution analysis in Taiwan, to study the relationship between landslide characteristics and different land use types etc. Reichenbach et al. (2014), conducted a study in Messina, Italy, where they generated landslide susceptibility maps to show the loss of forest lands and increase of bare lands caused the increase of unstable slope units. Land use change caused by anthropogenic factors was also found to cause new landslides or reactivate old ones in different inhabited parts of the world (Bruschi et al., 2013; Meusburger & Alewell, 2008; Vanacker et al., 2003). Glade (2003), showed how land use change altered the sediment generation processes in downhill basins in New Zealand. By examining the relationship between tea garden numbers and landslide density in northeast Turkey, Karsli et al. concluded that changes in land cover caused more landslides (Karsli et al., 2009). In the Andean watersheds Vanacker et al., (2003) used specific hydrologic parameter settings in a process-based slope stability model to find that the slope movement susceptibility depends largely on the recent land use change.

### **1.5 Research problem**

Research works so far, scarcely investigated the future landslide susceptibility based on a future land cover scenario. Chung and Fabbri in 2008, attempted to analyse the risk of landslides in Lisbon, Portugal by predicting the probability of future landslide occurrence based on some given scenarios and likely geomorphologic and topographic factors; the study followed a two stage approach (modified from (C.-J. F. Chung & Fabbri, 2005; C. J. F. Chung & Fabbri, 2003) ) and was validated through a cross-validation approach (C. J. Chung & Fabbri, 2008).

Shu et al. investigated the historical, present and future scenario of LULC (Land Use and Land Cover) in Pyrenees, Spain to analyse the impact of LULC changes on landslide susceptibility for 150 years, for this the authors relied on heuristic and deterministic models to predict landslide susceptibility and on Terrset software for predicting future LULC (Shu et al., 2019). The study found a clear influence of land use and land cover on landslide susceptibility.

Nevertheless, the approach to study the dynamic influence of land cover on landslide susceptibility and vice versa in a continuous feedback manner has not been found to exist in literature. This area of research is quite unadorned and the existing literature shows the need for in depth studies and experimenting with different models/techniques in different locations to gain knowledge about the existing and future relationship between land cover changes and landslide susceptibility. The research problem for this particular study is, therefore, to contribute to this area of scientific research by investigating the dynamic influence of future land cover on landslide susceptibility through a suitable methodological approach.

### **1.6 Study area**

The proposed study area, Idukki District in Kerala (Figure 1), India – is significantly characterized by landslides, since the mountainous Western Ghats cover a major portion of the district (Kalaranjini & Ramakrishnan, 2020; Sajinkumar et al., 2011). Several studies documented the presence of continuous land use and land cover changes and a sharp increase of annual landslide events in and around the study area since 1800 (George & Chattopadhyay, 2001; Jha et al., 2000; Kuriakose, 2010; Raju & Anil Kumar, 2006). Idukki has experienced a high population increase predominantly from migration for favourable agro-

climatic conditions and that eventually led to severe deforestation (Jha et al., 2000; Raju & Anil Kumar, 2006; Sajinkumar et al., 2011).

### 1.7 Background and state-of-art

India is a country where the occurrences of landslides are becoming more prominent over the years (Barnard et al., 2001). According to Rao, four zones of the country namely the western Himalayas, eastern and north-eastern Himalayas and plateau margins, Naga-Arakkon mountain belt and the Western Ghats along with some part of the eastern ghats are most prone to landslides (Rao, 1989).

Kerala – a state of southwestern India, located along the most significant physiographic and orographic feature of the Indian Peninsula- the Western Ghats, experiences a population migration, rapid land use and land cover changes and subsequent landslides (Kuriakose, 2010; Raju & Anil Kumar, 2006).

Several studies have been conducted in Kerala to study landslide susceptibility using different techniques. The methods include frequency-ratio technique, weights of evidence method, a combination of Dempster-Shafer, Bayesian probability and logistic regression methods, heuristic landslide susceptibility index (LSI) methods etc. (Achu et al., 2020; Ajin et al., 2014; Thampy et al., 1998; Vijith & Madhu, 2008).

The Dyna-CLUE model has been used in several locations of India, e.g. to analyze deforestation in Mahanadi and Brahmaputra river basin (M. D. Behera et al., 2018), to predict land use and land cover in the Ganga river basin (N. K. Behera & Behera, 2020), to study land use dynamics of future (2025) using decadal satellite images in Mahanadi river basin (Das et al., 2019), to model the land use of the pre-industrial time in Karnataka (S. Ghosh & Shetty, 2017), to analyze future land cover and land use with the prime objective of predicting future environmental vulnerability in the Dwarakeswar-Gandheswari river basin (Sahoo et al., 2019), to inspect the impact of water demand on the hydrological regime as a response to future land use and land cover change and climate change in Gandheswari river basin (Sahoo, Dhar, et al., 2018), to predict future agricultural sustainability based on future land-use suitability in the Dwarakeswar-Gandheswari river basin (Sahoo, Sil, et al., 2018), etc.

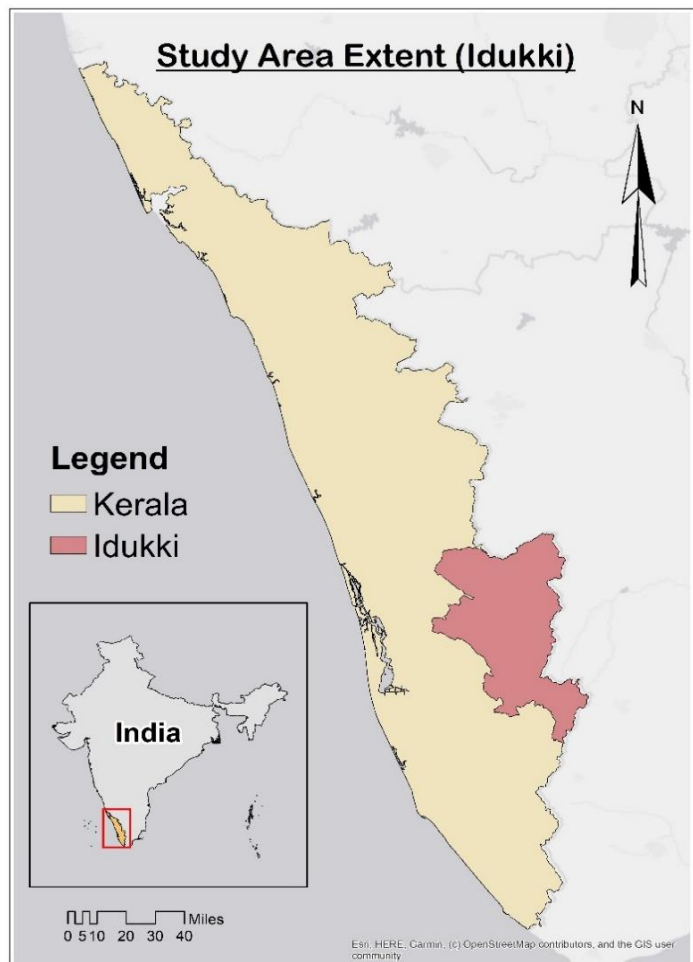


Figure 1: Study area extent

## 2. RESEARCH OBJECTIVES AND RESEARCH QUESTIONS

This study aims to analyse the interrelationship between landslide susceptibility and land cover change while illustrating their influence on characterizing each other in the future in a continuous feedback manner.

## 2.1 Overall objective

Predicting future landslide Susceptibility in Idukki district, Kerala based on the future land cover scenario by analyzing the land cover of the past.

## 2.2 Sub-objectives

1. Building a reference landslide susceptibility model trained with morphometric characteristics and historical land cover data.
2. Developing land cover scenarios by analyzing the past land cover change and future development plans.
3. Estimating the land cover of the future by learning from the past land cover.
4. Estimating landslide susceptibility using the estimated future land cover scenario.

## 2.3 Research questions

**Sub-objective 1: Building a reference landslide susceptibility model trained with morphometric characteristics and historical land cover data.**

- What are the most relevant covariates in the landslide susceptibility model?
- Do the land cover classes show a considerable influence on landslide susceptibility?

**Sub-objective 2: Developing land cover scenarios by analyzing the past land cover change and future development plans.**

- What are the prominent general trends in the past?
- What could possibly be the expected future trends?

**Sub-objective 3: Estimating the land cover of the future by learning from the past land cover and landslide susceptibility.**

- How well does the model perform in predicting the determined land cover classes?
- Does the landslide susceptibility influence the land cover change in the future?

**Sub-objective 4: Estimating landslide susceptibility scenarios in the future according to the estimated future land cover scenario.**

- How the landslide susceptibility of the future differs from that of the past in respect to the land cover evolution within Idukki?
- Is there any difference in predicted landslide susceptibility if it is accounted for in the future land cover change?

# 3. RESEARCH DESIGN AND METHODS

This chapter elaborates the combined methodological approach followed in this study to attain the aforementioned research objectives and answer the associated research questions. The research design consists of eight (8) phases through which the modelling methodology has been executed. Figure 2, illustrates the methodology process flow.

## 3.1 Beginning phase

### 3.1.1 Scenario development and setting boundary conditions

This study aims to investigate the influence of landslide susceptibility and land cover change on each other in a continuous feedback manner. It illustrates how changes in land cover in the future contribute to the change in future landslide susceptibility and vice versa. A time span of forty (40) years (2010-2050) was considered for this study but the modelling process was conducted for eight time steps – each corresponding

five years. They are: 2010-2015, 2015 -2020, 2020-2025, 2025-2030, 2030-2035, 2035-2040, 2040-2045 and 2045-2050. Landslide susceptibility was calculated for the beginning and end year of each time step.

For better understanding and clarity, adopting a scenario-based approach deemed appropriate. Therefore, a number of recent statistics, literature, future development plans were studied as well as an interview with a local expert (details mentioned in the Appendices) has been conducted.

To summarize the acquired information, Idukki though was recorded to experience a population decline (Board, 2014), settlements were reported to be doubled during 1990 to 2012 (Ramachandran & Reddy, 2017). Idukki often requires shifting of settlements due to landslide occurrence or susceptibility (KSDMA, 2018, 2019). To provide for the past loss of agricultural plantation, in 2021 the government has announced new projects to promote agricultural plantation (The Hindu, 2021). Reserved forests and wetlands are planned to be preserved and protected from conversions in the future (Board, 2014), though Idukki has been successfully controlling deforestation (Ramachandran & Reddy, 2017). Though Ramachandran and Reddy (2017) has recorded settlements to be doubled from 1990 to 2012, as a part of the 2030 plan - all sorts of constructions would be highly regulated (Board, 2014). According to the local expert, the villagers or land-owners are allowed to retain the ownership of their lands in landslide susceptible areas as well as continue agricultural activities but they are not allowed to live there anymore. The government also conducts some plantation activities as a part of a future plan in landslide susceptible areas.

Based on this information, for this research two different scenarios for both land cover and landslide susceptibility prediction have been developed.

- **Scenario – 1: Business as usual / No landslide mitigation (NL):** Land cover changes without any consideration of landslide susceptible zones. No private or public actions taken to account for the high-risk zones. Protected areas remain intact without any conversions. In the following parts of this document (including figures) the abbreviation- “NL” has been used to represent this scenario.
- **Scenario – 2: Sustainable future / With landslide mitigation (WL):** Land cover changes in a pre-meditated and controlled manner to account for landslide susceptibility. Controlled private or public actions are taken to reduce risk and effective land cover zonation policies are in effect. Land cover changes normally (business as usual) in non-susceptible areas whereas risk reduction measures e.g. plantation are undertaken in susceptible areas. Protected areas remain intact without any conversions. In the following parts of this document (including figures) the abbreviation- “WL” has been used to represent this scenario.

It was also assumed that in both the scenarios, the land cover demands for each year remain the same but for scenario-2 (sustainable future) land cover changes are only allowed in non-susceptible areas. Land cover and landslide susceptibility was estimated for every 5 years, for both the scenarios from 2010 to 2050.

For scenario -2 (sustainable future), land cover of the final year of each time step (5 years) was used to calculate landslide susceptibility of that year, which was then used to estimate land cover of the final year of the next time step. In other words, for scenario-2, the outputs of the model are considered as inputs of the landslide susceptibility model and vice versa, for better illustration of their influence on each other.

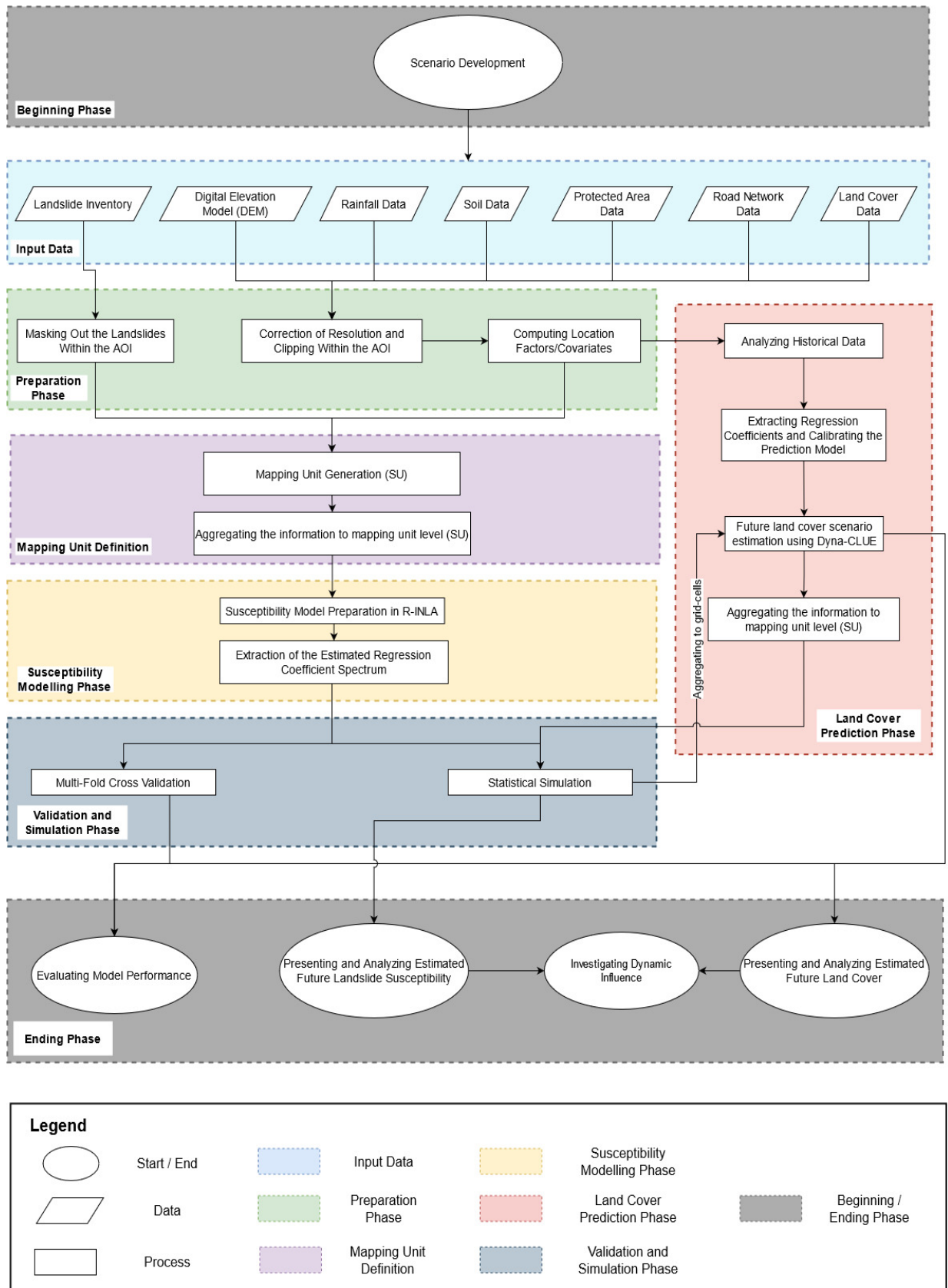


Figure 2: Methodology process flow

It was also assumed that in both the scenarios, the land cover demands for each year remains the same but for scenario-2 (sustainable future) land cover changes are only allowed in non-susceptible areas. Land cover and landslide susceptibility were estimated for every 5 years, for both scenarios from 2010 to 2050.

For scenario -2 (sustainable future), the land cover of the final year of each time step (5 years) was used to calculate landslide susceptibility of that year, which was then used to estimate land cover of the final year of the next time step. In other words, for scenario-2, the outputs of the model are considered as inputs of the landslide susceptibility model and vice versa, for better illustration of their influence on each other.

### 3.2 Input data

Several datasets from different sources with different resolutions were acquired for this research. The datasets and their sources are briefly presented in Table 1.

#### 3.2.1 DEM (digital elevation model)

For this study, the ASTER DEM with 30m resolution was selected which is made available by NASA, METI, AIST, Japan Spacesystems and U.S.-Japan ASTER Science Team (2019). It was subjected to thorough inspection and corrections for potholes/sinks within the study area in the preparation phase.

Table 1: Source and details of input datasets

Data type	Source	Description
Digital elevation model (dem)	Aster dem	30m resolution; good for modelling purposes.
Soil data	Soilgrid ( <a href="http://www.soilgrids.org">www.soilgrids.org</a> ) (hengl et al., 2017)	Global soil properties dataset with 250m resolution. Selected parameters: bulk density, cation exchange capacity, clay, coarse fragments, soil ph, sand, silt and soil organic carbon Selected depth: 60-100 cm
Land cover data	Kerala state disaster management authority (ksdma) ( <a href="http://www.sdma.kerala.gov.in">www.sdma.kerala.gov.in</a> )	Level 2 land cover data of 2010
Landslide point data	Doi: <a href="https://doi.org/10.17026/dans-x6c-y7x2">10.17026/dans-x6c-y7x2</a> (westen, 2020)	Point data of landslides mapped in 2018 (June to August).
Rainfall data	Worldclim ( <a href="http://www.worldclim.org">www.worldclim.org</a> )	Bioclimatic variables – annual average precipitation (bio12) – 30s
Road network data	Kerala state disaster management authority (ksdma) ( <a href="http://www.sdma.kerala.gov.in">www.sdma.kerala.gov.in</a> )	Major roads of Idukki – linear features
Protected area data	Protected planet – world database of protected areas (unep-wcmc & iucn, 2021) ( <a href="http://www.protectedplanet.net">www.protectedplanet.net</a> )	Authoritative data on protected areas and other effective area-based conservation measures.

### **3.2.2 Landslide point data**

A database of landslide point data created in 2018 for the entire state of Kerala, was acquired for this study (Westen, 2020). The database was created based on two inventories which were based on object-based image analysis (OBIA) and field surveys. Out of a total of 4728 landslides, 2477 by OBIA, 973 by field survey, 422 by both OBIA and field surveys and 856 were mapped by visual interpretation of Google Earth imageries (Hao et al., 2020; Westen, 2020).

### **3.2.3 Soil data**

The soil properties data were acquired from [www.soilgrids.org](http://www.soilgrids.org); this dataset is a set of global maps of soil properties for six depth intervals and has a resolution of 250m (Hengl et al., 2017). Eight soil parameters were selected for the study, namely: bulk density, cation exchange capacity, clay, coarse fragments, soil pH, sand, silt and soil organic carbon. The selected depth range of the obtained parameters was 60-100 cm.

### **3.2.4 Land cover data**

For this study, acquiring relevant land cover data, using that as a covariate in the susceptibility model and also for predicting the future land cover, are part of the initial goal. Therefore, the land cover data of the year 2010 was acquired from the Kerala State Disaster Management Authority (KSDMA). This dataset was selected because of its accuracy, reliability, collection method and completeness. The acquired land cover dataset was thoroughly examined and the Level-2 data was selected for it having the optimum level of details for the modelling purpose.

### **3.2.5 Rainfall data**

The rainfall data used in this study was acquired from WorldClim (Fick & Hijmans, 2017) – 30 seconds bioclimatic variables. This dataset contains the annual rainfall average for the initial year 2010 (the same year as the acquired land cover data).

### **3.2.6 Road network data**

The major road network data was acquired from KSDMA (Kerala State Disaster Management Authority). The dataset contains only the major roads of the Idukki district as a linear feature.

### **3.2.7 Protected area data**

Idukki contains a significant extent of protected areas that are maintained by the local government. The dataset containing the spatial extent of the protected areas in Idukki was acquired from Protected Planet ([www.protectedplanet.net](http://www.protectedplanet.net)) (UNEP-WCMC & IUCN, 2021). Figure 15, shows the spatial extent of the protected areas in Idukki.

## **3.3 Preparation phase**

### **3.3.1 Masking out landslides**

Out of 4728 mapped landslides in the Kerala-wide dataset, a subset of 2223 landslides was created that are located within the study area – Idukki district. In this stage, the landslide dataset was pre-processed and a matrix containing their presence or absence on the selected mapping unit level was prepared.

### **3.3.2 Correction of resolution and clipping**

All the datasets used in both the landslide susceptibility and land cover change model were projected to the same local coordinate system (UTM Zone 43N). A resolution of 100 meters was considered optimal for this study and all the acquired datasets were resampled to this resolution to maintain uniformity. The number of pixels, as well as the number of rows and columns, were also matched within the datasets to avoid errors during the modelling process explained in the following sections. All the input datasets were also ‘clipped’ to maintain their spatial extent as per that of the study area.

### 3.3.3 Computing location factors / covariates

The acquired datasets were used as location factors in the land cover model and as covariates in the landslide susceptibility model. The list of all the covariates/location factors considered in this study is presented in Table 2.

All the acquired soil properties, elevation and slope calculated from the DEM, Euclidean distance to roads and the rainfall data were considered as location factors in the reference land cover model. Additionally, for the 'WL' scenario (see section 3.1.1), the calculated landslide susceptibility of the final year of the previous time step was considered also as a location factor for modelling the land cover of the next time step.

A plethora of factors contribute to slope stability, slope dynamics and the occurrence of landslides (Juang et al., 1998; Lv et al., 2017). As considered in a number of relevant studies (Luigi Lombardo, Opitz, et al., 2018; Luigi Lombardo & Tanyas, 2020; L. Luo et al., 2020), slope and elevation were calculated from the DEM in a GIS platform and used as morphometric covariates (Luigi Lombardo, Saia, et al., 2018; Paola Reichenbach et al., 2018). Euclidean distance to roads and the acquired soil properties were also incorporated as locational covariates along with the size and shape of slope units as a mapping unit. The land cover data (past or estimated future scenarios) were considered as entropic covariates in the landslide susceptibility model.

### 3.4 Mapping unit definition

For this study, two different mapping units were used for landslide susceptibility and land cover modelling. For the land cover model (built-in DynaCLUE v2.0 - section 3.6.1), it is vital to use grid-cells as has been implemented with a native structure that only makes use of raster data. But for the landslide susceptibility model (built in R-INLA - section 3.5), the mapping unit could be either grid-cells or slope-units.

For this study, slope unit was chosen, which are geographical objects bound by ridges and streamlines (Alvioli et al., 2016). The reason behind this choice is mainly geomorphological; in fact, when a theoretical landslide occurs, unless of extremely large proportions, it initiates and propagates within the same slope unit. Therefore, this spatial partition reflects the morpho-dynamic behaviour of a landslide.

Moreover, considering the area of interest of this study (Idukki), which covers an entire district and contains a large number of landslides (Westen, 2020), grid-cells as a mapping unit might have a massive number of pixels requiring enormous computational time for landslide susceptibility modelling in R-INLA than that of the slope units. Hence, slope unit was considered as the most suitable mapping unit for susceptibility modelling in this particular study. Slope units were calculated from the DEM using the "r.slopeunits" software (Alvioli et al., 2016; Luigi Lombardo et al., 2019), where a small slope unit area is targeted to ensure that the landscape is well represented.

Finally, all the selected covariates or location factors were aggregated to the respective mapping units chosen for both models. As for the feedback process (WL scenario), where the outputs of the landslide susceptibility models are passed as an input for the land-cover prediction model, and vice-versa, an additional processing step is required. In fact, the output of the landslide susceptibility is expressed at the slope unit scale and needs to be downscaled at the pixel resolution required to run the land cover change model. In other words, the output of the land cover change model needs to be upscaled to the slope unit resolution, and this step is consistent irrespective of the NL or WL scenarios.

Table 2: List of location factors / covariates

Serial No.	Name	Source/ Name of input dataset	Used in
1	Bulk density	Soil data	Both land cover and landslide susceptibility model
2	Cation exchange capacity	Soil data	Both land cover and landslide susceptibility model
3	Clay content	Soil data	Both land cover and landslide susceptibility model
4	Coarse fragments	Soil data	Both land cover and landslide susceptibility model
5	Soil pH	Soil data	Both land cover and landslide susceptibility model
6	Sand	Soil data	Both land cover and landslide susceptibility model
7	Silt	Soil data	Both land cover and landslide susceptibility model
8	Soil organic carbon	Soil data	Both land cover and landslide susceptibility model
9	Elevation	DEM	Both land cover and landslide susceptibility model
10	Euclidean distance to roads	Road network data	Both land cover and landslide susceptibility model
11	Slope steepness	DEM	Both land cover and landslide susceptibility model
12	Rainfall	Rainfall data	Only in land cover model
13	Predicted land cover	Land cover data of 2010 and outputs of land cover model	Only in landslide susceptibility model (both NL and WL scenarios)
14	Predicted landslide susceptibility	Output of landslide susceptibility model	Only in land cover model (WL scenario)

### 3.5 Susceptibility modelling phase

The landslide susceptibility model used for this study is a Bayesian version of a binomial Generalized Additive Mixed Model (GAMM) (Brenning, 2008; Luigi Lombardo et al., 2020) with necessary modifications. The reasoning for choosing a Bayesian framework to model landslide susceptibility is to estimate the uncertainty in the landslide prediction (Luigi Lombardo & Tanyas, 2021). This allows for a robust simulation step (see section 3.7.2) where the posterior distributions of each model component are used to randomly generate a number of predictive functions to be solved for the same morphometric characteristics and the changing land cover distribution in space and time. GAMM models are reported to be extensively used in landslide susceptibility studies (Nefeslioglu et al., 2008; Paola Reichenbach et al., 2018). The model has a several implementations in R-studio (Team, 2013), one of which can be run by using the library R-INLA (Bakka et al., 2018; Martins et al., 2013). R-INLA was opted for due to its ability to precisely and promptly calculate Bayesian statistics (Rue et al., 2017). For landslide susceptibility calculation, the model used for this study can be summarized as:

$$\eta(P) = \beta_0 + \beta_1 X_1 + \dots + \beta_m X_m + f(Y_n) \quad 3.1$$

In equation 3.1,  $\eta$  is the logit link,  $\beta_0$  is the global intercept,  $\beta_1$  to  $\beta_m$  are the estimated regression coefficients of the corresponding covariates used linearly in the model and  $f$  represents a non-linear function of the 'Y' covariate discretized in a  $n$  number of classes. In this study, the chosen non-linear function is a first order random walk (RW1) (Bakka et al., 2018). The difference between GAMs and GLMs (Generalized Linear Model) is that, GLMs can only feature linear or fixed effects whereas GAMs is an extension that can feature different non-linear relationships (Luigi Lombardo & Tanyas, 2021). For the detailed procedure and scripting, the step-by-step methods of Lombardo et al. (2019) were followed.

In order to ensure that all the co covariates have comparable effects, they were rescaled with mean zero and unit variance (L. Luo et al., 2020). The regression coefficients were then estimated and the associated distributions were extracted at this stage.

From the estimated distribution of each regression coefficient, simulations were developed. Meaning that a number of predictive functions were extracted from the estimated regression coefficients' distributions and these were solved for all the time-invariant predictors which were kept constant, and for the time-variant component related to the land-cover. This means that the element corresponding to the land cover responsible for the landslide occurrences in 2010, was substituted with the estimated future land-cover (more explanation in section 3.7.2).

This procedure enables estimating the way landslide susceptibility may change in spatial patterns as a function of the spatial pattern of a potential future land-cover.

Slope, as known to have a random effect in various literature (Luigi Lombardo & Tanyas, 2020; L. Luo et al., 2020), was modelled as a first order random walk (RW1) with adjacent-class dependency (Lindgren & Rue, 2008). Whereas all the other covariates including land cover classes were considered as a fixed effect. In other words, they were modelled as linear covariates.

### 3.6 Land cover prediction phase

#### 3.6.1 DynaCLUE modelling

For estimating the future land cover the Dyna-CLUE model (P. H. Verburg & Overmars, 2009) was used in this study, which is a modified version of the CLUE-s model (Castella & Verburg, 2007; P. H. Verburg et al., 2002). The spatial allocation of demands for land cover types acts as the base of the model, whereas the model combines a top-down and bottom-up approach for allocating land-use change to grid cells and determining the conversions of land cover types respectively (P. H. Verburg & Overmars, 2009).

##### 3.6.1.1 Model structure and functioning

The model consists of one spatial and one non-spatial module. The land cover data of the starting year, restriction policies, and drivers are considered as input for the spatial module whereas locational characteristics, land cover conversion settings, conversion elasticity, demand information, and convergence conditions are the inputs of the non-spatial module (M. D. Behera et al., 2018; N. K. Behera & Behera, 2020).

The change of the area of the given land-use types are calculated within the non-spatial module and is considered as the demand input for the spatial module to allocate demands to grid cells in an iterative process until the demand has been satisfied (P. H. Verburg & Overmars, 2009).

The influence of the location factors on a particular land cover type to occur in a specific grid-cell can be explained through a binomial logit function in equation 3.2, where ' $P_k$ ' refers to the probability of that grid cell to have that particular land cover class in location 'k', 'F's refer to the location factors and ' $\beta$ 's refer to

the regression coefficients calculated from a logistic regression where the land cover is considered as the dependent variable (P. Verburg, 2010).

$$\log\left(\frac{P_k}{1 - P_k}\right) = \beta_0 + \beta_1 F_{1,k} + \dots + \beta_n F_{n,k} \quad 3.2$$

The total probability calculated by the model is the sum of location suitability, neighborhood suitability, iteration variables (representing competitive advantage of one land cover class over another) and conversion elasticity (P. Verburg, 2010; P. H. Verburg & Overmars, 2009). Equation 3.3, shows the total probability calculation, where Ptotal, Ploc, Pnbh, CElas and ItVar are total probability, location suitability, neighborhood suitability, conversion elasticity and iteration variable respectively, whereas, k, t and lc represent location/grid-cell, time and land cover type respectively.

$$P_{total_{k,t,lc}} = P_{loc_{k,t,lc}} + P_{nbh_{k,t,lc}} + CE_{las_{lc}} + ItVar_{lc} \quad 3.3$$

The location and neighborhood suitability are ascertained by empirical methods, expert and process knowledge, analysis, etc. The conversion elasticity determines the cost of conversion of the initial land cover types to another (P. H. Verburg & Overmars, 2009). Through a conversion matrix, the model determines which conversions are allowed for each type of land cover classes by taking the spatial policies and restrictions into account (N. K. Behera & Behera, 2020; P. H. Verburg & Overmars, 2009).

### 3.6.2 Analyzing historical data

For estimating the future land cover scenarios, the land cover of 2010 along with the demand assumed from the future development plans, current statistics and expert opinion was used (see section 3.1.1). The level 2 data of this dataset was considered in this study and the listed land cover classes were aggregated to eight (8) classes as per their relevance. Table 3, enlists the reclassified new land cover classes used for this study along with the class names in the level-2 dataset from which they were originally assigned from.

Table 3: List of land cover classes

Number	Assigned new land cover class	Class name in L-2 data/assigned from
1	Villages / Built-up	Villages (rural)
2	Cropland	Crop land (paddy), fallow
3	Agricultural plantation	Plantation
4	Grassland	Grassland, land with or without scrub
5	Forest	Evergreen/semi-evergreen, deciduous (dry/moist)
6	Forest plantation	Forest plantation
7	Waterbodies	Water bodies, river/stream, reservoir
8	Rocks & others	Barren rocky/stony waste, mining/industrial wasteland

Eight binary maps were prepared for each of the land cover classes and converted to ASCII file format. The protected area extent map was also used in this stage to apply restrictions to the land cover allocation process.

### 3.6.3 Extracting regression coefficients and calibrating the model

For the model to be able to detect, all the individual land cover classes and location factor maps were converted to binary and then to ASCII file format. A total of fifteen location factors were considered in this study, including landslide susceptibility for the ‘WL’ scenario, whereas for the ‘NL’ scenario, the landslide susceptibility did not have any influence on the model as a location factor. The land cover classes: ‘waterbodies’ and ‘rocks & others’ were assumed to be static throughout the timeline, hence they were also considered as location factors for this study. The model needs four system files namely, ‘demand’, ‘alloc1’, ‘allow’ and ‘main’ to perform and these were prepared based on all the location factors. Besides, the protected areas were considered as the “region1” file, which would not allow any changes within its extent.

### 3.6.3.1 Alloc1 file preparation

The 'alloc1' file includes the regression results for each land-cover type (except for the waterbodies and rocks & others) with all the significant location factors that might control the suitability of a location for the specific land-use type.

Before conducting the regression in a statistical software, the GIS data are converted to a supported file format for a statistical software using the "convert.exe" tool provided with the Dyna-CLUE package (P. H. Verburg & Overmars, 2009). Each land cover type was converted one by one with all the location factors using the convert tool. The resultant stat files were imported in SPSS (IBM, 2019). In SPSS, all the stat files were subjected to binary logistic regression with a forward-conditional method where the specific land cover types were considered as dependent variables. The Alloc1 file was constructed as per the outputs obtained from the "variables in equation" block. Regression was conducted for six land cover types except for 'waterbodies' and 'rocks & others', as they were considered static. Hence, for these two classes a fixed regression coefficient: 0.5 was used in the 'alloc1' file (Figure 16).

### 3.6.3.2 Allow file preparation

The 'allow' file contains the conversion matrix that determines the specific grid cells that are allowed to convert to other land use types and restricts those that are not (Figure 16). The value "0" and "1" of a cell indicates that conversion is respectively not allowed and allowed (P. Verburg, 2010). The number code of the land cover types starts from 0, so for this study, the land cover type code ranges from "lc0" to "lc7".

As per the knowledge gained from expert opinion and recent statistics (see section 3.1.1), for the 'NL' scenario we assumed that all the land cover classes can convert to their own classes, but 'grasslands' and 'forests' can convert to 'villages' and 'agricultural plantations'. In other words, 'villages' and 'agricultural plantations' can replace 'grasslands' and 'forests'. As for the 'WL' scenario, the same rules were assumed to be applicable but only in the 'non-susceptible areas. It is crucial to mention here that for the land cover model for the 'WL' scenario, 'susceptible' and 'non-susceptible areas are defined using a fixed susceptibility threshold of 0.95 from the susceptibility generated by the land cover model (in section 3.5) while passing it on to the land cover model as a location factor (explained at the beginning of section 3.6.3).

### 3.6.3.3 Demand file preparation

The demand file contains the land requirements of each year for all the land cover types. This helps the model to allocate land cover changes as per the land requirements for each year while keeping the difference between both in an iterative way (P. Verburg, 2010). The first line of the demand file contains the number of years including the initial year. The following lines of the demand file contain the individual requirements of all land cover types in a way that the total area (number of pixels) remains the same in each year (P. Verburg, 2010).

For this study, we assumed that from 2010 to 2050, 'villages' and 'agricultural plantation' would increase by 25% and 10% respectively, which they would gain from the 'grasslands' and 'forests' (in low susceptible areas in the WL scenario; see section 3.6.3.2) to maintain the total count of pixels. As per these assumptions, villages and agricultural plantations had 0.56% and 0.24% annual growth rate respectively. The annual growth rate was calculated from the compound annual growth rate equation suggested by Fernando (2021), equation 3.4 shows the modified version of it.

The demand file was populated considering the annual growth rate for the specified land cover types while maintaining the total count of pixels within the study area in each year (Figure 16).

$$\text{Compound annual growth rate} = \left( \frac{\text{Final year's demand}}{\text{Initial year's demand}} \right)^{\frac{1}{\text{Number of years}}} - 1 \quad 3.4$$

#### 3.6.3.4 Setting main parameters/main file preparation

The main file contains the values of several factors required for the model to run properly, e.g., number of land cover types, the maximum number of factors in one regression, conversion elasticity (0 – 1), iteration variables, etc. The iteration variables used for this study were ‘0.4’ for ‘cropland’, ‘agricultural plantation’, ‘forest’ and ‘forest plantation’, ‘1’ for ‘villages’ and ‘waterbodies’, ‘0.3’ for ‘grassland’ and ‘0.2’ for ‘rocks & others’. This indicates that a relative competitive strength (P. Verburg, 2010) assigned to the ‘villages’ and ‘waterbodies’ were the highest and lowest for ‘rocks & others’ (Figure 16).

#### 3.6.4 Aggregating to mapping unit level

The predicted land covers were used in the landslide susceptibility model as a covariate. Hence, the predicted land cover generated from the DynaCLUE model were aggregated to the slope unit level and applied as an input in the statistical simulation stage (see section 3.7.2).

### 3.7 Validation and simulation phase

#### 3.7.1 Multi-fold cross validation

For the validation, a multi-fold cross validation routine was adopted, and it was an internal validation performed only for one landslide inventory (2018) as a reliable multi-temporal description of landslide occurrences is not available after this period. The dataset was split into two parts, one for fitting the model and one for validating it through a series of constrained Bootstrap replicates. Overall, 90% of the data was used to train the model and 10% was used for the validation. More specifically, the same random process was repeated ten times to generate ten mutually exclusive subsets, whose union represent the entirety of the study area. In other words, at each random extraction the following one was constrained to not sample the same slope units as the previous, thus creating ten 10% partition of Idduki. To estimate the actual performance for each validation, the ROC (Receiver Operating Characteristics) curves and AUCs (Area Under the Curve) were computed.

#### 3.7.2 Statistical simulation

As mentioned in, section 3.5, the reference model returned a posterior distribution of potential regression coefficients. These were exploited in this simulation stage by removing the land cover component mapped in 2010. And, by adding instead the forecasted land cover for a specific future scenario. In reality, we generated 1000 simulations from these distributions and substituted the land cover component from the reference fit with the predicted future land cover, for a total of 16 combinations and 1000 simulations for each case. These 16 combinations consist of 8 scenarios, one every 5 years from 2010 to 2050, and the two different territorial management strategies, with (WL) or without (NL) landslide mitigation practices in place.

This way, we projected changes in the susceptibility patterns, due to the changes in the land management practices. Since the simulated susceptibility outputs and predicted land cover inputs in this stage needed to be represented through their respective mapping units, intermediate downscaling and upscaling steps were involved in this stage. Figure 3, adopted from Luo et al., (2020), represents a summary workflow to provide better visualization of the simulation stage adopted in this study. For each year and from the 1000 simulations generated, we then extracted the mean predictive map to represent the central tendency, together with the distance measured from the 2.5 and 97.5 percentiles to measure the 95% credible interval of all the simulated scenarios.

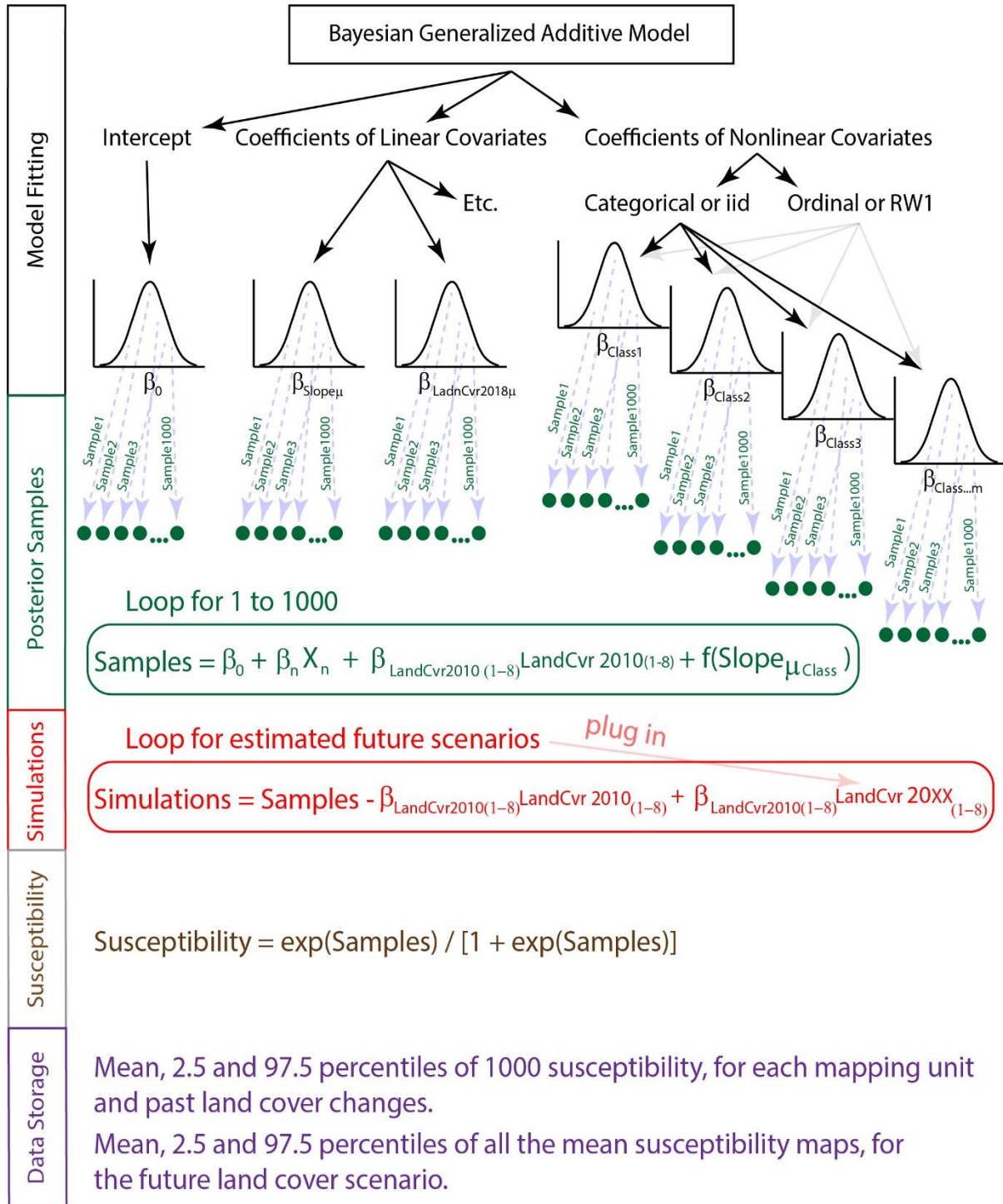


Figure 3: Process flow of statistical simulation (modified from Luo et al., 2020)

## 4. RESULTS AND DISCUSSIONS

This chapter consists of the generated results of all the processes performed in chapter 3: ‘Research design and methods’ as well as the discussions required to facilitate clearer insight. This was done through two broad sections namely ‘Land cover modelling’ and ‘Landslide susceptibility’. This chapter also includes an overall discussion, associated uncertainties and limitations and implications of further studies in three different sections.

### 4.1 Land cover modelling

This section contains an overview of the land cover modelling performed in section 3.6 and analyzes the predictive performance, presents the regression results and the model outputs with necessary explanations.

#### 4.1.1 Regression outputs

As mentioned in section 3.6.3.1, a binary logistic regression was conducted individually for six (6) land cover classes considering a specific land cover class as the dependent variable and all the location factors (other than landslide susceptibility) as independent variables. The number and type of the significant variables for each land cover class were different. For ‘villages’, ‘cropland’, ‘agricultural plantation’, ‘grassland’, ‘forests’ and ‘forest plantation’ classes the number of significant variables was 5, 9, 11, 8, 11 and 8 respectively. Table 4 lists all the location factors used in the regression and their respective significance for all the land cover classes. The regression coefficients of all the significant location factors for their particular land cover class were extracted and using those the “alloc1” file was prepared (Figure 16).

Table 4: Location factors and their significance as per regression

Test Variable(s)	Villages	Cropland	Agricultural Plantation	Grassland	Forest	Forest Plantation
Bulk Density	Not Significant	Significant	Significant	Not Significant	Significant	Significant
Cation	Significant	Significant	Significant	Significant	Significant	Not Significant
Clay	Not Significant	Not Significant	Significant	Significant	Significant	Not Significant
Coarse	Significant	Not Significant	Significant	Significant	Significant	Significant
DEM	Not Significant	Significant	Not Significant	Not Significant	Not Significant	Not Significant
Euclidean Distance to Roads	Significant	Significant	Significant	Not Significant	Significant	Significant
pH	Not Significant	Significant	Significant	Significant	Significant	Not Significant
Rainfall	Not Significant	Significant	Significant	Significant	Significant	Significant
Sand	Significant		Significant	Significant	Significant	Significant
Silt	Not Significant	Significant	Significant	Significant	Significant	Significant
Slope	Not Significant	Significant	Significant	Significant	Significant	Significant
Soil Organic Carbon	Significant	Significant	Significant	Not Significant	Significant	Not Significant

#### 4.1.2 Predictive performance

To analyze the model’s performance in predicting the probability of each of these land cover classes based on their significant location factors (according to the regression results), we computed the ROC curves and AUCs. Table 5 contains the AUCs for six land cover classes (‘villages’, ‘cropland’, ‘agricultural plantation’, ‘grassland’, ‘forests’ and ‘forest plantation’).

Table 5: AUCs (Area under the curves) of land cover prediction model

Land Cover Class	AUC	Performance Indicator (Yang & Berdine, 2015)
Villages	0.757	Excellent
Cropland	0.855	Excellent
Agricultural Plantation	0.855	Excellent
Grassland	0.643	Acceptable
Forests	0.839	Excellent
Forest Plantation	0.731	Excellent

Figure 4 shows the ROC curves for ‘cropland’ and ‘agricultural plantation’ – the two land cover classes with the best predictive performance (AUC 0.855). ROC curves of the rest of the land cover classes are presented in Figure 17.

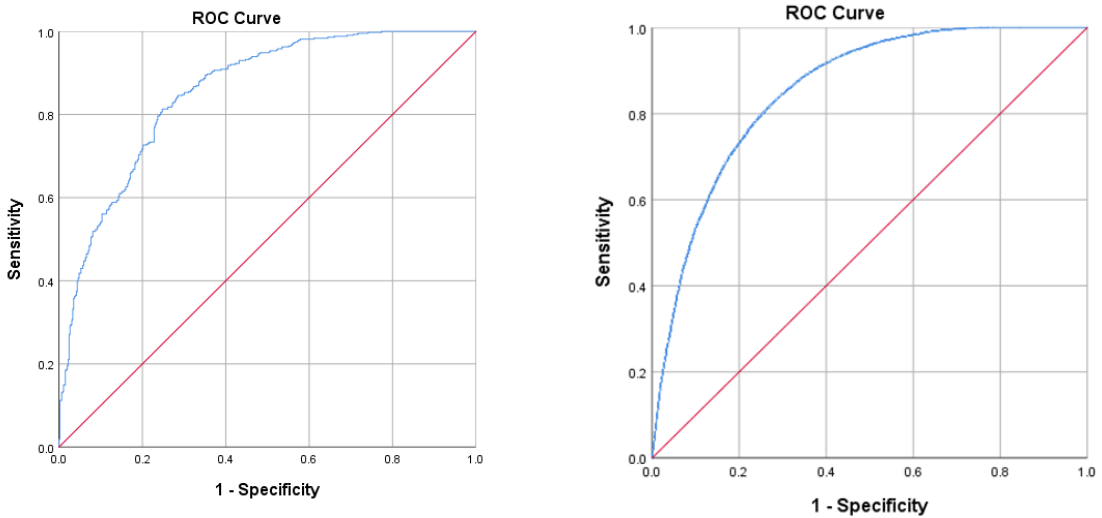


Figure 4: ROC curves of cropland (left panel) and agricultural plantation (right panel)

According to Yang & Berdine (2015), other than the ‘grassland’ class, the model performance in predicting all the other land cover classes was “excellent”. The model’s performance was the best in predicting “cropland” and “agricultural plantation” and the worst in predicting “grassland” class. Though the model performance for grassland can be considered “acceptable” by some scholars (Yang & Berdine, 2015), it can be considered “poor” by some others (Mandrekar, 2010).

To better understand the spatial extent of the probability for each land cover class we also computed the probability maps using the DynaCLUE v2.0’s built-in function. The probability maps of ‘cropland’ and ‘agricultural plantation’ is presented in Figure 5 and the rest of the maps are presented in Figure 18 and Figure 19.

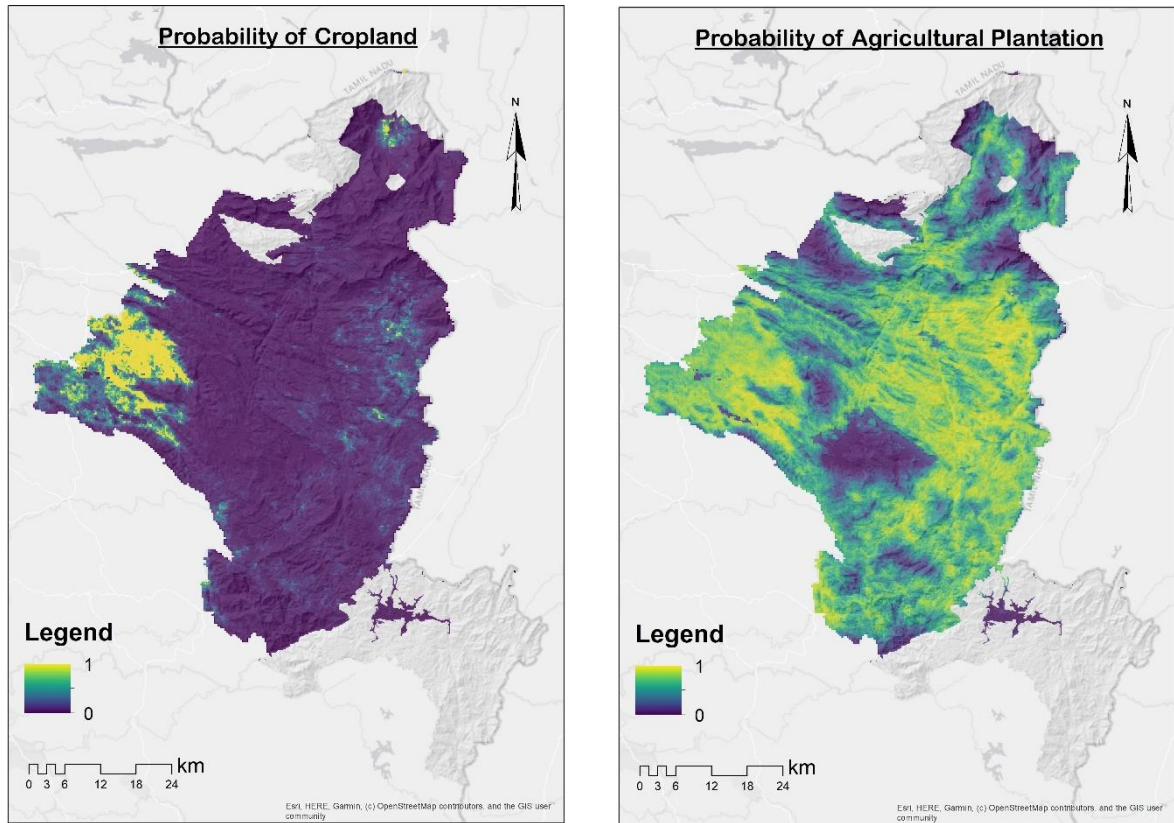


Figure 5: Probability maps of cropland (left panel) and agricultural plantation (right panel)

The missing parts in the northern and southern parts of the probability maps indicate the extent of the protected areas (Figure 15), and so the model did not calculate any probability for those areas. It's noticeable from the probability maps that all the land cover classes show different probabilities but some show significant variation. This occurs perhaps for the scenario based rule set and the allowed conversion settings implemented in the model as well as the pre-dominant location of a certain land cover class. For instance, agricultural plantations show a widespread high probability of occurrence whereas waterbodies show no probability throughout the study area other than very high probability in some places. Such differences occur because 'agricultural plantation' had an increased demand in the final year, allowed to replace other land cover types and was predominantly widespread, whereas waterbodies are modelled as 'static' and not allowed to convert to or from any other land cover classes, therefore the probability is very high only in its predominant locations.

#### 4.1.3 Land cover model outputs

The land cover model was first run for the 'NL' scenario for each time step (8 time steps: 2010-2050) without considering the landslide susceptibility. For the 'WL' or the landslide mitigation scenario, the model was run next for each time step with the simulated landslide susceptibility (outputs from section 3.7.2). Additionally, the same conversion rules were applied to both the scenarios but for the 'WL' scenario, conversions were only allowed in 'non-susceptible zones (see explanation in section 3.6.3.2). A total of sixteen (16) land cover maps were prepared (8 for each scenario) and presented in Figure 20 - Figure 24. The land cover map of the initial year as acquired from the dataset of 2010 with the redefined classes is presented in Figure 6. The predicted land cover maps of the final year (2050) for both the scenarios are presented in Figure 7.

It is clearly visible from the presented maps that the conversions took place as directed by the scenario rule sets. Replacement of grasslands by agricultural plantations is the most apparent phenomena from visual inspection.

To visualize the differences of the land cover maps of both the scenarios for each time step, we calculated their individual differences and presented them through maps in Figure 26 and Figure 27. Only the final year's (2050) difference of estimated land covers is shown in Figure 8. As seen in the difference maps, in the initial years the differences were very low between the two scenarios (notable: no difference in 2015). Though in the latter years some differences are noticeable along the northern parts, differences over the years are also mostly confined around the central Idukki. The differences were low in the initial years perhaps because of the fact that the scenario rule sets take a considerable amount of time to show notable differences, besides the modelling resolution might also be an imposing factor. Additionally, the northern and southern parts are mostly covered by the protected areas, thus no changes occurring in those directions can be justified. The landslide susceptibility differences occurring also in the central part of the study area (Figure 14), could be a significant imposing factor as it is considered as a location factor in the 'WL' scenario. The pixel differences among the land cover scenario difference maps for each time step is presented in Table 6. As the maps suggest, the year 2050 has the highest difference in terms of changed pixel count (0.5%-pixel change).

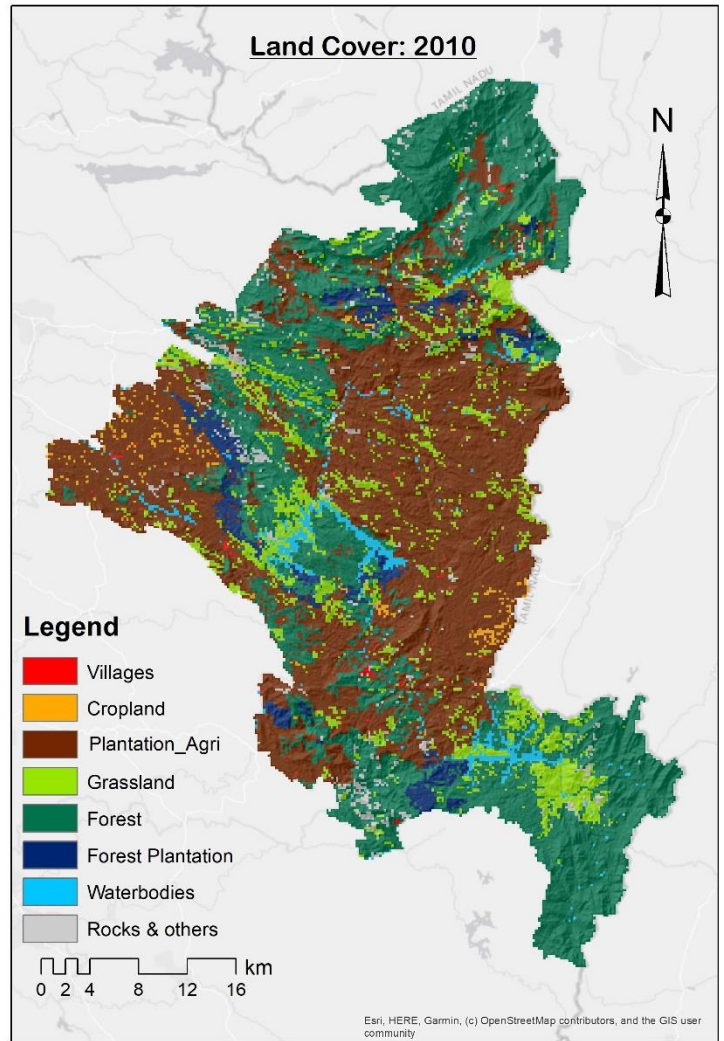


Figure 6: Land cover of year 2010 (Starting year)

Table 6: Pixel differences of land cover scenario difference maps

Year	Changed Pixel Count	Unchanged Pixel Count	Total Number of Pixels	Percent Pixel Change
2015	0	436803	436803	0%
2020	262	436541	436803	0.06%
2025	415	436388	436803	0.10%
2030	691	436112	436803	0.16%
2035	981	435822	436803	0.22%
2040	1337	435466	436803	0.31%
2045	1733	435070	436803	0.40%
2050	2168	434635	436803	0.50%

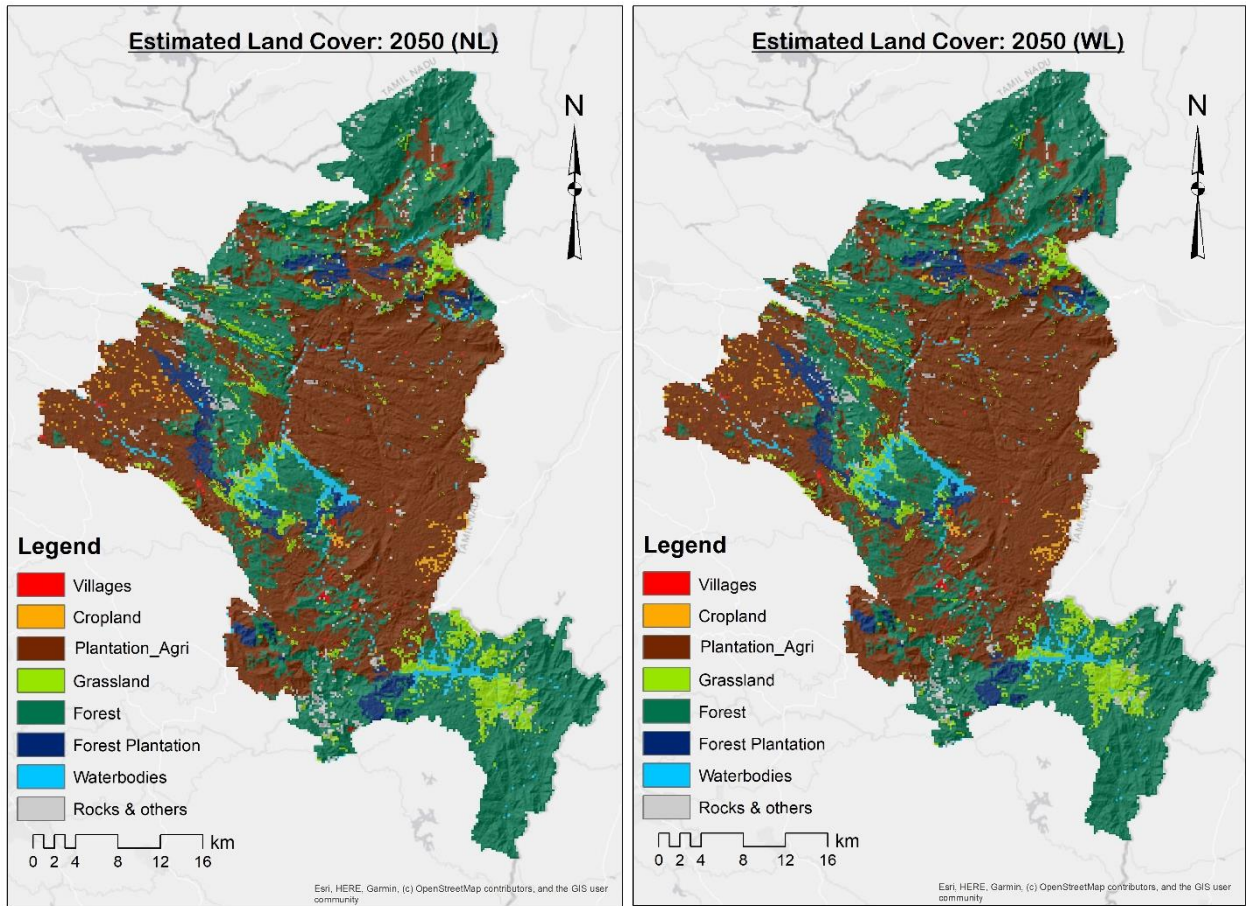


Figure 7: Estimated future land cover of 2050 (Left panel: 'No landslide mitigation' scenario, Right panel: 'With landslide mitigation' scenario)

Difference maps were also calculated for the initial year (2010) and the final year (2050) for both the scenarios, and they are presented in Figure 9 with their in-between difference map. Additionally, their pixel count differences (for each time step) are also presented in Table 7.

Table 7: Difference between 2010 & 2050 (Scenario NL, WL and scenario difference)

Scenario	Changed Pixel Count	Unchanged Pixel Count	Total Number of Pixels	Percent Pixel Change
Scenario NL	19085	417718	436803	4.37%
Scenario WL	19086	417717	436803	4.37%
Scenario Difference	2147	434656	436803	0.49%

It is evident from Figure 9, that for both scenarios the model successfully predicted future land cover with substantial difference between the starting and the final year as directed by the scenario conditions. The difference for each scenario appears quite spread out whereas the scenario difference shows they were varying mostly in the central part of Idukki. Table 7 suggests that there was almost no difference between the scenarios (only '1' extra pixel count in WL scenario, no change in percent pixel change) but their in-between difference (scenario difference) was about 0.49% (pixel change). That indicates that land cover

changes took place from 2010 to 2050 in different locations in different scenarios, though there is a negligible difference in their pixel count.

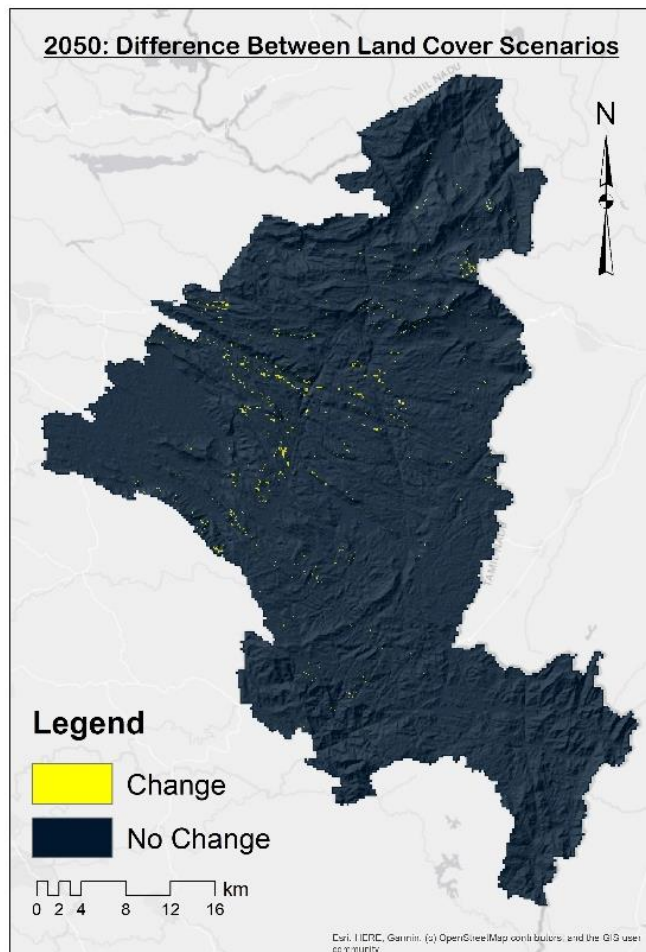


Figure 8: Difference between scenarios in 2050

Centralized land cover changes are perhaps influenced by the coarse resolution of the input datasets and also the landslide susceptibility being centralized (though landslide susceptibility and land cover influence each other in scenario 2). The restriction introduced by the protected areas is also a substantial factor in this regard.

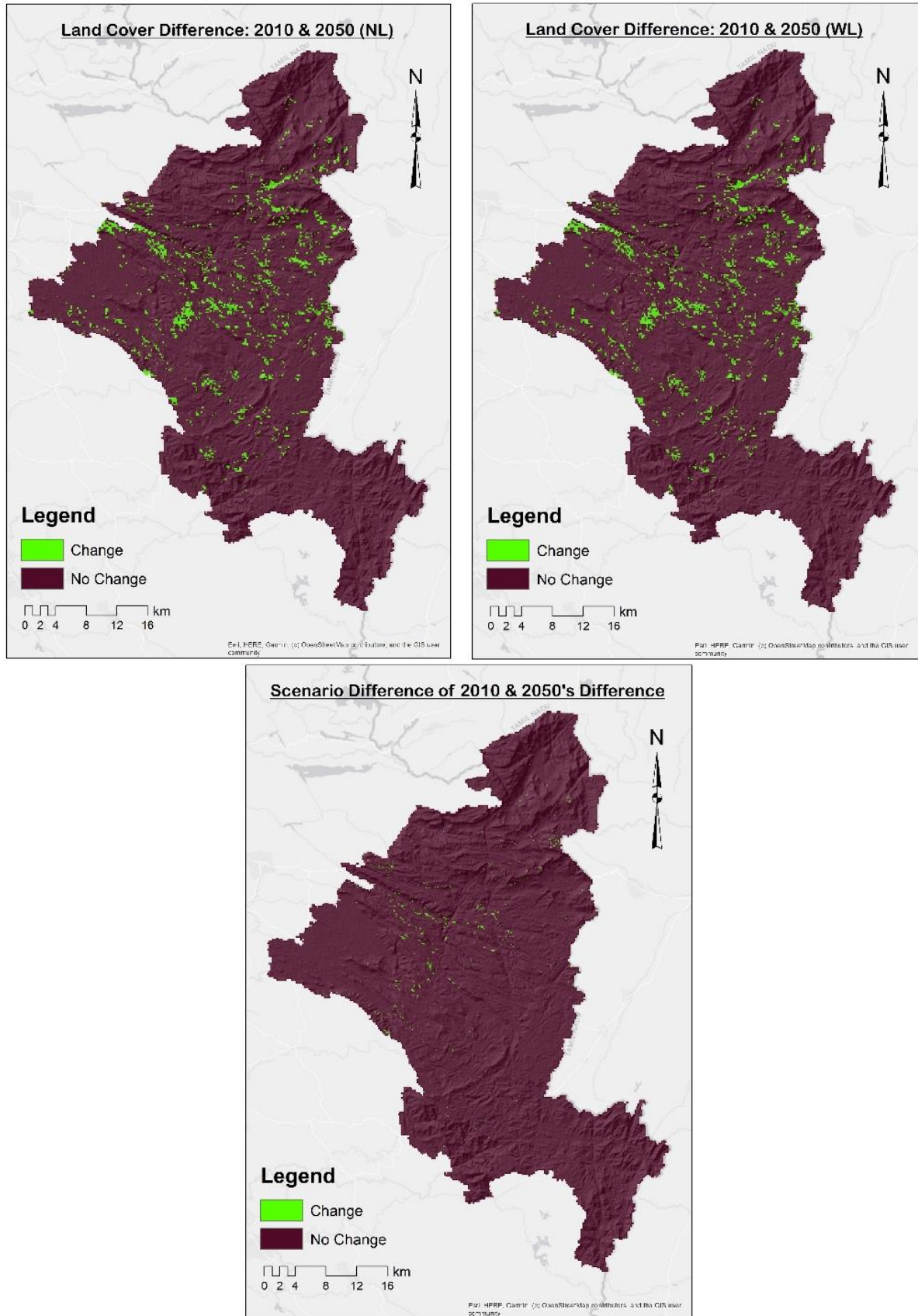


Figure 9: Land cover difference between the first (2010) and final (2050) year; TL : NL scenario, TR: WL scenario, Bottom: Difference between scenarios (TL vs. TR)

### 4.2 Landslide susceptibility

The outputs of the landslide susceptibility model developed in R-INLA (Bakka et al., 2018) along with the simulation results are presented in this section. The effect of the covariates, predictive performance of the model and the generated susceptibility and uncertainty maps are also presented and discussed in the following subsections.

The landslide model was ran initially for the year 2010. Its structure featured the variables whose effects on the landslide occurrences were modelled linearly (fixed effects) and a variable assumed to behave non-linearly (random effect). The latter corresponded to the mean slope steepness per slope unit, the ordinal structure of which was retained in the model by imposing an adjacent class dependence.

For both the scenarios considered in this study, the landslide susceptibility model was ran for each time steps from 2010 to 2050. Land covers of the final year of each time step (from the land cover model outputs of both scenarios) were used to calculate landslide susceptibility of that year.

#### 4.2.1 Covariates' effects

We considered both fixed and random effects in this study. Figure 10 shows the significant fixed effects (top) and random effect (bottom) estimated for the slope steepness.

The narrow posterior distributions of these covariates suggest that the model well estimated the contribution of each parameter with respect to landslide occurrences. As the covariates were rescaled by mean zero and unit variance in a pre-processing step, their respective posterior distributions are expressed in the same unitless scale, making their contribution to the model comparable (L. Luo et al., 2020). Clay mean and clay standard deviation show remarkable influence on the susceptibility pattern, which is also the highest of all the covariates. This can be interpreted in terms of clays' expansion capacity when imbued with water during a rainfall event. An opposite effect has been estimated for the bulk density. In this case, one can assume that a greater density implies greater compaction of the soil cover draping over the bedrock. Thus, greater compaction should be associated with a proportional cohesion, which in turn may reduce the probability of landslide occurrence per slope unit. It is crucial to mention that five land cover classes ('villages', 'agricultural plantation', 'grassland', 'forest' and 'forest plantation') show a significant and positive influence on the landslide susceptibility, of

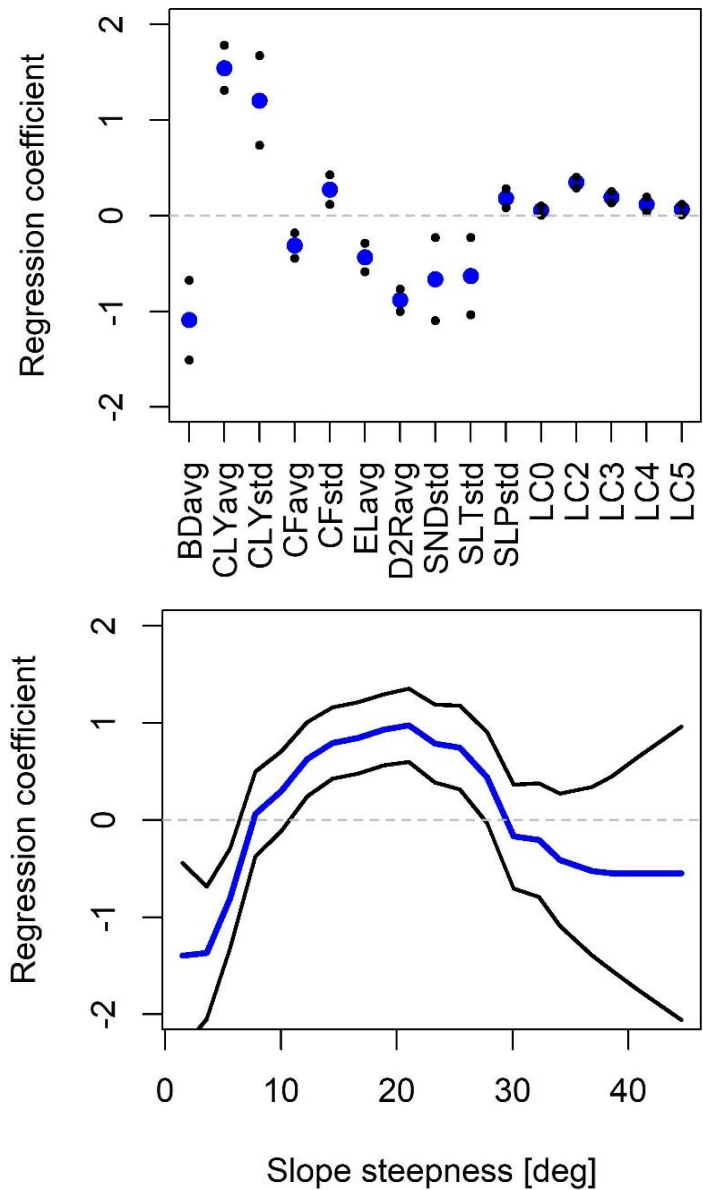


Figure 10: Top: Significant fixed effects (blue dots depict the posterior mean and black dots depict 95% CI); Bottom: Random ordinal effect of slope steepness (blue line highlights the mean and black lines highlight 95% CI)

which ‘agricultural plantation’ influences the susceptibility pattern the most. These agricultural plantations mostly correspond to cardamom, cinnamon, tea and some other herbs and shrubs. Their influence on slope instability may be mostly due to the way local farmers manage the slope. The harvesting cycle for such plants is quite frequent, thus as the plants are removed, the soil surface gets exposed to rainfall discharges and weathering.

As shown in Figure 10, the distribution of slope steepness depicts a clear non-linear trend, behaving as a sigmoidal function. This sigmoid rapidly increases the landslide susceptibility as the mean slope steepness per slope unit increases, up to approximately 22 degrees. After that, there is an inversion that still presents positive regression coefficients until 29 degrees and becomes much more uncertain and negative on average for steepness values up to 45 degrees. This is a typical trend for slope steepness especially when shallow landslides are involved. An important reminder here is that the slope steepness is an aggregation over the whole slope unit, which means that the higher portion of the mapping unit will most likely exhibit an even higher steepness. Therefore, for average steepness values greater than 30 degrees per slope unit, the common source areas for landslides will not have much soil available because, at very high steepness, even common erosional processes would remove the soil cover. Hence, the negative contribution to the susceptibility at high steepness conditions ( $>30^\circ$ ) as well as at very low steepness conditions ( $<8^\circ$ ) coincide with floodplain characteristics.

#### 4.2.2 Predictive performance

The model performance was estimated via a multi-fold cross validation (10-fold) scheme. This operation was executed by splitting the whole dataset into two subsets, one where 90% of the data is contained and used to train our model and the complementary 10% data used for validation. This random partition was repeated ten times, at each time constraining the 10% extraction to not share any slope unit with the others. This in turn produces ten 10% subsets that are mutually exclusive and represent the variability of the whole study area. As presented in Figure 11, each validation was estimated by using ROC (Receiver Operating Characteristics) curves and their area under the curve (AUC) distributions.

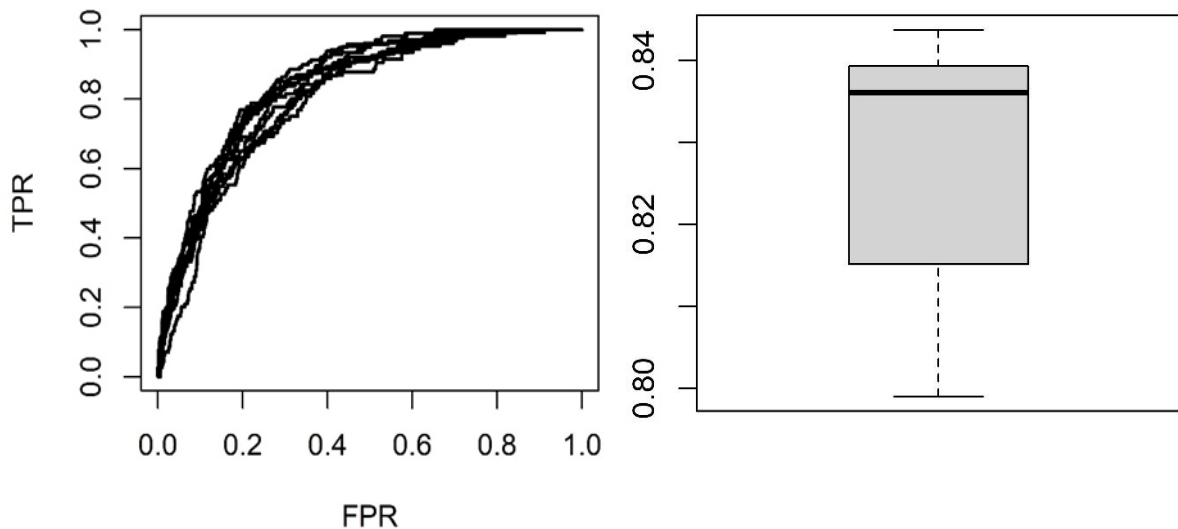


Figure 11: Left: Ten cross validated ROC curves of the reference landslide susceptibility model; Right: Associated AUC distribution

As for the ROC curves, (left) they clearly do not spread, which graphically confirms the very low variability among cross-validated subsets. This is once again depicted in the AUC distribution (right), where the interquartile distance is less than 0.03 and the difference between the maximum and minimum AUC is less than 0.05.

#### 4.2.3 Susceptibility model outputs

The reference landslide susceptibility model was run for the landcover of 2010, the resulting landslide susceptibility and the associated uncertainty are reported in Figure 12. Higher susceptible zones are mostly noticeable in the central sector of Idukki.

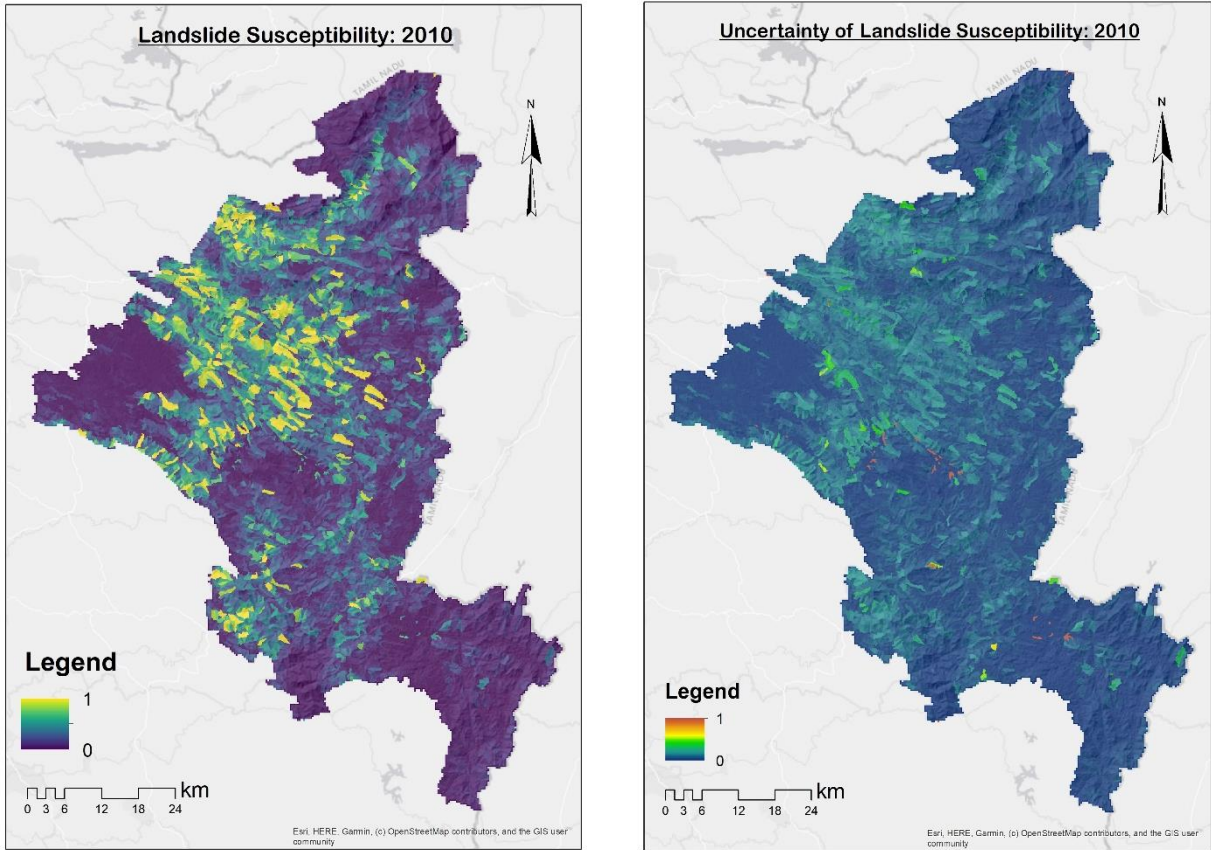


Figure 12: Calculated landslide susceptibility (left panel) and uncertainty (right panel) of year 2010

The subsequent scenario simulations at changing land cover have been run for two situations, one where no landslide mitigations strategies are put into place by local authorities and on a private accord (denoted as 'NL', which stands for No-Landslide mitigation) and the other one where local authorities and land-owners act on unstable slopes (i.e., slope units previously estimated with a probability of landslide occurrence equal or greater than 0.95) by assigning different mitigation strategies (denoted as 'WL', which stands for With-Landslide mitigation). For both the mitigation scenarios, the landslide susceptibility model was ran with a time step of five (5) years, keeping all morphometric covariates the same and varying the land cover distribution in accordance with the respective simulations obtained from the land cover model's output. In other words, for each scenario landslide susceptibility was calculated for eight (8) years: 2015, 2020, 2025, 2030, 2035, 2040, 2045 and 2050.

All the generated landslide susceptibility and uncertainty maps are presented in Figure 28 - Figure 35 and only the final year's (2050) susceptibility and uncertainty maps of both the scenarios are presented in Figure 13. Judging from the low uncertainty values in all the maps, it can be said that the model performance in simulating landslide susceptibility was quite satisfactory. To better visualize the differences between both the scenarios, difference maps for all simulated years were also prepared and presented in Figure 36 & Figure 37. The difference maps were prepared by subtracting the landslide susceptibility simulated for WL scenario from the susceptibility simulated for the NL scenario (No landslide mitigation – With landslide mitigation).

Figure 14 shows this difference for year 2050. There, the clear difference between the two mostly resulted in positive values indicate a larger landslide susceptibility for the NL scenario with respect to WL scenario.

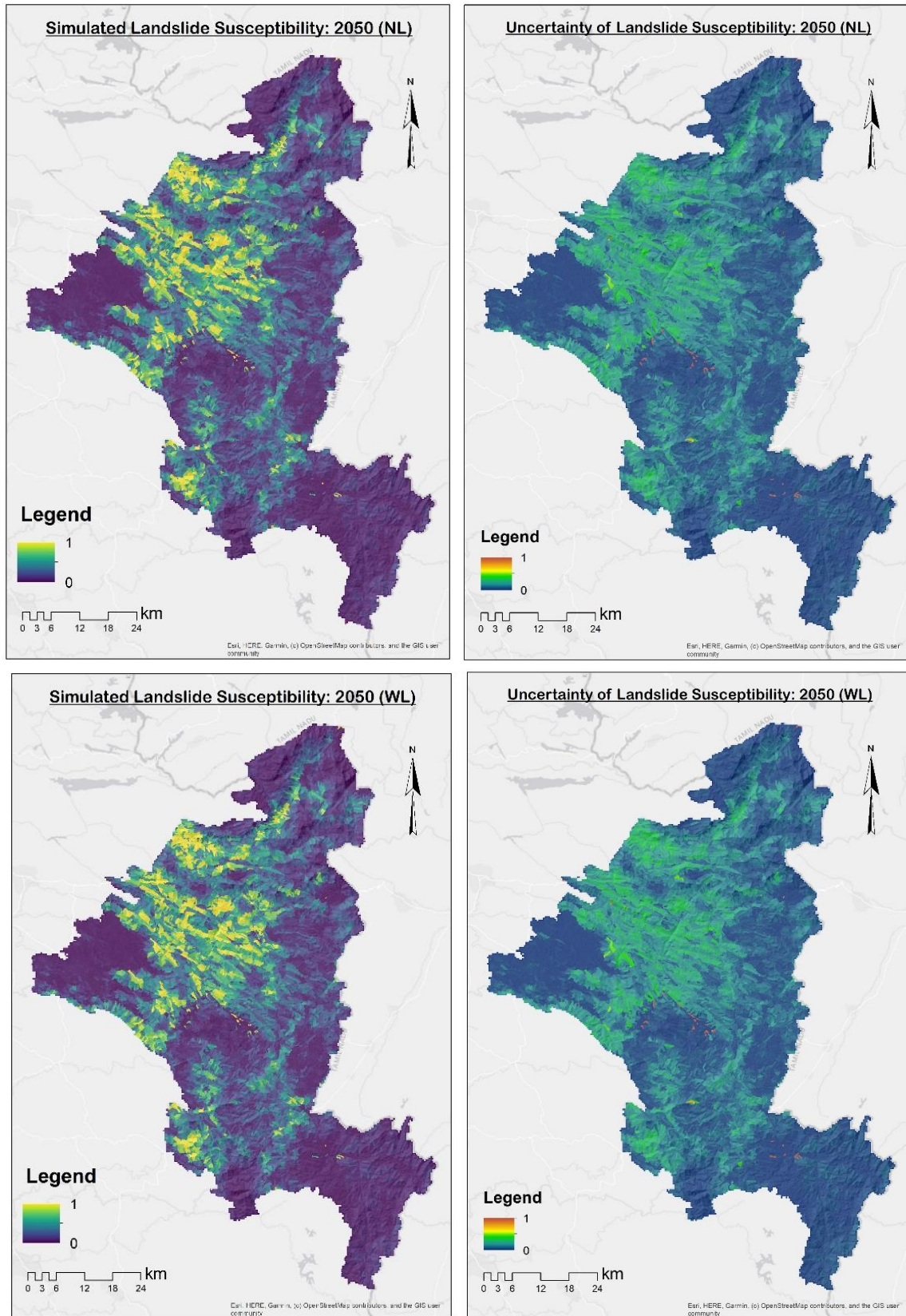


Figure 13: Simulated landslide susceptibility (top and bottom left) and uncertainty (top and bottom right) of 2050; Top panels: NL scenario, Bottom panels: WL scenario

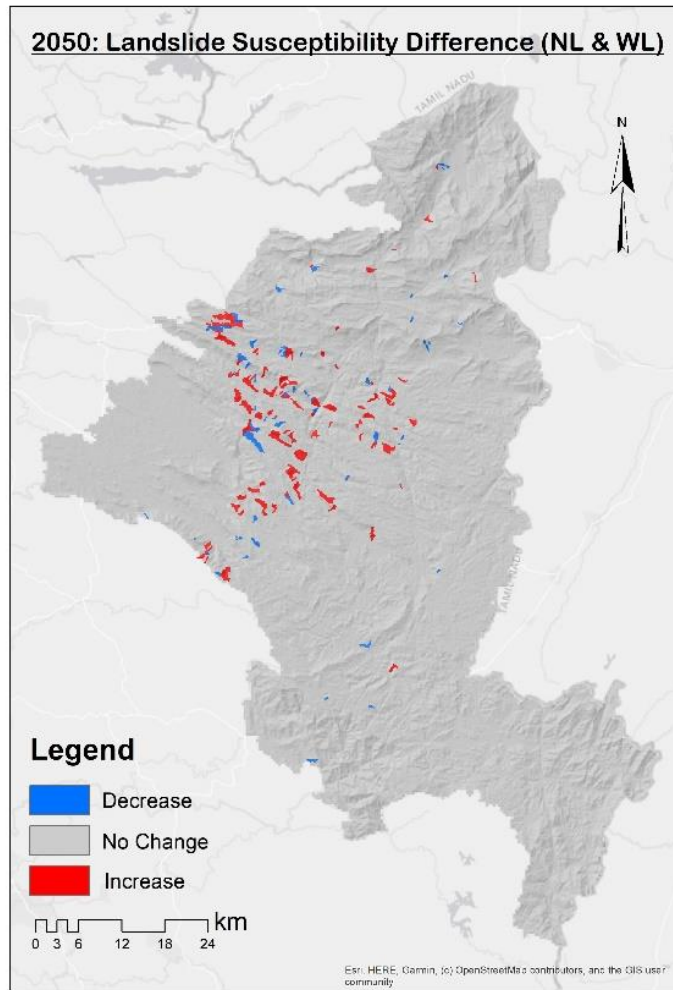


Figure 14: Difference of landslide susceptibility in 2050

This is to be expected, as in scenario NL, no consideration to slope instability mitigation strategies is given whereas in scenario WL the land cover is constrained to include mitigation measures to account for landslide susceptibility (see section 3.1.1).

It is also noticeable from the difference maps of each time step, that in the initial years the differences are quite low and it increases with time, also the differences become more noticeable in the central part of Idukki. Land cover changes being confined to central Idukki as well as their differences being low in the initial years are probably the reasoning behind this.

#### 4.3 Overall discussion

In order to assess the reciprocal influence of landslide susceptibility and land cover, it was crucial for the land cover classes to appear significant in the susceptibility model. Five out of the eight selected land cover classes actually show a mean regression coefficient and a significant posterior distribution. This supports the logic of following this methodological approach. However, it should be noted that the mean regression coefficients are quite small compared to those estimated for other covariates (see Figure 10).

This in turn implies that the susceptibility model is mostly controlled by morphometric characteristics and that the variations in the simulations, as the land cover changes, may be only slightly visible as it actually appeared. This being said, the overall proposed workflow is at least theoretically correct, because despite

the relatively small contribution of land cover, the overall model performance is constantly above the “excellence” AUC threshold.

From the presented landslide susceptibility, land cover and the difference maps, it is apparent that the changes over the years mostly occur around the central part of the study area. The scenario differences of landslide susceptibility maps imply that if land cover changes in the future can be directed in a manner that essentially addresses the landslide susceptible zones (through risk reduction measures e.g. afforestation/reforestation/plantation activities), then the number of landslide susceptible zones becomes less than the scenario where no consideration was given towards landslide susceptibility.

#### **4.4 Novelty in modelling approach**

Investigating the influence of landslide susceptibility and land cover change on each other through a continuous feedback process is a novel modelling approach as per best knowledge. Besides, calculating landslide susceptibility using R-INLA is a relatively new area of research and such an approach have not been adopted to calculate landslide susceptibility in the study area – Idukki or in Kerala. Estimating future land cover change using the DynaCLUE model is also a growing field of research and in the context of the study area this model has not been used to estimate land cover of the future. Overall, the combined approach of predicting future landslide susceptibility based on a separately estimated future land cover scenario using R-INLA and DynaCLUE models is a novel approach. In terms of statistical modelling, the combination of Bayesian (for landslide susceptibility) and Frequentist (for land cover) approach also introduces modelling novelty in the study.

#### **4.5 Uncertainties and limitations of the study**

Other than the associated uncertainties of both the landslide susceptibility and land cover models, an additional degree of uncertainty was also introduced to this study from a number of factors.

Firstly, the two scenarios that we considered in this study were developed mostly based on an “educated-guess” from the knowledge gained from statistics, literature, future development plans and expert opinions. We have used the land cover data of the past and modelled until present and beyond, but the modelled outputs of until present (e.g., until 2021) might be very different from the reality. In scenario-based modelling approaches this is quite common as such approaches do not necessarily thrive to represent reality as it is but create simplified versions of reality through different scenarios. Which not only gives the advantage of incorporating the broad local knowledge and future plans but also aids in extensive analysis (Swetnam et al., 2011).

As all the input datasets were resampled to a certain (100 meter) resolution to maintain uniformity (specially for the land cover model), the upscaling and downscaling of datasets might have caused a loss of some details (Singh & Kumar, 2017). In other words, 100m resolution might be a bit too coarse for modelling fine details, especially because an additional aggregation step is required to express the modelled information at the respective mapping unit for both models.

During the modelling process, the outputs of the landslide susceptibility and land cover model needed to be repeatedly converted to raster from vector and vice versa, for the output of one to be regarded as input of the other. This process might have also introduced a degree of uncertainty and loss of details for the algorithms used by the GIS platform to perform such conversions (Arnone et al., 2016).

To implement WL mitigation strategy, we informed the land cover model of the unstable slopes by using a fixed susceptibility threshold equal to 0.95. This choice is arbitrary and we opted for it as the most conservative one we could come up with. For instance, any slope unit with an estimated susceptibility greater than 0.95 should be very unstable and therefore most likely to undergo a slope failure in the future. However, even slope units with  $0.9 < \text{susceptibility} < 0.95$  could experience slope instability, which we did not account for. So, an additional degree of uncertainty may originate from the probability threshold one may choose.

#### 4.6 Implications of the study

The methodological approach followed in this study provides a novel framework for assessing the interrelationship between future land cover and landslide susceptibility. The outcomes of this study though might not replicate exact reality, they can provide crucial insights of what can be expected in the future in respect to the applied scenario rulesets.

Calibrating the models with high resolution and more recent datasets can significantly improve the model outputs whereas iterating this modelling approach for more scenarios would certainly give greater insight, and therefore, help in efficient decision making. Incorporating predictive meteorological modelling with the framework proposed in this study would also unveil a new area of research and provide outputs that can better resemble reality.

This study can set the basis for numerous fields of scientific research such as vulnerability and risk studies, urban planning, geological studies, agricultural research, forestry, watershed management studies and so on. The local government if not directly make use of the outcomes, can surely use this framework to have a glimpse of the future.

More specifically, this framework can be used to analyze what might happen in the future if certain choices are made in the present and based on that formulate effective policies, enact relevant construction and agricultural legislations, assemble efficient preparedness and mitigation plans and accordingly educate the mass population for ultimate capacity development. This in turn would reduce landslide risk significantly, increase community resilience and redefine sustainable land use while exploiting land cover in a pre-informed and planned manner.

## 5. CONCLUDING REMARKS

The effects of future land cover dynamics on landslide susceptibility do not only possess great research importance but also of extensive importance in terms of legislation and practical applications. In order to meet the overall objective, the methodology followed in this study estimated future land cover until 2050 and using that information predicted future landslide susceptibility. The following paragraphs attempt to address each sub-objectives and the associated research questions with a view to facilitating greater comprehension.

#### **Sub-objective: 1: Building a reference landslide susceptibility model trained with morphometric characteristics and historical land cover data.**

As explained in section 3.5, using the INLA libraries in R, a (Bayesian version of GAMM model) reference landslide model was built based on the land cover data of year 2010. Besides the redefined land cover classes, a number of morphometric covariates were used to train the model. The outputs of the model aid in answering the two associated research questions.

- What are the most relevant covariates in the landslide susceptibility model?

In this study, slope steepness was modelled non-linearly and the rest of the covariates were modelled linearly. Slope steepness thus, having a random effect on the susceptibility showed a sigmoidal behavior depicting a significant increase of landslide susceptibility as the slopes get steeper until about 29°. From thereafter, it shows high uncertainty and a negative influence. Of the fixed effect covariates, clay mean and clay standard deviations showed highest positive significance whereas bulk density mean had a significant negative influence on the landslide susceptibility.

- Do the land cover classes show a considerable influence on landslide susceptibility?

Out of eight land cover classes considered in this study, five classes ('villages', 'agricultural plantation', 'grassland', 'forest' and 'forest plantation') were found to have a significant and positive influence on the landslide susceptibility (see section 4.2.1). Though, 'cropland' was found to have the most effect than the four other land cover classes, in comparison to the morphometric covariates the effect of land cover classes on the landslide susceptibility was quite low (see Figure 10).

**Sub-objective 2: Developing land cover scenarios by analyzing the past land cover change and future development plans.**

For this study we developed two scenarios initially for estimating the future land cover and using that the future landslide susceptibility scenarios. The scenarios denoted as 'NL' and 'WL' represent two situations where no consideration is given to landslide susceptibility and landslide susceptibility is well-accounted for with necessary mitigation strategies in the other (explained in 3.1.1).

- What are the prominent general trends in the past?

Statistics show that Idukki experienced a population decline in the past (Board, 2014) but the settlement showed an increasing trend (Ramachandran & Reddy, 2017). The fact that the settlements often had to be relocated due to landslide occurrences could be the reason behind this. It was also understood that Idukki experienced some losses in terms of 'agricultural plantation'. 'Forests' (also forest plantation) and 'waterbodies' are well protected and did not experience any significant change over the years.

- What could possibly be the expected future trends?

As suggested by future development plans and expert opinions, agricultural plantations are expected to increase as budgets have been allocated within the study area to invest more in this sector. Villages are also likely to increase following the past increasing trend and settlement relocations. Protected areas containing mostly forest plantations and waterbodies are not likely to change other than having some fringe effects.

**Sub-objective 3: Estimating the land cover of the future by learning from the past land cover and landslide susceptibility.**

- How well does the model perform in predicting the determined land cover classes?

According to the logistic regression conducted for the land cover classes individually (other than waterbodies and rocks as they are modelled as 'static'), the predictive performance of the model was tested through AUCs and ROC curves. Cropland and agricultural plantations have the highest AUC value (AUC = 0.855) of all the land cover classes. For the other land cover classes, the model performed also relatively well other than the 'grassland' class. AUCs for 'villages', 'forests' and 'forest plantation' were 0.757, 0.839 and 0.731. Whereas for 'grassland' the model performance was just acceptable/poor (as argued by different researchers) as the AUC was 0.643.

The DynaCLUE model also calculated probability maps for each land cover class, where significant and logical probability distribution across the study area were noticed for different land cover types. The model also performed well in not assigning any probability within the protected areas (more explanation in section 4.1.2).

- Does the landslide susceptibility influence the land cover change in the future?

As modelled in the 'WL' scenario (with landslide susceptibility mitigation scenario) the future land cover was estimated using the calculated landslide susceptibility (of the initial year of each time step) as a location factor. The outcomes suggest that there were some notable differences between the predicted land cover of the two scenarios. Though in the initial years there are little to no differences, the differences become more prominent in the latter years. So, it can be asserted that the landslide susceptibility influenced and characterized the predicted land cover (see section 4.1.3).

**Sub-objective 4: Estimating landslide susceptibility scenarios in the future according to the estimated future land cover scenario.**

- How the landslide susceptibility of the future differs from that of the past in respect to the land cover evolution within Idukki?

As elaborated in section 3.5 and 3.7.2, the land cover component was used as a time variant fixed effect covariate in the calculation of landslide susceptibility. Hence, the susceptibility results are characterized by the estimated land cover scenarios. As portrayed in section 4.2.3, the calculated susceptibilities show significant differences over the years. Though its mostly confined (high susceptible zones) to the central part of the study area, it shows some increases and decreases as per the mapping unit. In other words, over the time span modelled in this study, landslide susceptibility increases and decreases in different locations as a response to the estimated future land cover dynamics.

- Was there any difference in predicted landslide susceptibility if it is accounted for in the future land cover change?

The landslide susceptibility was calculated for two scenarios as mentioned in section 3.1.1. The results suggest that if landslide susceptibility is accounted for through mitigation measures, then the susceptibilities over the years show a declining trend as opposed to the scenario where landslide susceptibility is not accounted for. As portrayed in Figure 14, the susceptibility increases in the NL scenario as compared to the WL scenario for the final year (2050), clarifies that there were more slope units (as a mapping unit) experiencing increased susceptibility than those experiencing a decrease in respect to the estimated future land cover.

It is crucial to mention here that this study was designed based on two different scenarios with specific rulesets. Though, the scenarios were developed mostly based on an 'educated-guess' from expert opinion, statistics and future plans, it tried to reflect reality to a great extent. Hence, the actual reality might have substantial difference with the outcomes of this study.

However, the modelling approach followed in this study and the outcomes can be an important tool for policy formulation, planning and future developments. It also sets the basis for further research in a plethora of scientific fields.

## LIST OF REFERENCES

- Achu, A. L., Aju, C. D., & Reghunath, R. (2020). Spatial modelling of shallow landslide susceptibility: a study from the southern Western Ghats region of Kerala, India. *Annals of GIS*, 26(2), 113–131. <https://doi.org/10.1080/19475683.2020.1758207>
- Ajin, R. S., Loghin, A. M., Vinod, P. G., Jacob, M. K., & Krishnamurthy, R. R. (2014). Landslide susceptible zone mapping using ARS and GIS techniques in selected taluks of Kottayam district, Kerala, India. *International Journal of Applied Remote Sensing and GIS*. <https://www.researchgate.net/publication/308208121>
- Alvioli, M., Marchesini, I., Reichenbach, P., Rossi, M., Ardizzone, F., Fiorucci, F., & Guzzetti, F. (2016). Automatic delineation of geomorphological slope units with *r.slopeunits* v1.0 and their optimization for landslide susceptibility modeling. *Geoscientific Model Development*, 9(11), 3975–3991. <https://doi.org/10.5194/gmd-9-3975-2016>
- Arnone, E., Francipane, A., Scarbaci, A., Puglisi, C., & Noto, L. V. (2016). Effect of raster resolution and polygon-conversion algorithm on landslide susceptibility mapping. *Environmental Modelling and Software*, 84, 467–481. <https://doi.org/10.1016/j.envsoft.2016.07.016>
- Arsanjani, J. J., Helbich, M., Kainz, W., & Boloorani, A. D. (2012). Integration of logistic regression, Markov chain and cellular automata models to simulate urban expansion. *International Journal of Applied Earth Observation and Geoinformation*, 21(1), 265–275. <https://doi.org/10.1016/j.jag.2011.12.014>
- Atkinson, P. M., & Massari, R. (1998). Generalised linear modelling of susceptibility to landsliding in the central Apennines, Italy. *Computers and Geosciences*, 24(4), 373–385. [https://doi.org/10.1016/S0098-3004\(97\)00117-9](https://doi.org/10.1016/S0098-3004(97)00117-9)
- Bakka, H., Rue, H., Fuglstad, G. A., Riebler, A., Bolin, D., Illian, J., Krainski, E., Simpson, D., & Lindgren, F. (2018). Spatial modeling with R-INLA: A review. *Wiley Interdisciplinary Reviews: Computational Statistics*, 10(6), e1443. <https://doi.org/10.1002/wics.1443>
- Barnard, P. L., Owen, L. A., Sharma, M. C., & Finkela, R. C. (2001). Natural and human-induced landsliding in the Garhwal Himalaya of Northern India. *Geomorphology*, 40(1–2), 21–35. [https://doi.org/10.1016/S0169-555X\(01\)00035-6](https://doi.org/10.1016/S0169-555X(01)00035-6)
- Beguieria, S. (2006). Validation and Evaluation of Predictive Models in Hazard Assessment and Risk Management. *Natural Hazards*, 37(3), 315–329. <https://doi.org/10.1007/s11069-005-5182-6>
- Behera, M. D., Tripathi, P., Das, P., Srivastava, S. K., Roy, P. S., Joshi, C., Behera, P. R., Deka, J., Kumar, P., Khan, M. L., Tripathi, O. P., Dash, T., & Krishnamurthy, Y. V. N. (2018). Remote sensing based deforestation analysis in Mahanadi and Brahmaputra river basin in India since 1985. *Journal of Environmental Management*, 206, 1192–1203. <https://doi.org/10.1016/j.jenvman.2017.10.015>
- Behera, N. K., & Behera, M. D. (2020). Predicting land use and land cover scenario in Indian national river basin: the Ganga. *Tropical Ecology*, 61(1), 51–64. <https://doi.org/10.1007/s42965-020-00073-x>
- Bell, E. J. (1974). Markov analysis of land use change—an application of stochastic processes to remotely sensed data. *Socio-Economic Planning Sciences*, 8(6), 311–316. [https://doi.org/10.1016/0038-0121\(74\)90034-2](https://doi.org/10.1016/0038-0121(74)90034-2)
- Board, K. S. P. (2014). *Perspective Plan 2030 - Kerala, Volume III*.
- Brabb, E. E. (1984). *Innovative approaches to landslide hazard and risk mapping*. 1, 17–22.
- Brenning, A. (2008). Statistical geocomputing combining R and SAGA: The example of landslide susceptibility analysis with generalized additive models. *Hamburger Beiträge Zur Physischen Geographie Und Landschaftsökologie*, 19, 23–32. <http://www.academia.edu/download/4945109/Brenning-2008-RSAGA.pdf>

- Bruschi, V. M., Bonachea, J., Remondo, J., Gómez-Arozamena, J., Rivas, V., Barbieri, M., Capocchi, S., Soldati, M., & Cendrero, A. (2013). Land management versus natural factors in land instability: Some examples in northern Spain. *Environmental Management*, 52(2), 398–416. <https://doi.org/10.1007/s00267-013-0108-7>
- Cai, Y., Liu, Y., Yu, Z., & Verburg, P. H. (2004). Progress in spatial simulation of land use change-CLUE-s model and its application. *Progress in Geography*, 23(4), 63–71. [http://en.cnki.com.cn/Article\\_en/CJFDTotol-DLKJ200404007.htm](http://en.cnki.com.cn/Article_en/CJFDTotol-DLKJ200404007.htm)
- Camilo, D. C., Lombardo, L., Mai, P. M., Dou, J., & Huser, R. (2017). Handling high predictor dimensionality in slope-unit-based landslide susceptibility models through LASSO-penalized Generalized Linear Model. *Environmental Modelling and Software*, 97, 145–156. <https://doi.org/10.1016/j.envsoft.2017.08.003>
- Carrara, A., Cardinali, M., Detti, R., Guzzetti, F., Pasqui, V., & Reichenbach, P. (1991). GIS techniques and statistical models in evaluating landslide hazard. *Earth Surface Processes and Landforms*, 16(5), 427–445. <https://doi.org/10.1002/esp.3290160505>
- Carro, M., De Amicis, M., Luzi, L., & Marzorati, S. (2003). The application of predictive modeling techniques to landslides induced by earthquakes: The case study of the 26 September 1997 Umbria-Mache earthquake (Italy). *Engineering Geology*, 69(1–2), 139–159. [https://doi.org/10.1016/S0013-7952\(02\)00277-6](https://doi.org/10.1016/S0013-7952(02)00277-6)
- Castella, J. C., & Verburg, P. H. (2007). Combination of process-oriented and pattern-oriented models of land-use change in a mountain area of Vietnam. *Ecological Modelling*, 202(3–4), 410–420. <https://doi.org/10.1016/j.ecolmodel.2006.11.011>
- Cendrero, A., & Dramis, F. (1996). The contribution of landslides to landscape evolution in Europe. *Geomorphology*, 15(3-4 SPEC. ISS.), 191–211. [https://doi.org/10.1016/0169-555x\(95\)00070-1](https://doi.org/10.1016/0169-555x(95)00070-1)
- Chen, C. Y., & Huang, W. L. (2013). Land use change and landslide characteristics analysis for community-based disaster mitigation. *Environmental Monitoring and Assessment*, 185(5), 4125–4139. <https://doi.org/10.1007/s10661-012-2855-y>
- Chung, C.-J. F., & Fabbri, A. G. (2005). Systematic Procedures of Landslide Hazard Mapping for Risk Assessment Using Spatial Prediction Models. In *Landslide Hazard and Risk* (pp. 139–174). John Wiley & Sons, Ltd. <https://doi.org/10.1002/9780470012659.ch4>
- Chung, C. J. F., & Fabbri, A. G. (2003). Validation of spatial prediction models for landslide hazard mapping. *Natural Hazards*, 30(3), 451–472. <https://doi.org/10.1023/B:NHAZ.0000007172.62651.2b>
- Chung, C. J., & Fabbri, A. G. (2008). Predicting landslides for risk analysis - Spatial models tested by a cross-validation technique. *Geomorphology*, 94(3–4), 438–452. <https://doi.org/10.1016/j.geomorph.2006.12.036>
- Clark, W. A. V. (1965). Markov chain analysis in geography: An application to the movement of rental housing areas. *Annals of the Association of American Geographers*, 55(2), 351–359. <https://doi.org/10.1111/j.1467-8306.1965.tb00523.x>
- Contreras-Hermosilla, A. (2000). The underlying causes of forest decline. *CIFOR OCCAS Pap.30*. <http://dlc.dlib.indiana.edu/dlc/handle/10535/3875>
- Corner, R. J., Dewan, A. M., & Chakma, S. (2014). Monitoring and prediction of land-use and land-cover (LULC) change. In *Dhaka Megacity: Geospatial Perspectives on Urbanisation, Environment and Health* (pp. 75–97). Springer Netherlands. [https://doi.org/10.1007/978-94-007-6735-5\\_5](https://doi.org/10.1007/978-94-007-6735-5_5)
- Cruden, D. M. (1991). A simple definition of a landslide. *Bulletin of the International Association of Engineering Geology - Bulletin de l'Association Internationale de Géologie de l'Ingénieur*, 43(1), 27–29. <https://doi.org/10.1007/BF02590167>

- Cruden, D. M., & Varnes, D. J. (1996). LANDSLIDE TYPES AND PROCESSES. *LANDSLIDES: INVESTIGATION AND MITIGATION*. National Research Council, Transportation Research Board, Special Report 247, Chapter 3. <https://trid.trb.org/view/462501>
- Dai, E., Wu, S., Shi, W., Cheung, C. K., & Shaker, A. (2005). Modeling Change-Pattern-Value dynamics on land use: An integrated GIS and Artificial Neural Networks approach. *Environmental Management*, 36(4), 576–591. <https://doi.org/10.1007/s00267-004-0165-z>
- Dams, J., Woldeamlak, S. T., & Batelaan, O. (2008). Predicting land-use change and its impact on the groundwater system of the Kleine Nete catchment, Belgium. *Hydrological Earth System Science*, 12, 1369–1385. <http://dspace.flinders.edu.au/dspace/www.hydrol-earth-syst-sci.net/12/1369/2008/>
- Das, P., Behera, M. D., Pal, S., Chowdary, V. M., Behera, P. R., & Singh, T. P. (2019). Studying land use dynamics using decadal satellite images and Dyna-CLUE model in the Mahanadi River basin, India. *Environmental Monitoring and Assessment*, 191(3), 1–17. <https://doi.org/10.1007/s10661-019-7698-3>
- Ercanoglu, M., & Gokceoglu, C. (2002). Assessment of landslide susceptibility for a landslide-prone area (north of Yenice, NW Turkey) by fuzzy approach. *Environmental Geology*, 41(6), 720–730. <https://doi.org/10.1007/s00254-001-0454-2>
- Erener, A., & Düzgün, H. S. B. (2012). Landslide susceptibility assessment: What are the effects of mapping unit and mapping method? *Environmental Earth Sciences*, 66(3), 859–877. <https://doi.org/10.1007/s12665-011-1297-0>
- Fernando, J. (2021). *Compound Annual Growth Rate (CAGR) Definition*. <https://www.investopedia.com/terms/c/cagr.asp>
- Fick, S. E., & Hijmans, R. J. (2017). WorldClim 2: new 1-km spatial resolution climate surfaces for global land areas. *International Journal of Climatology*, 37(12), 4302–4315. <https://doi.org/10.1002/joc.5086>
- Geist, H. J., & Lambin, E. F. (2002). Proximate causes and underlying driving forces of tropical deforestation. *BioScience*, 52(2), 143–150. [https://doi.org/10.1641/0006-3568\(2002\)052\[0143:PCAUDF\]2.0.CO;2](https://doi.org/10.1641/0006-3568(2002)052[0143:PCAUDF]2.0.CO;2)
- George, P. S. ., & Chattopadhyay, S. (2001). Population and land use in Kerala. *Growing Populations, Changing Landscapes: Studies from India, China and the United States*, 79–106.
- Ghosh, P., Mukhopadhyay, A., Chanda, A., Mondal, P., Akhand, A., Mukherjee, S., Nayak, S. K., Ghosh, S., Mitra, D., Ghosh, T., & Hazra, S. (2017). Application of Cellular automata and Markov-chain model in geospatial environmental modeling- A review. *Remote Sensing Applications: Society and Environment*, 5, 64–77. <https://doi.org/10.1016/j.rsase.2017.01.005>
- Ghosh, S., & Shetty, A. (2017). Modelling the land use system process for a pre-industrial landscape in India. *Modeling Earth Systems and Environment*, 3(2), 703–717. <https://doi.org/10.1007/s40808-017-0329-5>
- Glade, T. (2003). Landslide occurrence as a response to land use change: A review of evidence from New Zealand. *Catena*, 51(3–4), 297–314. [https://doi.org/10.1016/S0341-8162\(02\)00170-4](https://doi.org/10.1016/S0341-8162(02)00170-4)
- Goff, J. R. (1997). A chronology of natural and anthropogenic influences on coastal sedimentation, New Zealand. *Marine Geology*, 138(1–2), 105–117. [https://doi.org/10.1016/S0025-3227\(97\)00018-2](https://doi.org/10.1016/S0025-3227(97)00018-2)
- GOFF, J. R., & HICOCK, S. R. (1995). Origin of Downstream Variation in Clast Size in a Small, Mountain Catchment, British Columbia. *Geographical Review of Japan, Series B.*, 68(2), 209–217. <https://doi.org/10.4157/grj1984b.68.209>
- Gokceoglu, C., Sonmez, H., & Ercanoglu, M. (2000). Discontinuity controlled probabilistic slope failure risk maps of the Altındag (settlement) region in Turkey. *Engineering Geology*, 55(4), 277–296. [https://doi.org/10.1016/S0013-7952\(99\)00083-6](https://doi.org/10.1016/S0013-7952(99)00083-6)
- González Díez, A., Salas, L., Díaz De Terán, J. R., & Cendrero, A. (1996). Late quaternary climate changes and mass movement frequency and magnitude in the Cantabrian region, Spain. *Geomorphology*, 15(3–4)

- SPEC. ISS.), 291–309. [https://doi.org/10.1016/0169-555x\(95\)00076-h](https://doi.org/10.1016/0169-555x(95)00076-h)
- Guan, D. J., Li, H. F., Inohae, T., Su, W., Nagaie, T., & Hokao, K. (2011). Modeling urban land use change by the integration of cellular automaton and Markov model. *Ecological Modelling*, 222(20–22), 3761–3772. <https://doi.org/10.1016/j.ecolmodel.2011.09.009>
- Halmy, M. W. A., Gessler, P. E., Hicke, J. A., & Salem, B. B. (2015). Land use/land cover change detection and prediction in the north-western coastal desert of Egypt using Markov-CA. *Applied Geography*, 63, 101–112. <https://doi.org/10.1016/j.apgeog.2015.06.015>
- Han, H., Yang, C., & Song, J. (2015). Scenario Simulation and the Prediction of Land Use and Land Cover Change in Beijing, China. *Sustainability*, 7(4), 4260–4279. <https://doi.org/10.3390/su7044260>
- Hao, L., van Westen, C., Martha, T. R., Jaiswal, P., & McAdoo, B. G. (2020). Constructing a complete landslide inventory dataset for the 2018 monsoon disaster in Kerala, India, for land use change analysis. *Earth System Science Data*, 12(4), 2899–2918. <https://doi.org/10.5194/essd-12-2899-2020>
- Hengl, T., Mendes de Jesus, J., Heuvelink, G. B. M., Ruiperez Gonzalez, M., Kilibarda, M., Blagotić, A., Shangguan, W., Wright, M. N., Geng, X., Bauer-Marschallinger, B., Guevara, M. A., Vargas, R., MacMillan, R. A., Batjes, N. H., Leenaars, J. G. B., Ribeiro, E., Wheeler, I., Mantel, S., & Kempen, B. (2017). SoilGrids250m: Global gridded soil information based on machine learning. *PLOS ONE*, 12(2), e0169748. <https://doi.org/10.1371/journal.pone.0169748>
- Hyandye, C., & Martz, L. W. (2017). A Markovian and cellular automata land-use change predictive model of the Usangu Catchment. *International Journal of Remote Sensing*, 38(1), 64–81. <https://doi.org/10.1080/01431161.2016.1259675>
- IBM. (2019). *IBM SPSS Statistics for Windows* (26.0).
- Jha, C. S. ., Dutt, C. B. S. ., & Bawa, K. S. (2000). Deforestation and land use changes in Western Ghats, India on JSTOR. *Current Science*, 79(2), 231–238. [https://www.jstor.org/stable/24103455?seq=1#metadata\\_info\\_tab\\_contents](https://www.jstor.org/stable/24103455?seq=1#metadata_info_tab_contents)
- Jia, X., Khandelwal, A., Nayak, G., Gerber, J., Carlson, K., West, P., & Kumar, V. (2017). Incremental dual-memory LSTM in land cover prediction. *Proceedings of the 23rd ACM SIGKDD International Conference on Knowledge Discovery and Data Mining, Part F129685*, 867–876. <https://doi.org/10.1145/3097983.3098112>
- Jibson, R. W., Harp, E. L., & Michael, J. A. (2000). A method for producing digital probabilistic seismic landslide hazard maps. *Engineering Geology*, 58(3–4), 271–289. [https://doi.org/10.1016/S0013-7952\(00\)00039-9](https://doi.org/10.1016/S0013-7952(00)00039-9)
- Juang, C. H., Jhi, Y. Y., & Lee, D. H. (1998). Stability analysis of existing slopes considering uncertainty. *Engineering Geology*, 49(2), 111–122. [https://doi.org/10.1016/S0013-7952\(97\)00078-1](https://doi.org/10.1016/S0013-7952(97)00078-1)
- Kalaranjini, V. S., & Ramakrishnan, S. S. (2020). Landslide investigation using SAR Interferometry on selected regions of Idukki district, Kerala, India. *Indian Journal of Geo Marine Sciences*, 49 (05), 882–888. <http://nopr.niscair.res.in/handle/123456789/54719>
- Karimi, H., Jafarnezhad, J., Khaledi, J., & Ahmadi, P. (2018). Monitoring and prediction of land use/land cover changes using CA-Markov model: a case study of Ravansar County in Iran. *Arabian Journal of Geosciences*, 11(19), 1–9. <https://doi.org/10.1007/s12517-018-3940-5>
- Karsli, F., Atasoy, M., Yalcin, A., Reis, S., Demir, O., & Gokceoglu, C. (2009). Effects of land-use changes on landslides in a landslide-prone area (Ardesen, Rize, NE Turkey). *Environmental Monitoring and Assessment*, 156(1–4), 241–255. <https://doi.org/10.1007/s10661-008-0481-5>
- KSDMA. (2018). *Landslides 2018*. <https://sdma.kerala.gov.in/landslides-2018/>
- KSDMA. (2019). *Landslides 2019*. <https://sdma.kerala.gov.in/landslides-2019/>

- Kucsicsa, G., Popovici, E. A., Bălteanu, D., Grigorescu, I., Dumitraşcu, M., & Mitrică, B. (2019). Future land use/cover changes in Romania: regional simulations based on CLUE-S model and CORINE land cover database. *Landscape and Ecological Engineering*, 15(1), 75–90. <https://link.springer.com/content/pdf/10.1007/s11355-018-0362-1.pdf>
- Kuriakose, S. L. (2010). *Physically-based dynamic modelling of the effects of land use changes on shallow landslide initiation in the Western Ghats, Kerala, India*. s.n.].
- Lambin, E. F., Geist, H. J., & Lepers, E. (2003). Dynamics of Land-Use and Land-Cover Change in Tropical Regions. *Annual Review of Environment and Resources*, 28(1), 205–241. <https://doi.org/10.1146/annurev.energy.28.050302.105459>
- Lee, C. T., Huang, C.-C., Lee, J.-F., Pan, K.-L., Lin, M.-L., & Dong, J.-J. (2008). Statistical approach to storm event-induced landslides susceptibility. *Natural Hazards and Earth System Sciences*, 8(4), 941–960. <https://doi.org/10.5194/nhess-8-941-2008>
- Lee, S., Ryu, J. H., Min, K., & Won, J. S. (2003). Landslide susceptibility analysis using GIS and artificial neural network. *Earth Surface Processes and Landforms*, 28(12), 1361–1376. <https://doi.org/10.1002/esp.593>
- Lee, S., Ryu, J. H., Won, J. S., & Park, H. J. (2004). Determination and application of the weights for landslide susceptibility mapping using an artificial neural network. *Engineering Geology*, 71(3–4), 289–302. [https://doi.org/10.1016/S0013-7952\(03\)00142-X](https://doi.org/10.1016/S0013-7952(03)00142-X)
- Lee, S., & Talib, J. A. (2005). Probabilistic landslide susceptibility and factor effect analysis. *Environmental Geology*, 47(7), 982–990. <https://doi.org/10.1007/s00254-005-1228-z>
- Lima, M. L., Romanelli, A., & Massone, H. E. (2015). Assessing groundwater pollution hazard changes under different socio-economic and environmental scenarios in an agricultural watershed. *Science of the Total Environment*, 530–531, 333–346. <https://doi.org/10.1016/j.scitotenv.2015.05.026>
- Lindgren, F., & Rue, H. (2008). On the second-order random walk model for irregular locations. *Scandinavian Journal of Statistics*, 35(4), 691–700. <https://doi.org/10.1111/j.1467-9469.2008.00610.x>
- Lombardo, L., Cama, M., Maerker, M., & Rotigliano, E. (2014). A test of transferability for landslides susceptibility models under extreme climatic events: Application to the Messina 2009 disaster. *Natural Hazards*, 74(3), 1951–1989. <https://doi.org/10.1007/s11069-014-1285-2>
- Lombardo, Luigi, Opitz, T., & Huser, R. (2018). Point process-based modeling of multiple debris flow landslides using INLA: an application to the 2009 Messina disaster. *Stochastic Environmental Research and Risk Assessment*, 32(7), 2179–2198. <https://doi.org/10.1007/s00477-018-1518-0>
- Lombardo, Luigi, Opitz, T., & Huser, R. (2019). Numerical Recipes for Landslide Spatial Prediction Using R-INLA. In *Spatial Modeling in GIS and R for Earth and Environmental Sciences* (pp. 55–83). Elsevier. <https://doi.org/10.1016/b978-0-12-815226-3.00003-x>
- Lombardo, Luigi, Saia, S., Schillaci, C., Mai, P. M., & Huser, R. (2018). Modeling soil organic carbon with Quantile Regression: Dissecting predictors' effects on carbon stocks. *Geoderma*, 318, 148–159. <https://doi.org/10.1016/j.geoderma.2017.12.011>
- Lombardo, Luigi, & Tanyas, H. (2020). Chrono-validation of near-real-time landslide susceptibility models via plug-in statistical simulations. *Engineering Geology*, 278, 1–15. <https://doi.org/10.1016/j.enggeo.2020.105818>
- Lombardo, Luigi, & Tanyas, H. (2021). From scenario-based seismic hazard to scenario-based landslide hazard: fast-forwarding to the future via statistical simulations. *Stochastic Environmental Research and Risk Assessment*, 1–14. <https://doi.org/10.1007/s00477-021-02020-1>
- Lombardo, Luigi, Tanyas, H., & Nicu, I. C. (2020). Spatial modeling of multi-hazard threat to cultural heritage sites. *Engineering Geology*, 277, 105776. <https://doi.org/10.1016/j.enggeo.2020.105776>

- Luo, G., Yin, C., Chen, X., Xu, W., & Lu, L. (2010). Combining system dynamic model and CLUE-S model to improve land use scenario analyses at regional scale: A case study of Sangong watershed in Xinjiang, China. *Ecological Complexity*, 7(2), 198–207. <https://doi.org/10.1016/j.ecocom.2010.02.001>
- Luo, L., Lombardo, L., van Westen, C., Pei, X., & Huang, R. (2020). *From scenario-based seismic hazard to scenario-based landslide hazard: rewinding to the past via statistical simulations*. <http://arxiv.org/abs/2004.00539>
- Luzi, L., Pergalani, F., & Terlien, M. T. J. (2000). Slope vulnerability to earthquakes at subregional scale, using probabilistic techniques and geographic information systems. *Engineering Geology*, 58(3–4), 313–336. [https://doi.org/10.1016/S0013-7952\(00\)00041-7](https://doi.org/10.1016/S0013-7952(00)00041-7)
- Lv, Q., Liu, Y., & Yang, Q. (2017). Stability analysis of earthquake-induced rock slope based on back analysis of shear strength parameters of rock mass. *Engineering Geology*, 228, 39–49. <https://doi.org/10.1016/j.enggeo.2017.07.007>
- Mandrekar, J. N. (2010). Receiver operating characteristic curve in diagnostic test assessment. *Journal of Thoracic Oncology*, 5(9), 1315–1316. <https://doi.org/10.1097/JTO.0b013e3181ec173d>
- Martins, T. G., Simpson, D., Lindgren, F., & Rue, H. (2013). Bayesian computing with INLA: New features. *Computational Statistics and Data Analysis*, 67, 68–83. <https://doi.org/10.1016/j.csda.2013.04.014>
- Marutani, T., Kasai, M., Ebisu, N., & Trustrum, N. (2000). Sediment Generation from Numerous Shallow Landslides Related with Clear Cutting at Granite Mountain, Mt. Ichifusa, Japan. *Internationales Symposium INTERPRAEVENT*, 271–279.
- Marutani, Tomomi, Kasai, M., Reid, L. M., & Trustrum, N. A. (1999). Influence of storm-related sediment storage on the sediment delivery from tributary catchments in the Upper Waipaoa River, New Zealand. *Earth Surface Processes and Landforms*, 24(10), 881–896. [https://doi.org/10.1002/\(SICI\)1096-9837\(199909\)24:10<881::AID-ESP17>3.0.CO;2-I](https://doi.org/10.1002/(SICI)1096-9837(199909)24:10<881::AID-ESP17>3.0.CO;2-I)
- Matthews, J. (1997). Rapid mass movement as a source of climatic evidence for the Holocene. *Palaöklimateforschung Paleoclimate Research. Gustav Fischer Verlag, Stuttgart*, 19, 444.
- Matthews, R. B., Gilbert, N. G., Roach, A., Polhill, J. G., & Gotts, N. M. (2007). Agent-based land-use models: A review of applications. *Landscape Ecology*, 22(10), 1447–1459. <https://doi.org/10.1007/s10980-007-9135-1>
- Meusburger, K., & Alewell, C. (2008). Impacts of anthropogenic and environmental factors on the occurrence of shallow landslides in an alpine catchment (Urseren Valley, Switzerland). *Natural Hazards and Earth System Science*, 8(3), 509–520. <https://doi.org/10.5194/nhess-8-509-2008>
- Mohmand, A., Aljoufi, M., Flacke, J., Brussels, M., Karimi, M., & Ali, A. (2011). Developing a cellular automata land use model for Jeddah City, Kingdom of Saudi Arabia. *Proceedings of GTC*. <https://pdfs.semanticscholar.org/a072/2a6e4ae516bcd86296c76a2d8558feedaef.pdf>
- NASA/METI/AIST/Japan Spacesystems and U.S./Japan ASTER Science Team. (2019). ASTER DEM. *ASTER Global Digital Elevation Model V003, ASTGTM*(NASA EOSDIS Land Processes DAC). <https://doi.org/DOI:10.5067/ASTER/ASTGTM.003>
- Nefeslioglu, H. A., Gokceoglu, C., & Sonmez, H. (2008). An assessment on the use of logistic regression and artificial neural networks with different sampling strategies for the preparation of landslide susceptibility maps. *Engineering Geology*, 97(3–4), 171–191. <https://doi.org/10.1016/j.enggeo.2008.01.004>
- Oh, Y. G., Choi, J. Y., Bae, S. J., Yoo, S. H., & Lee, S. H. (2010). A probability mapping for land cover change prediction using CLUE model. *Journal of Korean Society of Rural Planning*, 16(2), 47–55. <https://www.koreascience.or.kr/article/JAKO201030159716186.page>
- Oh, Y. G., Choi, J. Y., Yoo, S. H., & Lee, S. H. (2011). Prediction of Land-cover Change Based on Climate Change Scenarios and Regional Characteristics using Cluster Analysis. *Journal of The Korean Society of*

- Agricultural Engineers*, 53(6), 31–41. <https://doi.org/10.5389/ksae.2011.53.6.031>
- Ohlmacher, G. C., & Davis, J. C. (2003). Using multiple logistic regression and GIS technology to predict landslide hazard in northeast Kansas, USA. *Engineering Geology*, 69(3–4), 331–343. [https://doi.org/10.1016/S0013-7952\(03\)00069-3](https://doi.org/10.1016/S0013-7952(03)00069-3)
- Ojima, D. S., Galvin, K. A., & Turner, B. L. I. I. (1994). The global impact of land-use change. *BioScience*, 44(5), 300–304. <https://doi.org/10.2307/1312379>
- Page, M. J., Trustrum, N. A., & DeRose, R. C. (1994). A high resolution record of storm-induced erosion from lake sediments, New Zealand. *Journal of Paleolimnology*, 11(3), 333–348. <https://doi.org/10.1007/BF00677993>
- Parise, M., & Jibson, R. W. (2000). A seismic landslide susceptibility rating of geologic units based on analysis of characteristics of landslides triggered by the 17 January, 1994 Northridge, California earthquake. *Engineering Geology*, 58(3–4), 251–270. [https://doi.org/10.1016/S0013-7952\(00\)00038-7](https://doi.org/10.1016/S0013-7952(00)00038-7)
- Pistocchi, A., Luzi, L., & Napolitano, P. (2002). The use of predictive modeling techniques for optimal exploitation of spatial databases: a case study in landslide hazard mapping with expert system-like methods. *Environmental Geology*, 41(7), 765–775. <https://www.researchgate.net/publication/259822769>
- Pourghasemi, H. R., & Rossi, M. (2017). Landslide susceptibility modeling in a landslide prone area in Mazandarn Province, north of Iran: a comparison between GLM, GAM, MARS, and M-AHP methods. *Theoretical and Applied Climatology*, 130(1–2), 609–633. <https://doi.org/10.1007/s00704-016-1919-2>
- Promper, C., Puissant, A., Malet, J. P., & Glade, T. (2014). Analysis of land cover changes in the past and the future as contribution to landslide risk scenarios. *Applied Geography*, 53, 11–19. <https://doi.org/10.1016/j.apgeog.2014.05.020>
- Rahman, M. T. U., Tabassum, F., Rasheduzzaman, M., Saba, H., Sarkar, L., Ferdous, J., Uddin, S. Z., & Zahedul Islam, A. Z. M. (2017). Temporal dynamics of land use/land cover change and its prediction using CA-ANN model for southwestern coastal Bangladesh. *Environmental Monitoring and Assessment*, 189(11), 1–18. <https://doi.org/10.1007/s10661-017-6272-0>
- Raju, K., & Anil Kumar, R. (2006). Land use changes in Udumbanchola Taluk, Idukki District - Kerala: An analysis with the application of remote sensing data. *Journal of the Indian Society of Remote Sensing*, 34(2), 161–169. <https://doi.org/10.1007/BF02991821>
- Ramachandran, R. M., & Reddy, C. S. (2017). Monitoring of deforestation and land use changes (1925–2012) in Idukki district, Kerala, India using remote sensing and GIS. *Journal of the Indian Society of Remote Sensing*, 45(1), 163–170. <https://doi.org/10.1007/s12524-015-0521-x>
- Rao, P. J. (1989). General Report on Landslides. *Symposium on Preparedness, Mitigation and Management of Natural Disaster*, 2.
- Refice, A., & Capolongo, D. (2002). Probabilistic modeling of uncertainties in earthquake-induced landslide hazard assessment. *Computers and Geosciences*, 28(6), 735–749. [https://doi.org/10.1016/S0098-3004\(01\)00104-2](https://doi.org/10.1016/S0098-3004(01)00104-2)
- Reichenbach, P., Busca, C., Mondini, A. C., & Rossi, M. (2014). The Influence of Land Use Change on Landslide Susceptibility Zonation: The Briga Catchment Test Site (Messina, Italy). *Environmental Management*, 54(6), 1372–1384. <https://doi.org/10.1007/s00267-014-0357-0>
- Reichenbach, Paola, Rossi, M., Malamud, B. D., Mihir, M., & Guzzetti, F. (2018). A review of statistically-based landslide susceptibility models. *Earth-Science Reviews*, 180, 60–91. <https://doi.org/10.1016/j.earscirev.2018.03.001>
- Restrepo, C., & Alvarez, N. (2006). Landslides and Their Contribution to Land-cover Change in the

- Mountains of Mexico and Central America<sup>1</sup>. *Biotropica*, 38(4), 446–457. <https://doi.org/10.1111/j.1744-7429.2006.00178.x>
- Rindfuss, R. R., Walsh, S. J., Turner, B. L., Fox, J., & Mishra, V. (2004). Developing a science of land change: Challenges and methodological issues. *Proceedings of the National Academy of Sciences of the United States of America*, 101(39), 13976–13981. <https://doi.org/10.1073/pnas.0401545101>
- Romeo, R. (2000). Seismically induced landslide displacements: A predictive model. *Engineering Geology*, 58(3–4), 337–351. [https://doi.org/10.1016/S0013-7952\(00\)00042-9](https://doi.org/10.1016/S0013-7952(00)00042-9)
- Rue, H., Riebler, A., Sørbye, S. H., Illian, J. B., Simpson, D. P., & Lindgren, F. K. (2017). Bayesian computing with INLA: A review. *Annual Review of Statistics and Its Application*, 4, 395–421. <https://doi.org/10.1146/annurev-statistics-060116-054045>
- Sahoo, S., Dhar, A., Debsarkar, A., & Kar, A. (2018). Impact of water demand on hydrological regime under climate and LULC change scenarios. *Environmental Earth Sciences*, 77(9), 341. <https://doi.org/10.1007/s12665-018-7531-2>
- Sahoo, S., Dhar, A., Debsarkar, A., & Kar, A. (2019). Future Scenarios of Environmental Vulnerability Mapping Using Grey Analytic Hierarchy Process. *Natural Resources Research*, 28(4), 1461–1483. <https://doi.org/10.1007/s11053-019-09462-z>
- Sahoo, S., Sil, I., Dhar, A., Debsarkar, A., Das, P., & Kar, A. (2018). Future scenarios of land-use suitability modeling for agricultural sustainability in a river basin. *Journal of Cleaner Production*, 205, 313–328. <https://doi.org/10.1016/j.jclepro.2018.09.099>
- Sajinkumar, K. S., Anbazhagan, S., Pradeepkumar, A. P., & Rani, V. R. (2011). Weathering and landslide occurrences in parts of Western Ghats, Kerala. *Journal of the Geological Society of India*, 78(3), 249–257. <https://doi.org/10.1007/s12594-011-0089-1>
- Shen, T. Y., Wang, W. D., Hou, M., Guo, Z. C., Xue, L., & Yang, K. Z. (2007). Study on spatio-temporal system dynamic models of urban growth. *Xitong Gongcheng Lilun Yu Shijian/System Engineering Theory and Practice*, 27(1), 10–17. [https://doi.org/10.1016/s1874-8651\(08\)60002-2](https://doi.org/10.1016/s1874-8651(08)60002-2)
- Shou, K. J., & Wang, C. F. (2003). Analysis of the Chiufengershan landslide triggered by the 1999 Chi-Chi earthquake in Taiwan. *Engineering Geology*, 68(3–4), 237–250. [https://doi.org/10.1016/S0013-7952\(02\)00230-2](https://doi.org/10.1016/S0013-7952(02)00230-2)
- Shu, H., Hürlimann, M., Molowny-Horas, R., González, M., Pinyol, J., Abancó, C., & Ma, J. (2019). Relation between land cover and landslide susceptibility in Val d’Aran, Pyrenees (Spain): Historical aspects, present situation and forward prediction. *Science of the Total Environment*, 693, 133557. <https://doi.org/10.1016/j.scitotenv.2019.07.363>
- Sidle, R., Pearce, A., & O’Laughlin, C. (1985). Hillslope Stability and Land Use: American Geophysical Union Water Resources Monograph 11. *AGU Publications, National Transportation Research*.
- Singh, G., & Kumar, E. (2017). Input data scale impacts on modeling output results: A review. *Journal of Spatial Hydrology*, 13(1). [https://www.researchgate.net/profile/Gurdeep\\_Singh22/publication/321759023\\_Input\\_data\\_scale\\_impacts\\_on\\_modeling\\_output\\_results\\_A\\_review/links/5a30b748a6fdccb7ef154da/Input-data-scale-impacts-on-modeling-output-results-A-review.pdf](https://www.researchgate.net/profile/Gurdeep_Singh22/publication/321759023_Input_data_scale_impacts_on_modeling_output_results_A_review/links/5a30b748a6fdccb7ef154da/Input-data-scale-impacts-on-modeling-output-results-A-review.pdf)
- Slymaker, O., Spencer, T., & Embleton-Hamann, C. (Eds.). (2009). *Geomorphology and Global Environmental Change*. Cambridge University Press.
- Solonenko, V. P. (1977). Landslides and collapses in seismic zones and their prediction. *Bulletin of the International Association of Engineering Geology - Bulletin de l’Association Internationale de Géologie de l’Ingénieur*, 15(1), 4–8. <https://doi.org/10.1007/BF02592633>
- Swetnam, R. D., Fisher, B., Mbilinyi, B. P., Munishi, P. K. T., Willcock, S., Ricketts, T., Mwakalila, S.,

- Balmford, A., Burgess, N. D., Marshall, A. R., & Lewis, S. L. (2011). Mapping socio-economic scenarios of land cover change: A GIS method to enable ecosystem service modelling. *Journal of Environmental Management*, 92(3), 563–574. <https://doi.org/10.1016/j.jenvman.2010.09.007>
- Tatem, A. J., Lewis, H. G., Atkinson, P. M., & Nixon, M. S. (2002). Super-resolution land cover pattern prediction using a Hopfield neural network. *Remote Sensing of Environment*, 79(1), 1–14. [https://doi.org/10.1016/S0034-4257\(01\)00229-2](https://doi.org/10.1016/S0034-4257(01)00229-2)
- Team, R. C. (2013). *R: A language and environment for statistical computing*.
- Thampi, P. K., Mathai, J., Sankar, G., & Sidharthan, S. (1998). *Evaluation study in terms of landslide mitigation in parts of Western Ghats*.
- The Hindu. (2021, February 26). ₹12,000 crore package for Idukki district. <https://www.thehindu.com/news/national/kerala/special-packagefor-idukki-district/article33935416.ece>
- Thomas, M. F. (1994). *Geomorphology in the tropics: a study of weathering and denudation in low latitudes. Geomorphology in the Tropics: A Study of Weathering and Denudation in Low Latitudes*.
- UNEP-WCMC, & IUCN. (2021). *Protected Planet: The World Database on Protected Areas (Wdpa) and World Database on Other Effective Area-based Conservation Measures (WD-OECM) [Online]*. [www.protectedplanet.net](http://www.protectedplanet.net).
- Vanacker, V., Vanderschaeghe, M., Govers, G., Willems, E., Poesen, J., Deckers, J., & De Bievre, B. (2003). Linking hydrological, infinite slope stability and land-use change models through GIS for assessing the impact of deforestation on slope stability in high Andean watersheds. *Geomorphology*, 52(3–4), 299–315. [https://doi.org/10.1016/S0169-555X\(02\)00263-5](https://doi.org/10.1016/S0169-555X(02)00263-5)
- Veldkamp, A., & Fresco, L. O. (1996). CLUE: A conceptual model to study the conversion of land use and its effects. *Ecological Modelling*, 85(2–3), 253–270. [https://doi.org/10.1016/0304-3800\(94\)00151-0](https://doi.org/10.1016/0304-3800(94)00151-0)
- Verburg, P. (2010). *The CLUE model Hands-on exercises Course material*.
- Verburg, P. H., & Overmars, K. P. (2009). Combining top-down and bottom-up dynamics in land use modeling: Exploring the future of abandoned farmlands in Europe with the Dyna-CLUE model. *Landscape Ecology*, 24(9), 1167–1181. <https://doi.org/10.1007/s10980-009-9355-7>
- Verburg, P. H., Soepboer, W., Veldkamp, A., Limpiada, R., Espaldon, V., & Mastura, S. S. (2002). Modeling the Spatial Dynamics of Regional Land Use: The CLUE-S Model. *Environmental Management*, 30(3), 391–405. <https://doi.org/10.1007/s00267-002-2630-x>
- Vijith, H., & Madhu, G. (2008). Estimating potential landslide sites of an upland sub-watershed in Western Ghat's of Kerala (India) through frequency ratio and GIS. *Environmental Geology*, 55(7), 1397–1405. <https://doi.org/10.1007/s00254-007-1090-2>
- Westen, D. C. J. van. (2020). Landslide inventory of the 2018 monsoon rainfall in Kerala, India. In *DANS*. <https://easy.dans.knaw.nl/ui/datasets/id/easy-dataset:161398/tab/1>
- Yang, S., & Berdine, G. (2015). The receiver operating characteristic (ROC) curve. *The Southwest Respiratory and Critical Care Chronicles*, 3(9). <https://doi.org/10.12746/swrccc2015.0309.125>
- Zhou, G., Esaki, T., Mitani, Y., Xie, M., & Mori, J. (2003). Spatial probabilistic modeling of slope failure using an integrated GIS Monte Carlo simulation approach. *Engineering Geology*, 68(3–4), 373–386. [https://doi.org/10.1016/S0013-7952\(02\)00241-7](https://doi.org/10.1016/S0013-7952(02)00241-7)

# APPENDICES

**Name of Interviewed local expert:** Dr. Sekhar L. Kuriakose

**Designation:** Head, Kerala State Emergency Operations Centre – Member Secretary (Ex-officio)

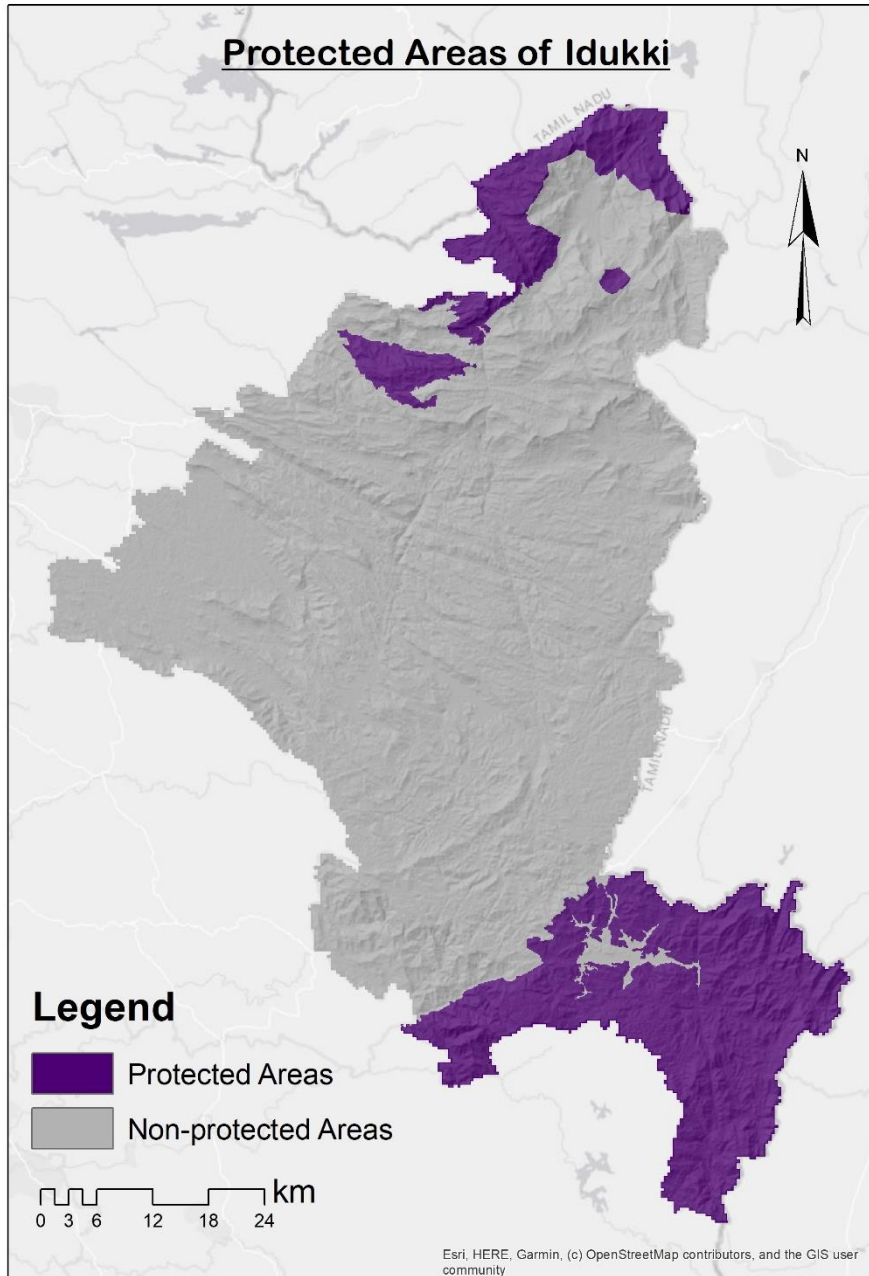


Figure 15: Protected Areas of Idukki

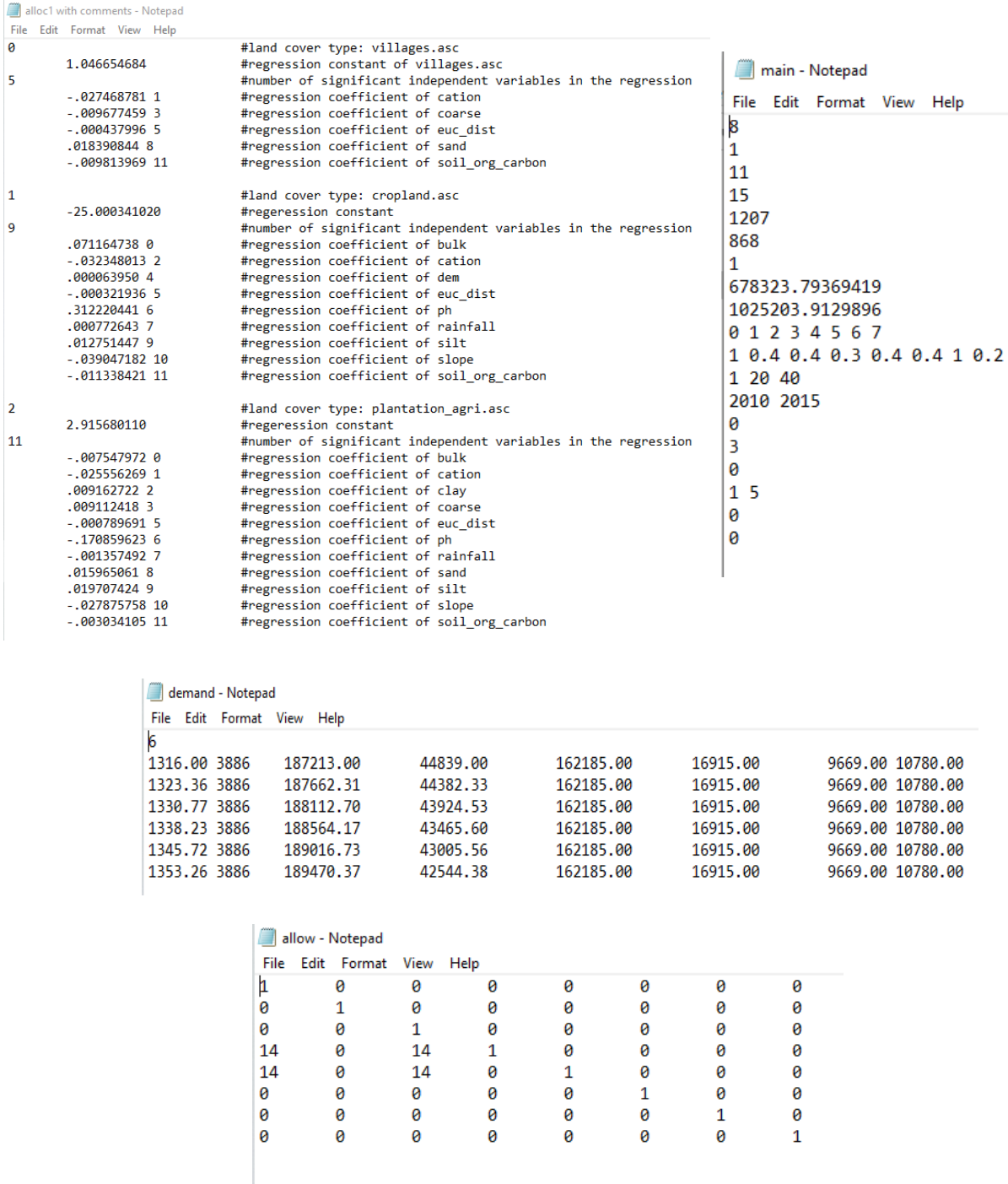


Figure 16: DynaCLUE system files (TL: Alloc1 file, TR: Main file, Middle: Demand file, Bottom: Allow file)

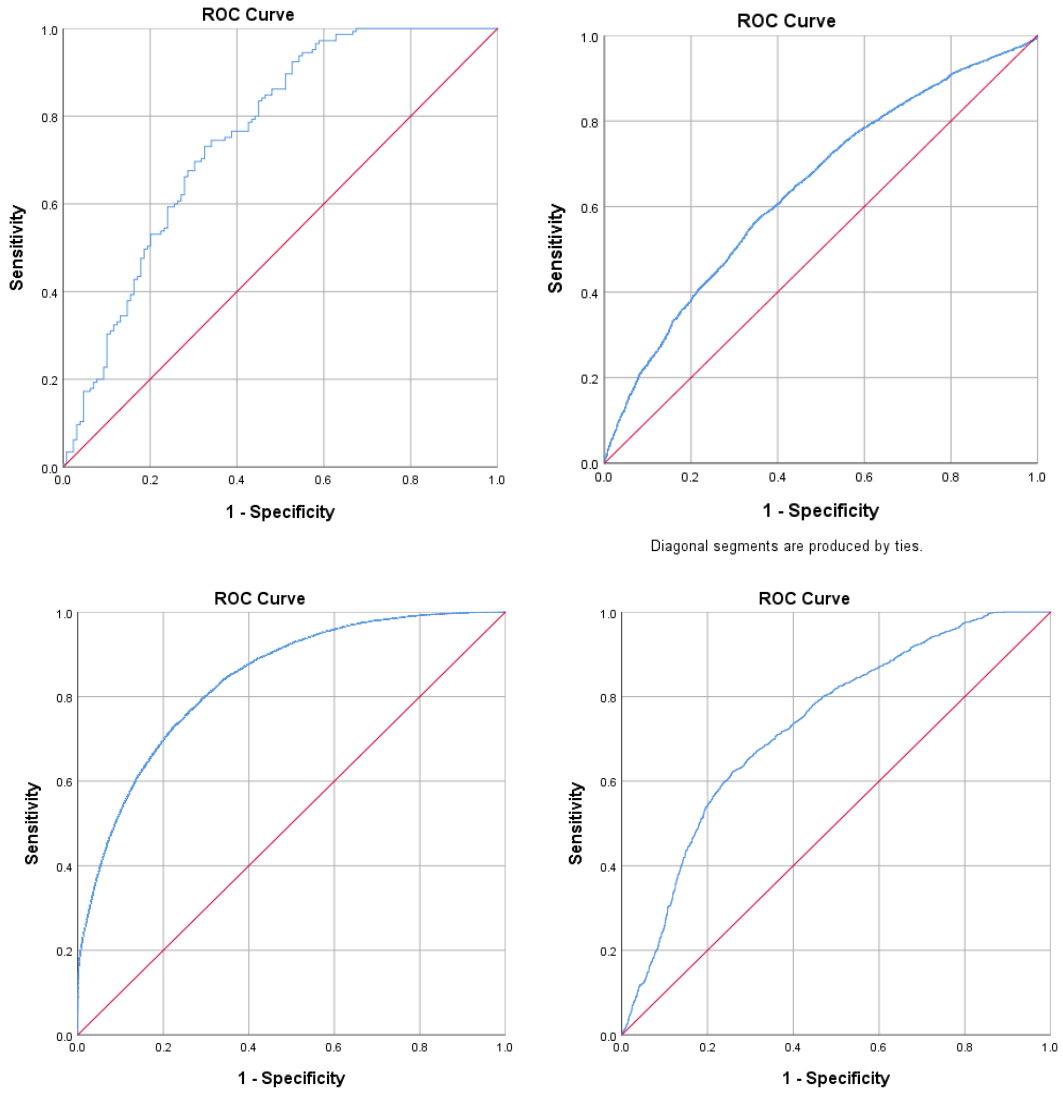


Figure 17: ROC curves of villages (top left), grassland (top right), forests (bottom left) and forest plantation (bottom right)

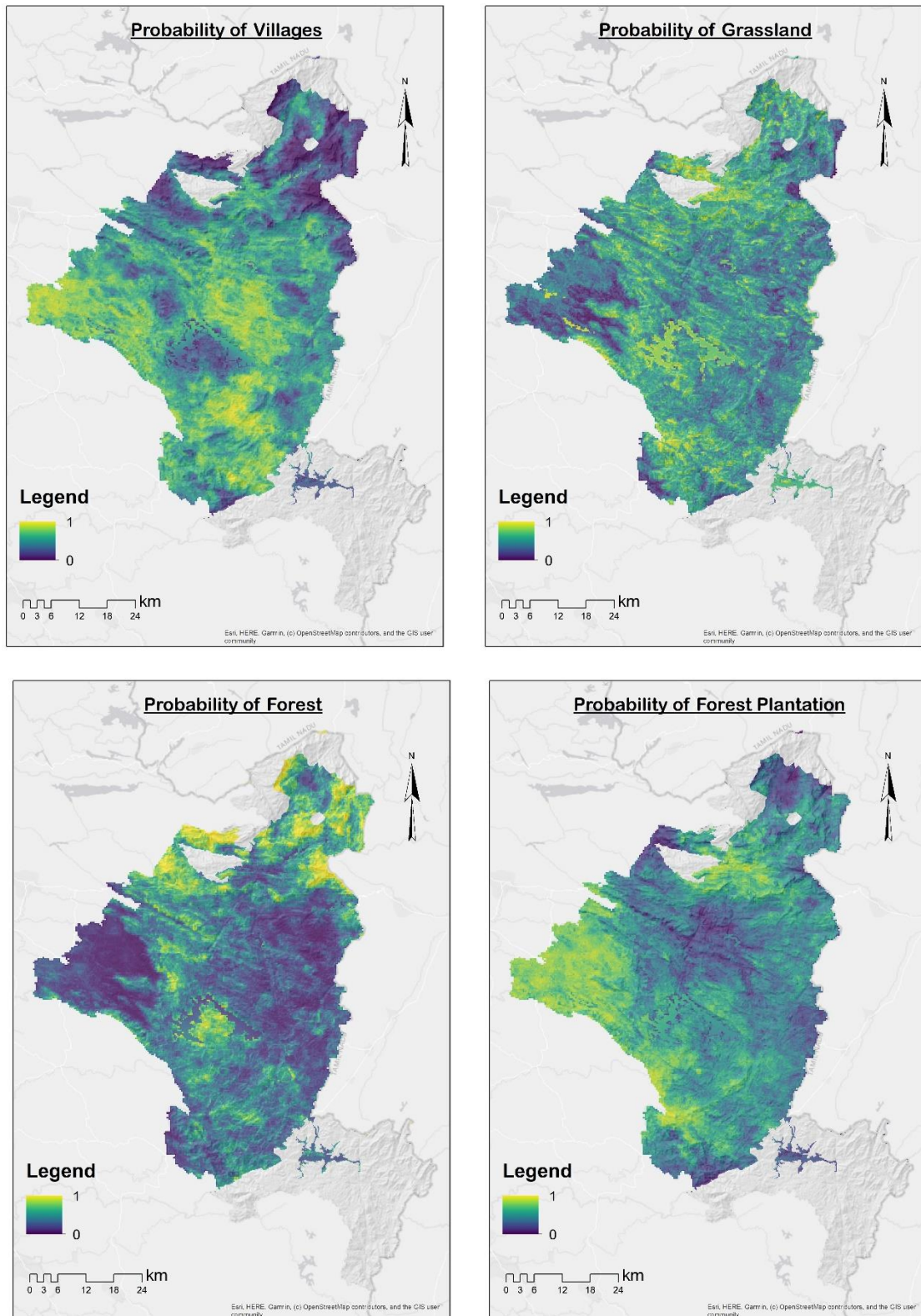


Figure 18: Probability maps of villages (TL), grassland (TR), forest (BL) and forest plantation (BR)

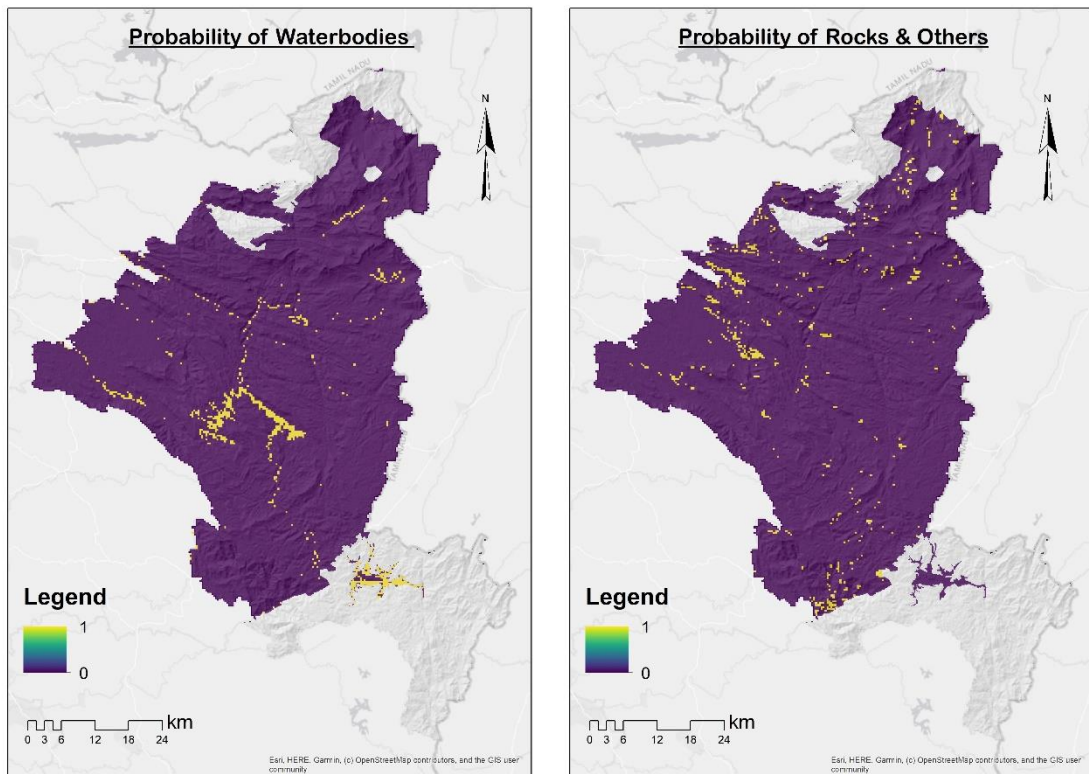


Figure 19: Probability maps of waterbodies (L) and Rocks & others (R)

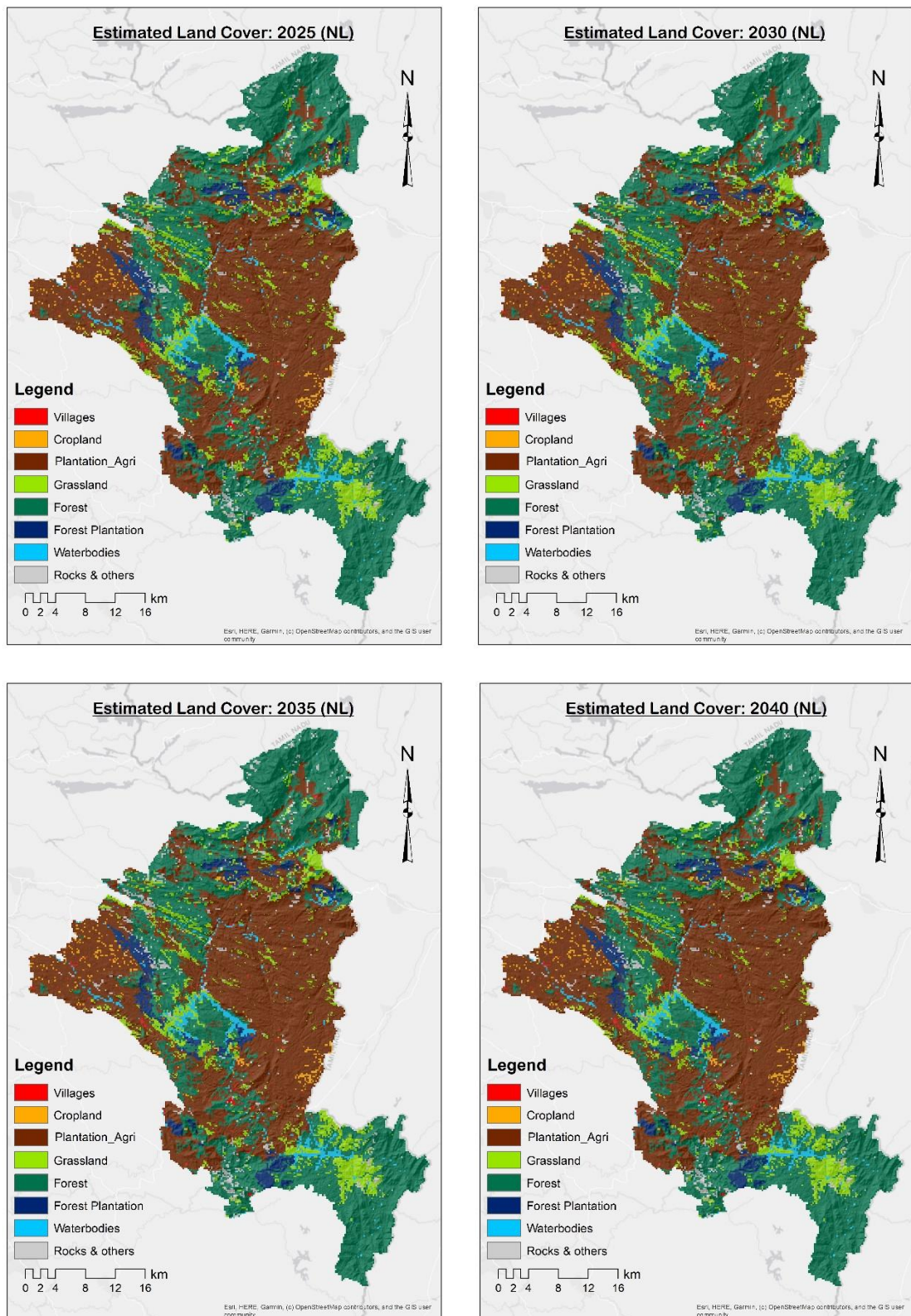


Figure 20: Estimated future land cover (NL scenario) (2025, 2030, 2035, 2040)

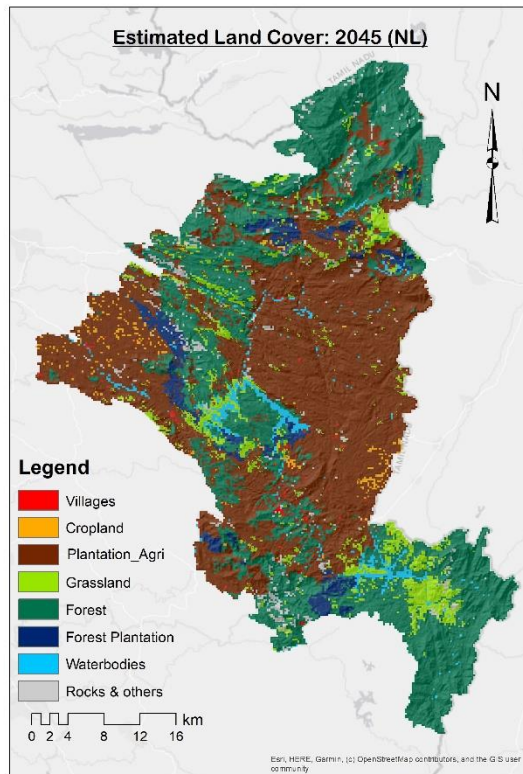


Figure 21: Estimated future land cover (NL scenario) of 2045

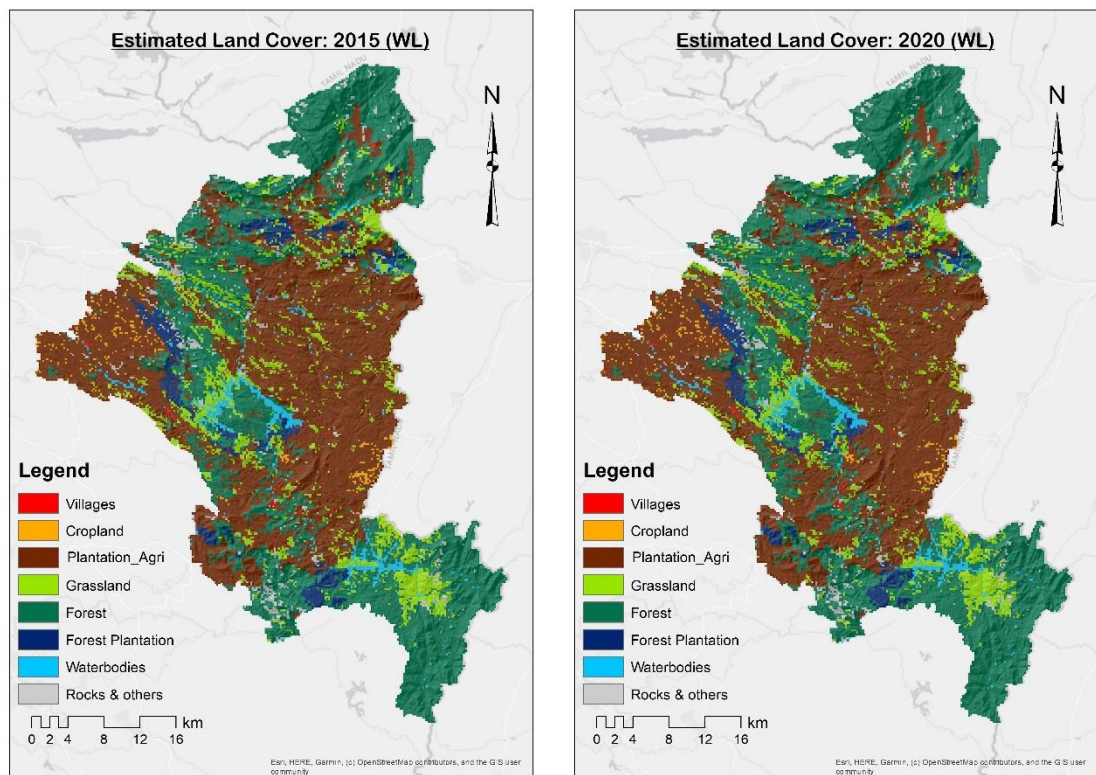


Figure 22: Estimated future land cover (WL scenario) (2015 & 2020)

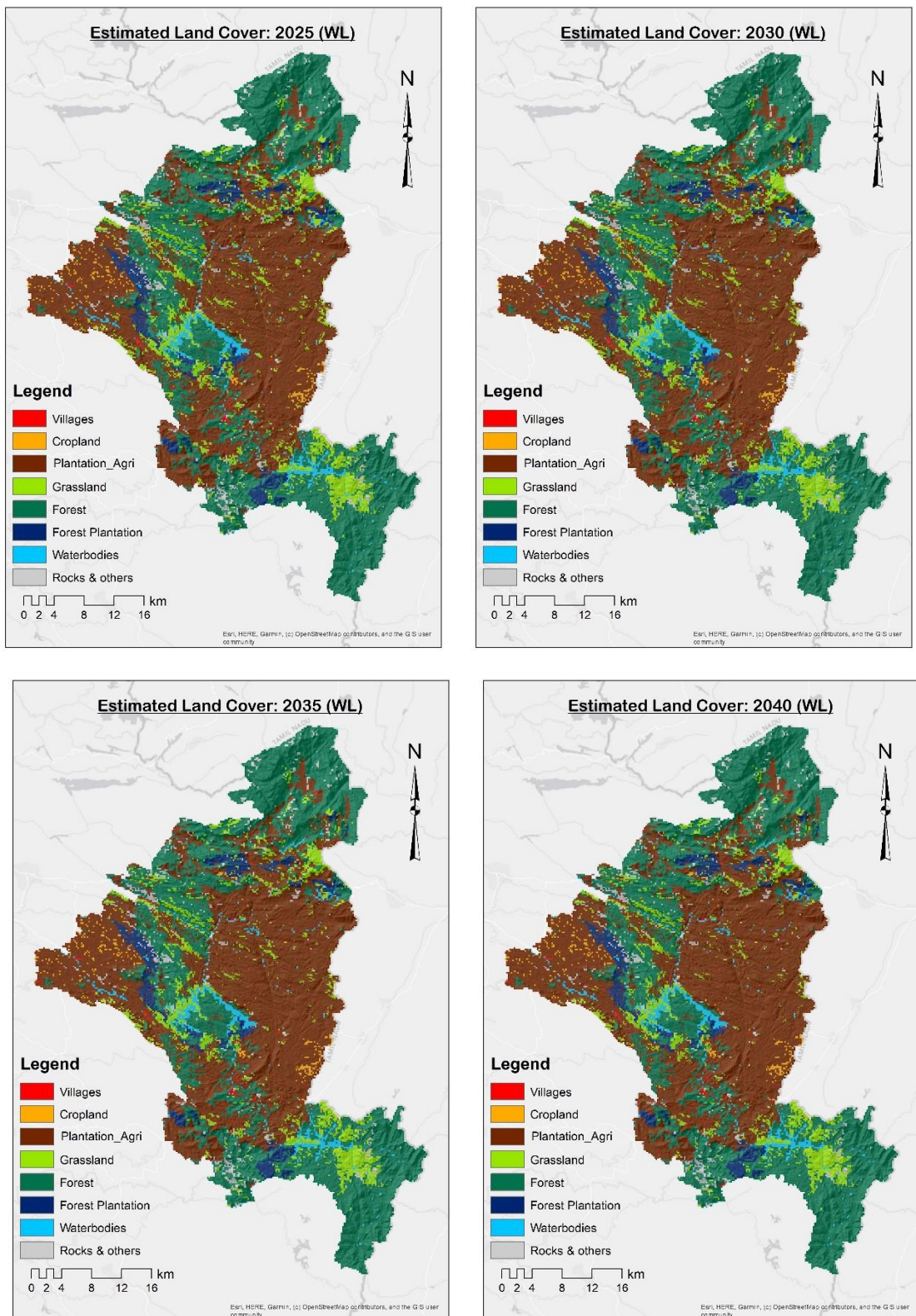


Figure 23: Estimated future land cover (WL scenario) (2025, 2030, 2035, 2040)

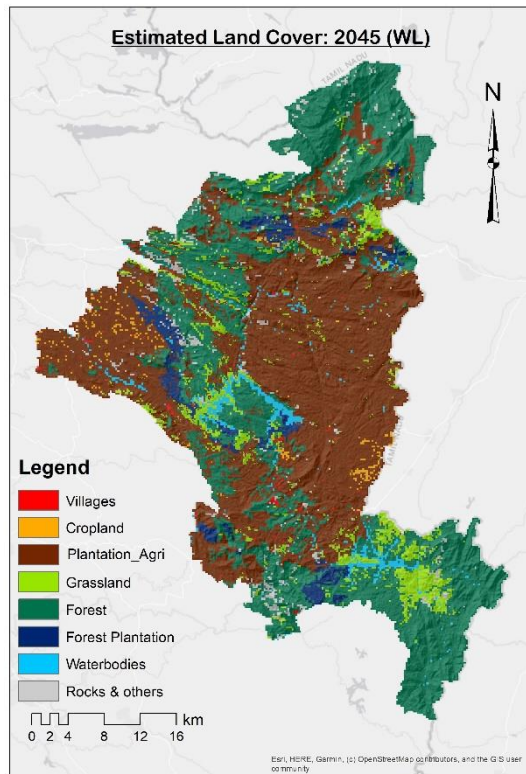


Figure 24: Estimated future land cover (WL scenario) of 2045

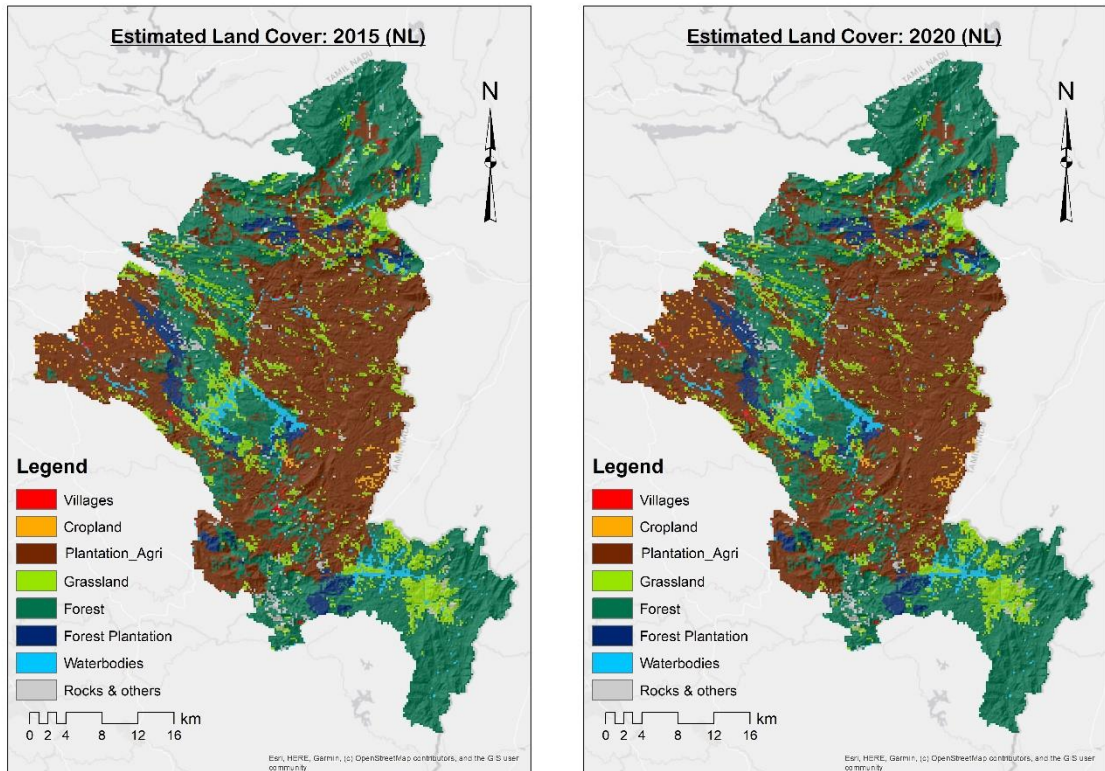


Figure 25: Estimated future land cover (WL scenario) (2015 and 2020)

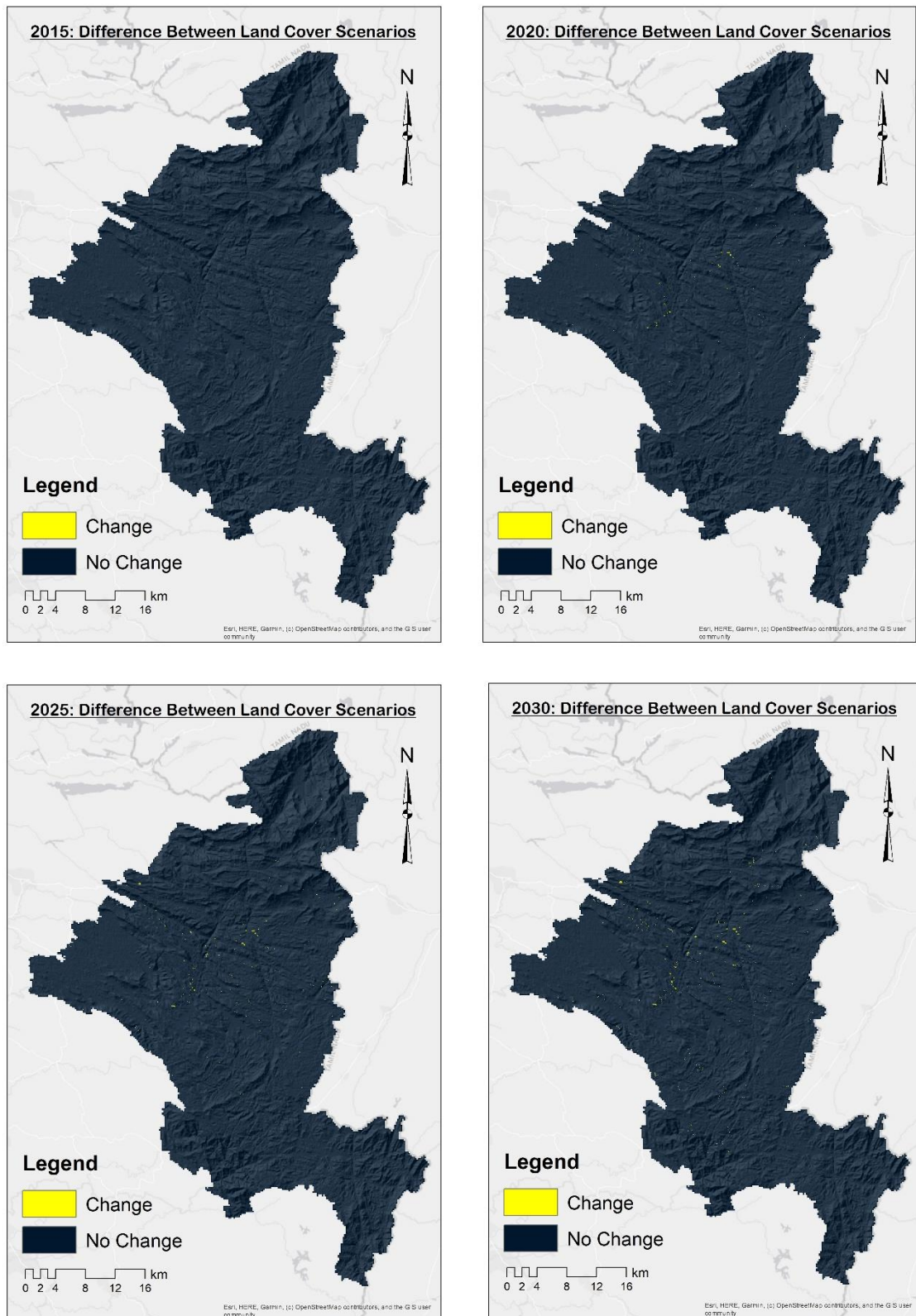


Figure 26: Difference between land cover scenarios (2015, 2020, 2025 and 2030)

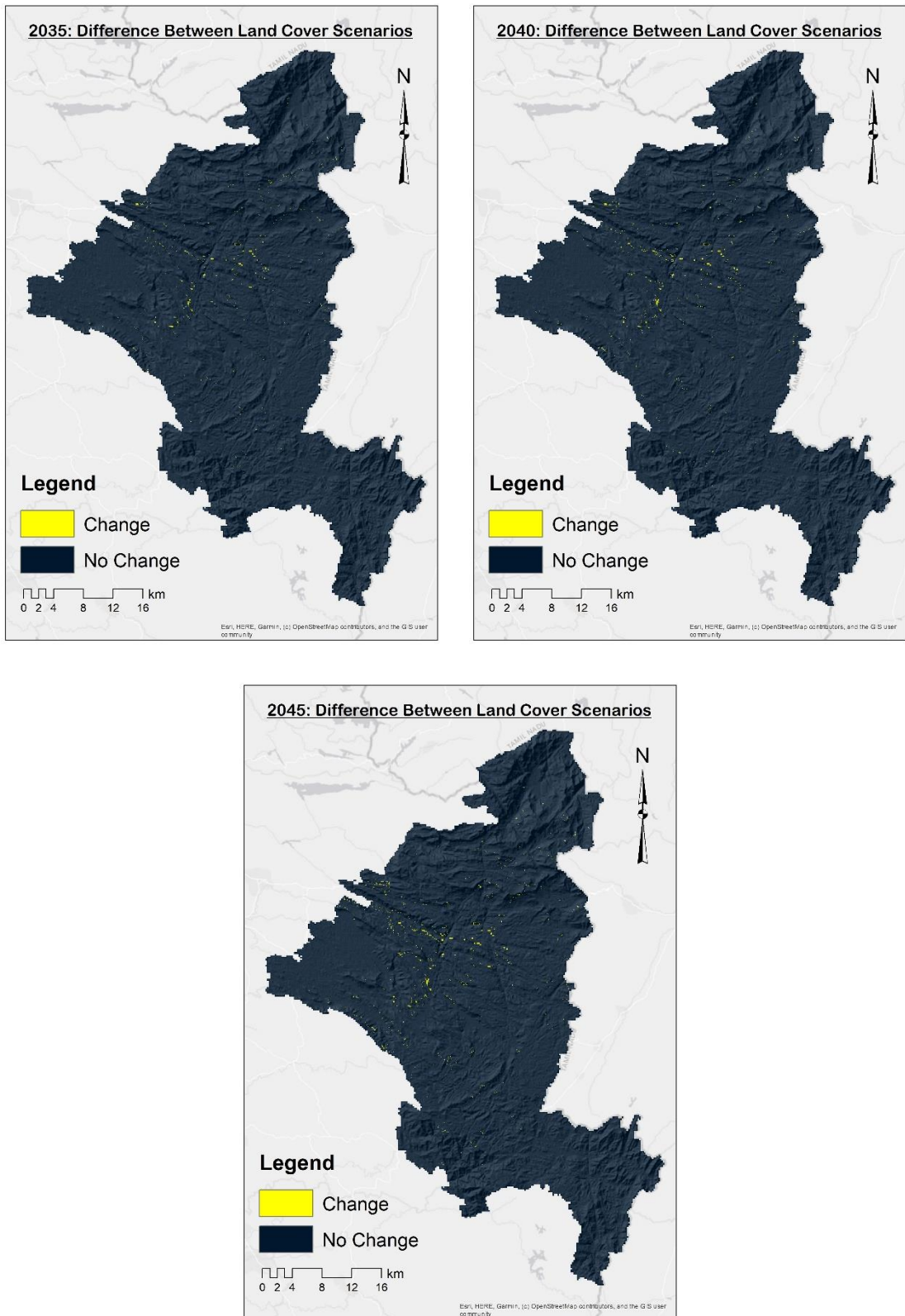


Figure 27: Difference between land cover scenarios (2035, 2040 and 2045)

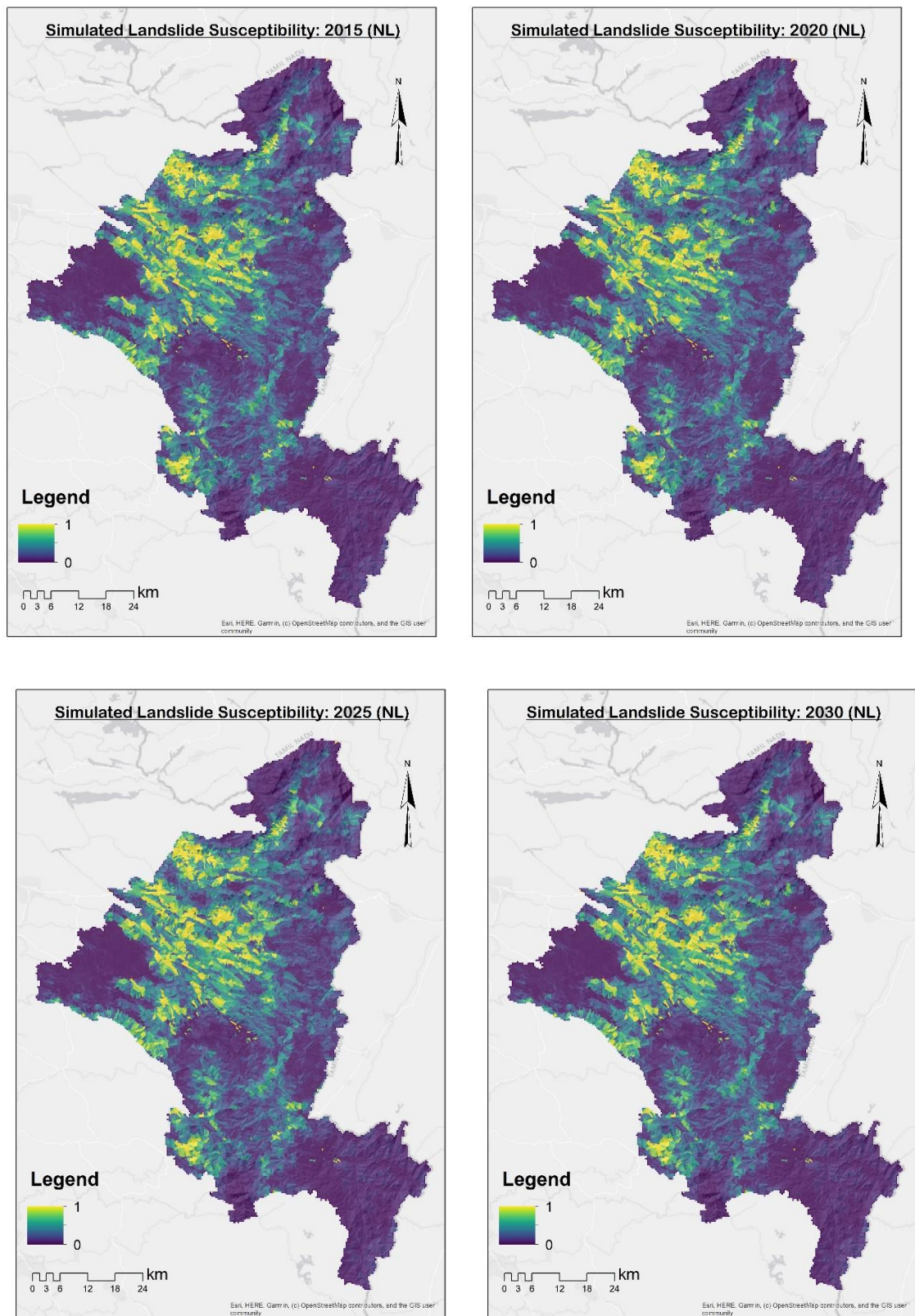


Figure 28: Simulated landslide susceptibility (2015, 2020, 2025 & 2030) – Scenario NL

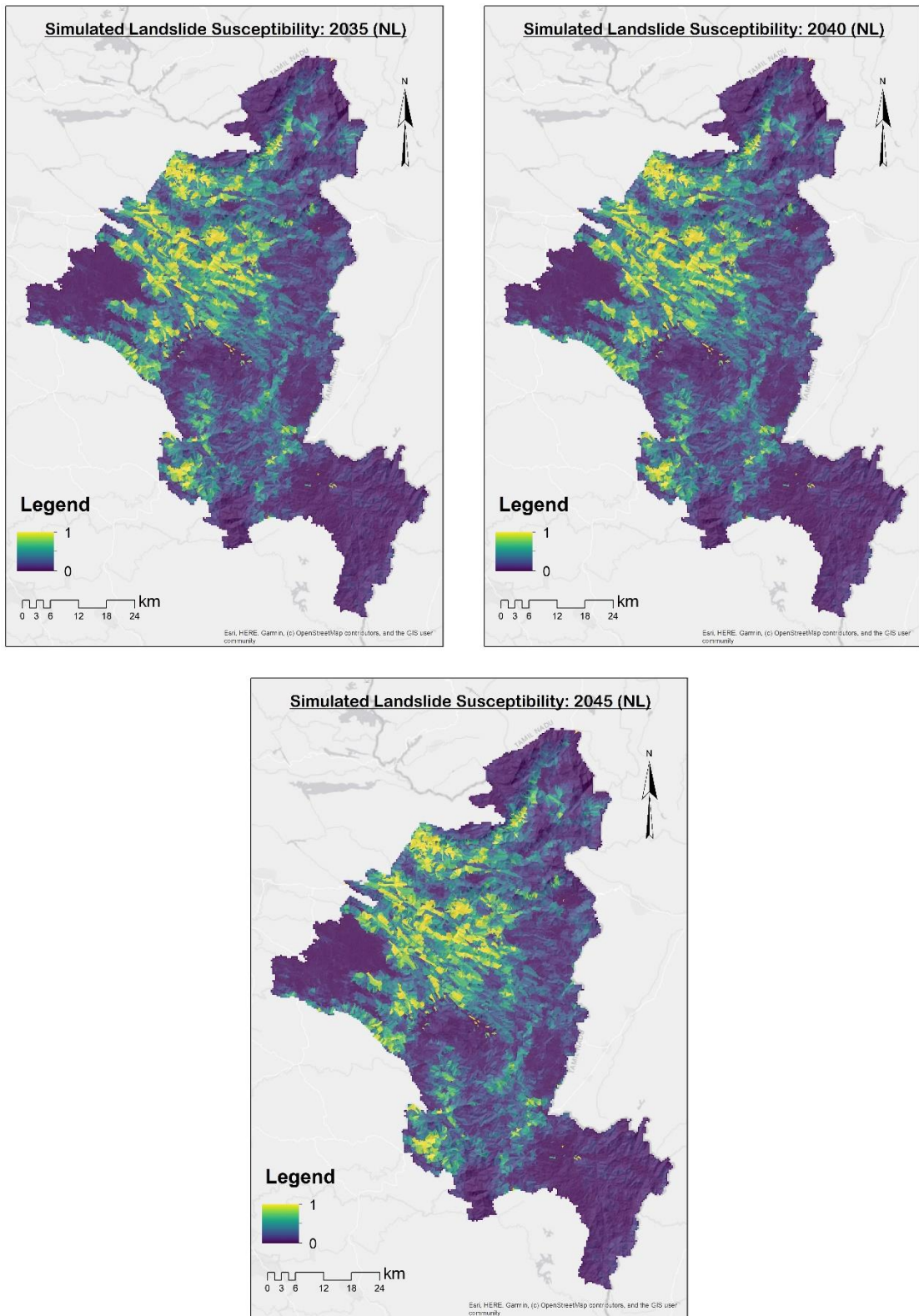


Figure 29: Simulated landslide susceptibility (2035, 2040 and 2045) - Scenario NL

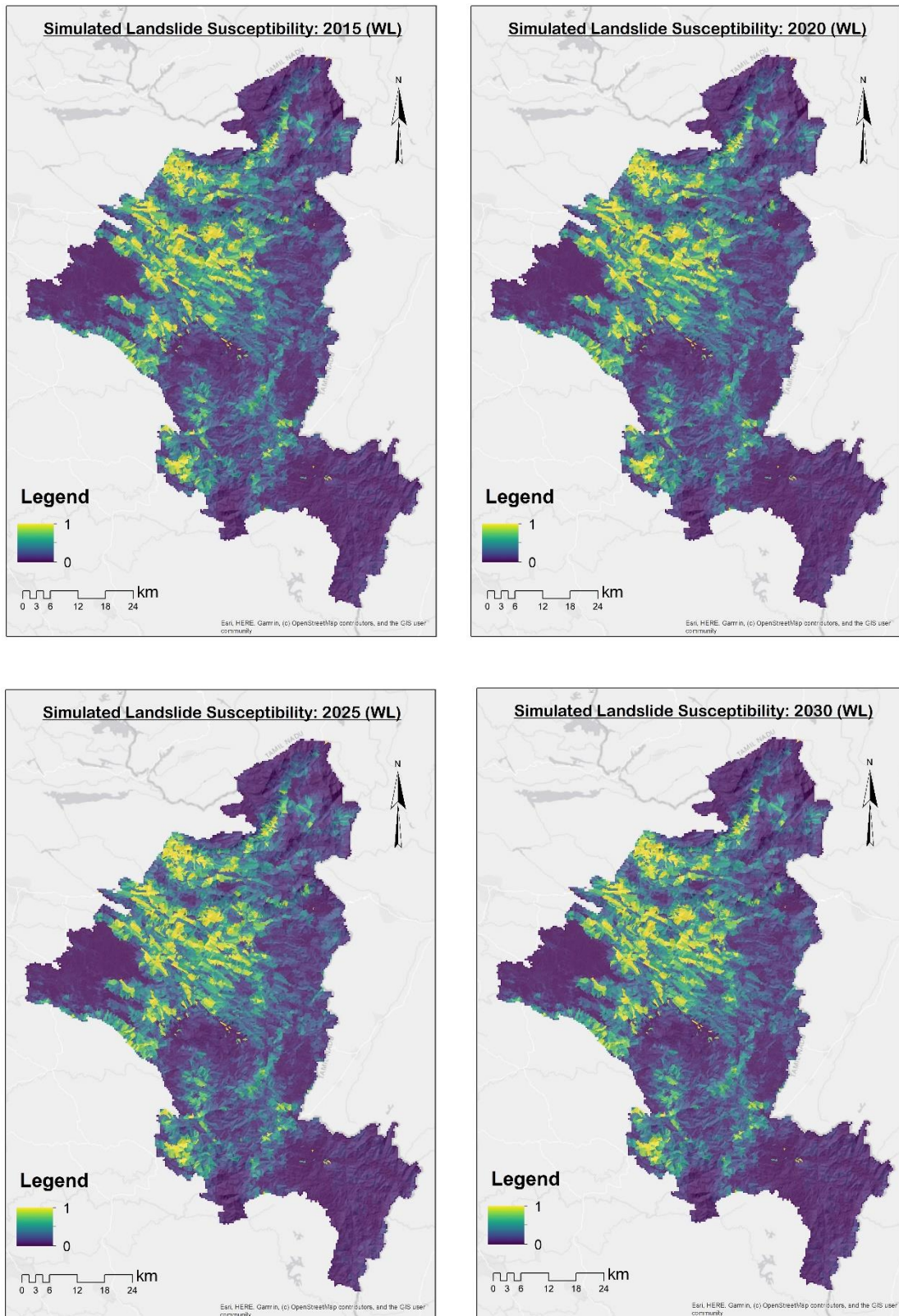


Figure 30: Simulated landslide susceptibility (2015, 2020, 2025, 2030) - Scenario WL

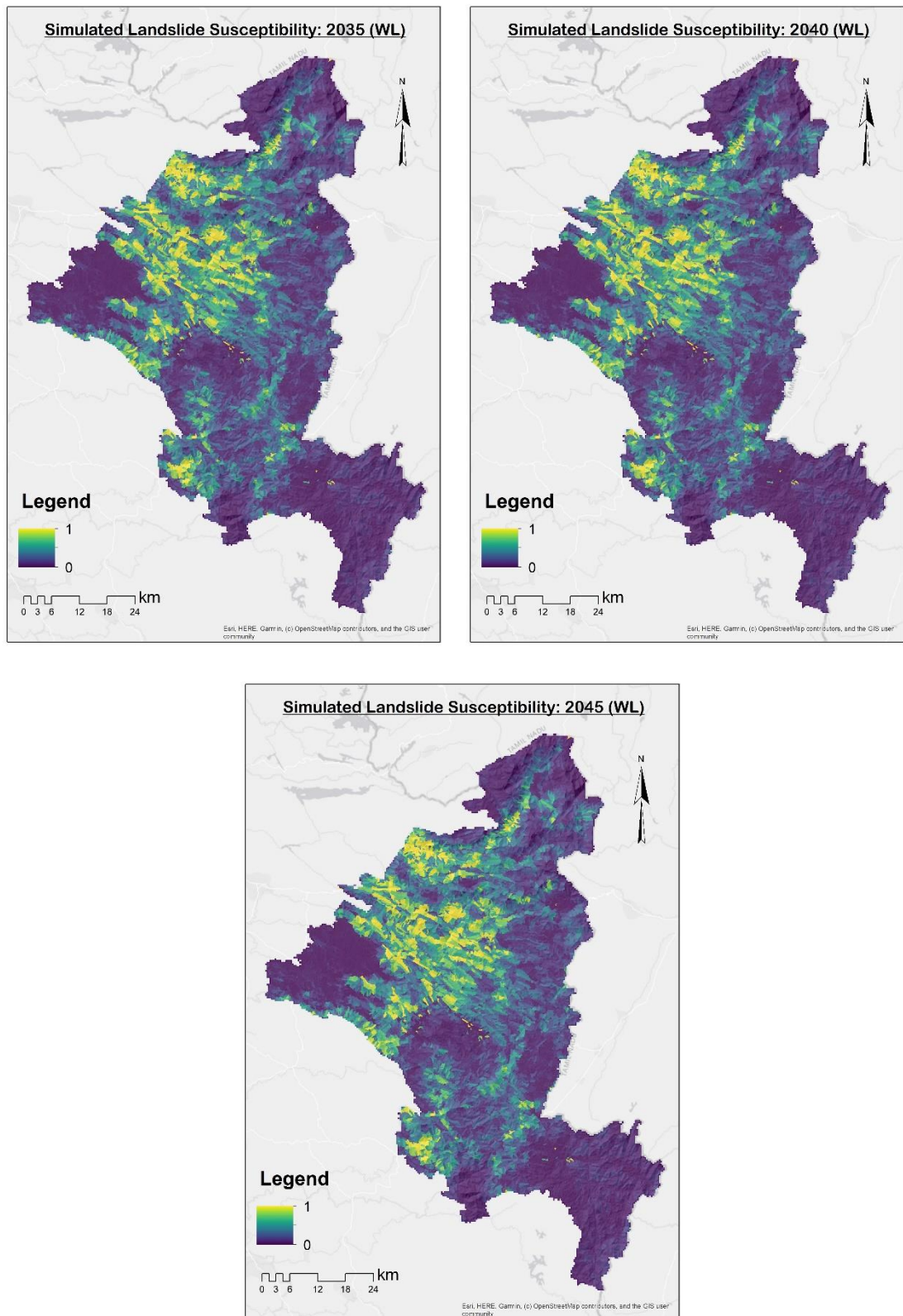


Figure 31: Simulated landslide susceptibility (2035, 2040 and 2045) - Scenario WL

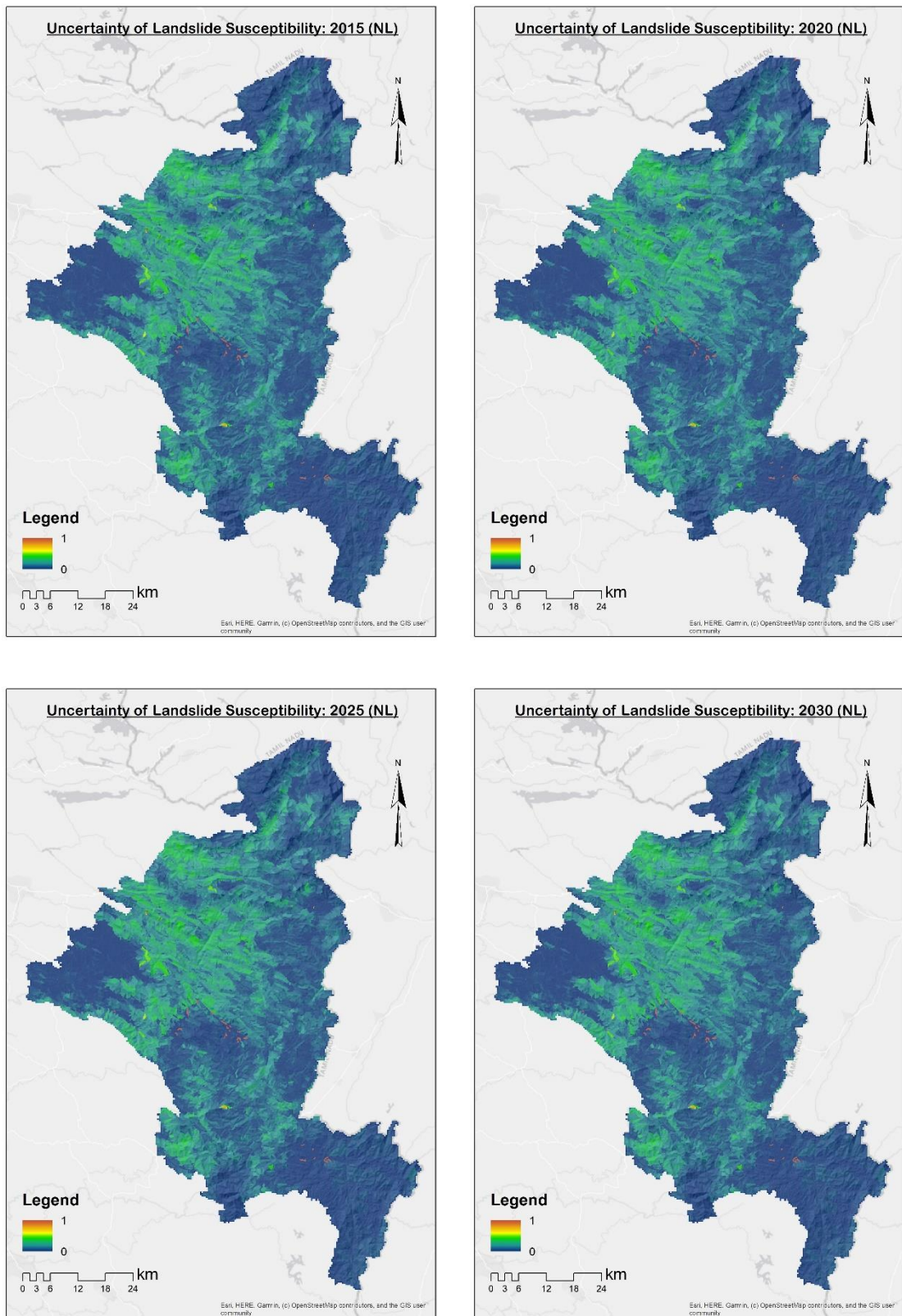


Figure 32: Simulated uncertainty (2015, 2020, 2025, 2030) - NL scenario

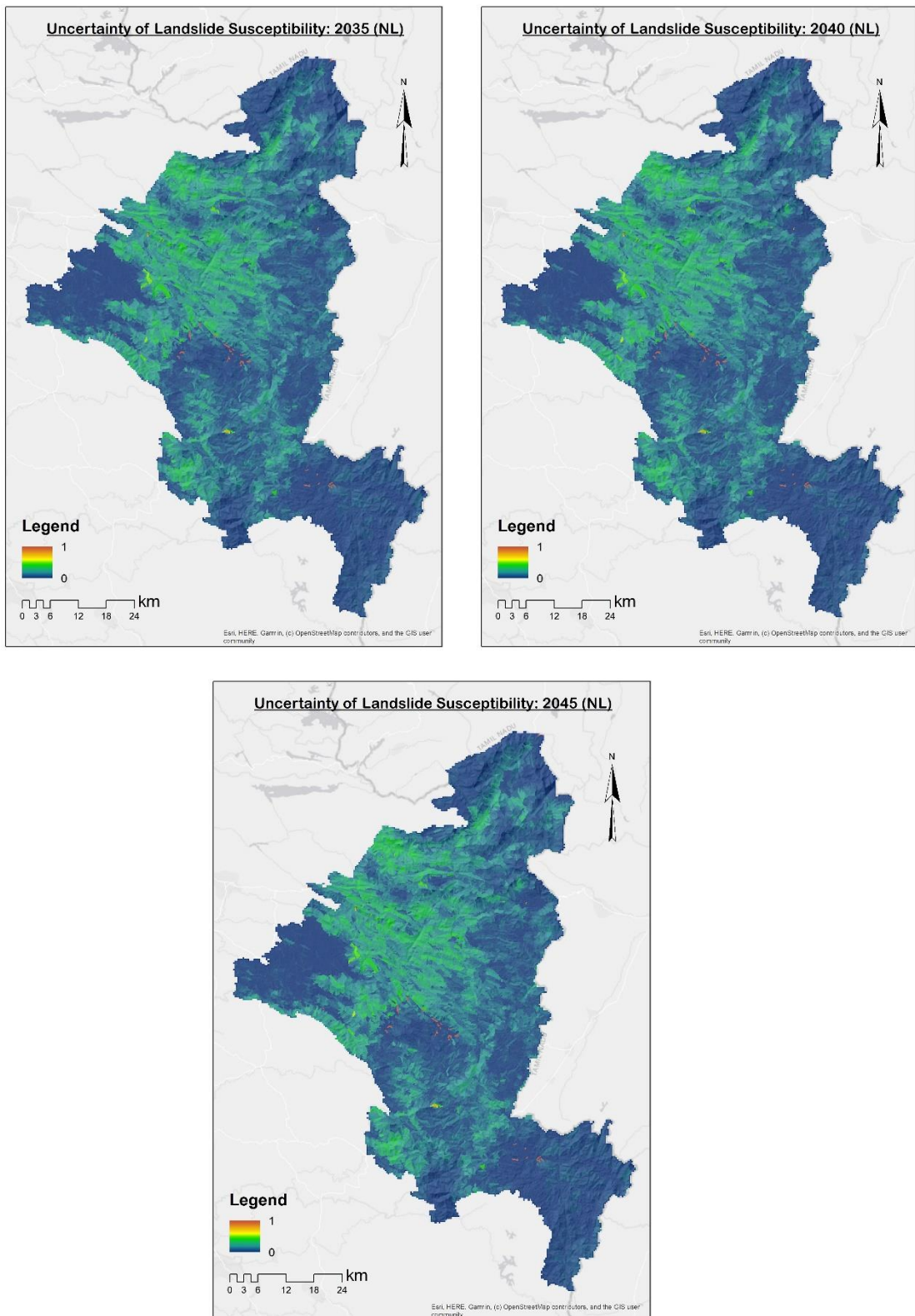


Figure 33: Simulated uncertainty (2035, 2040 and 2045) - NL scenario

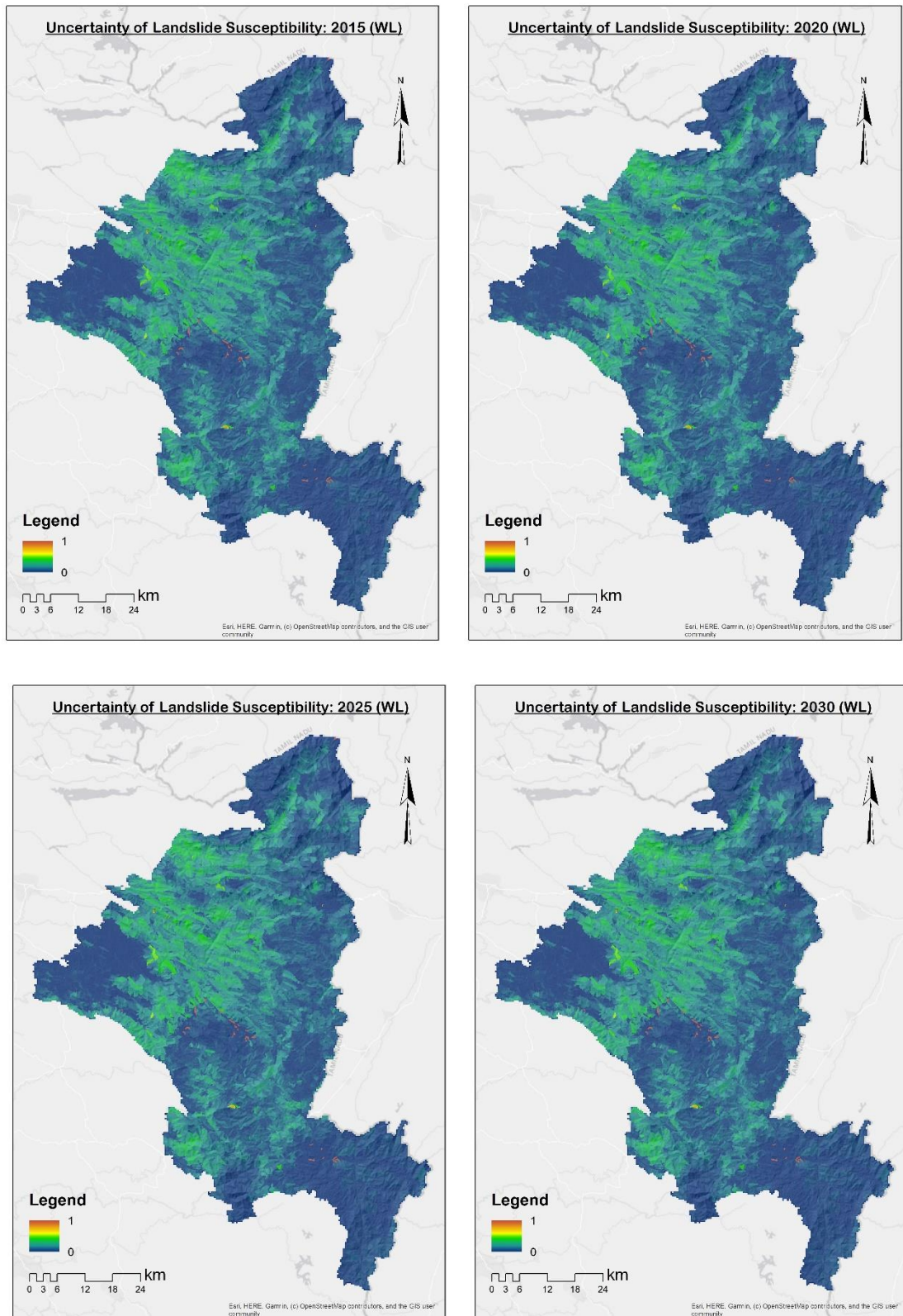


Figure 34: Simulated uncertainty (2015, 2020, 2025 and 2030) - WL scenario

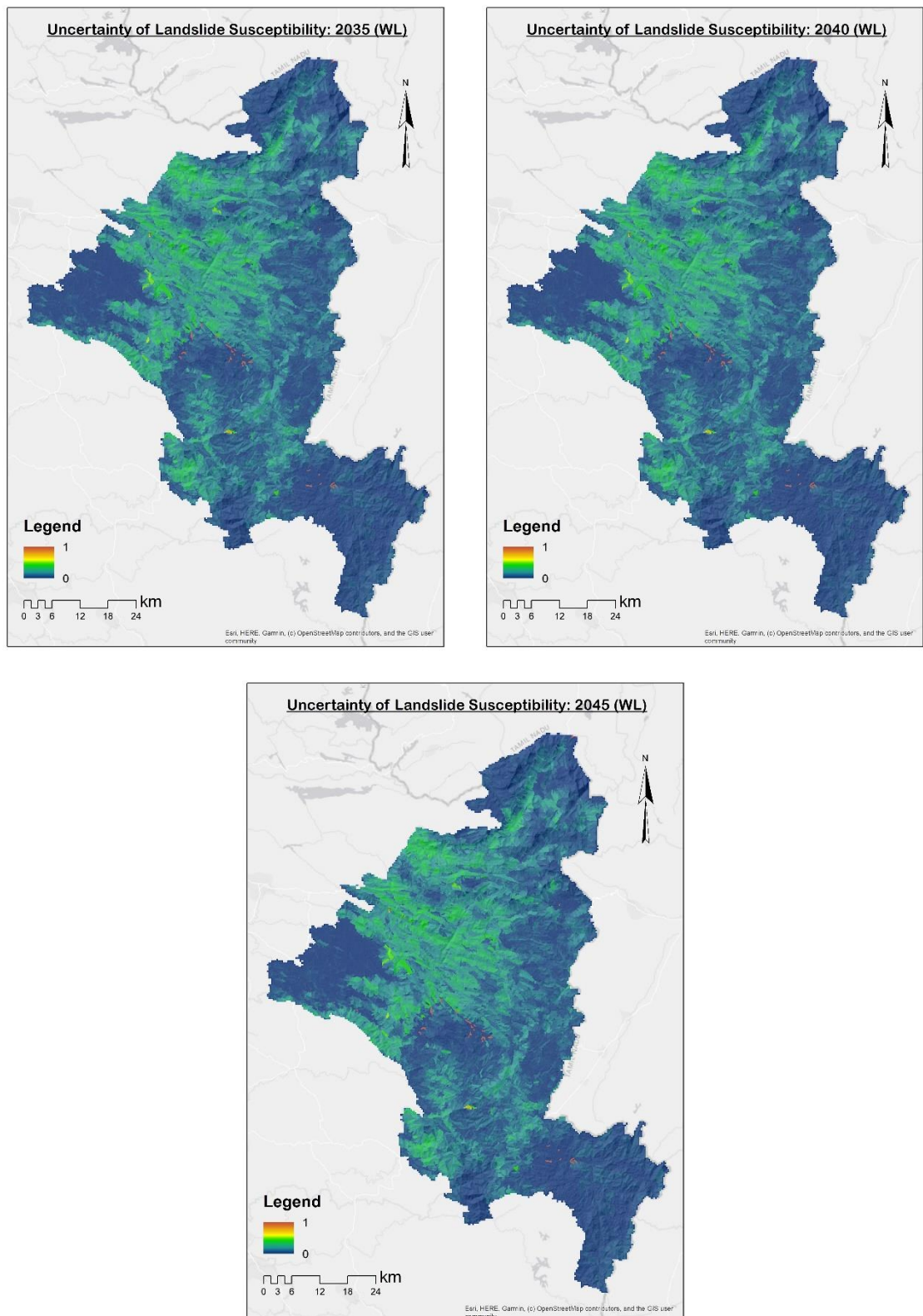


Figure 35: Simulated uncertainty (2035, 2040 and 2045) - WL scenario

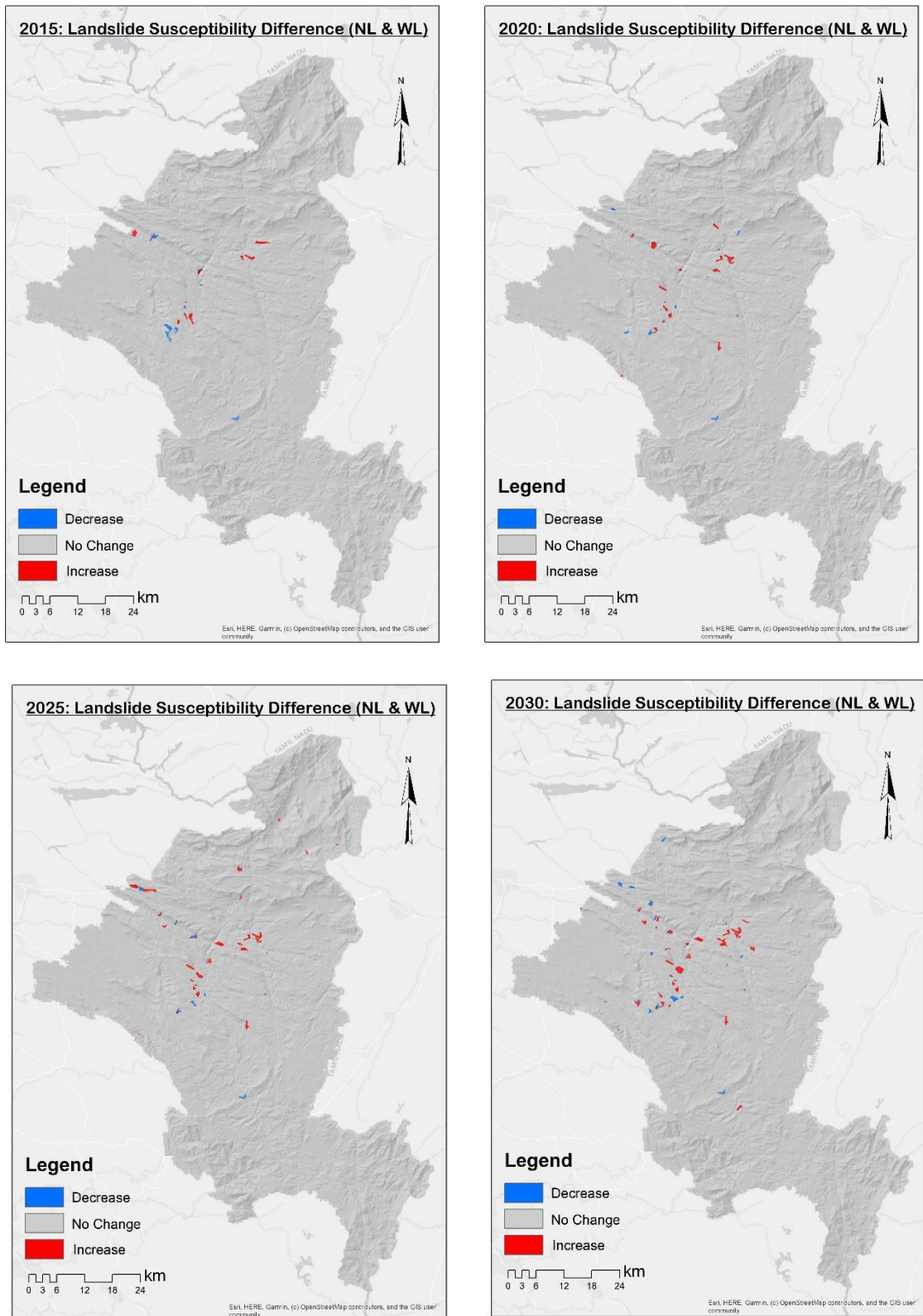


Figure 36: Landslide susceptibility differences (2015, 2020, 2025 and 2030)

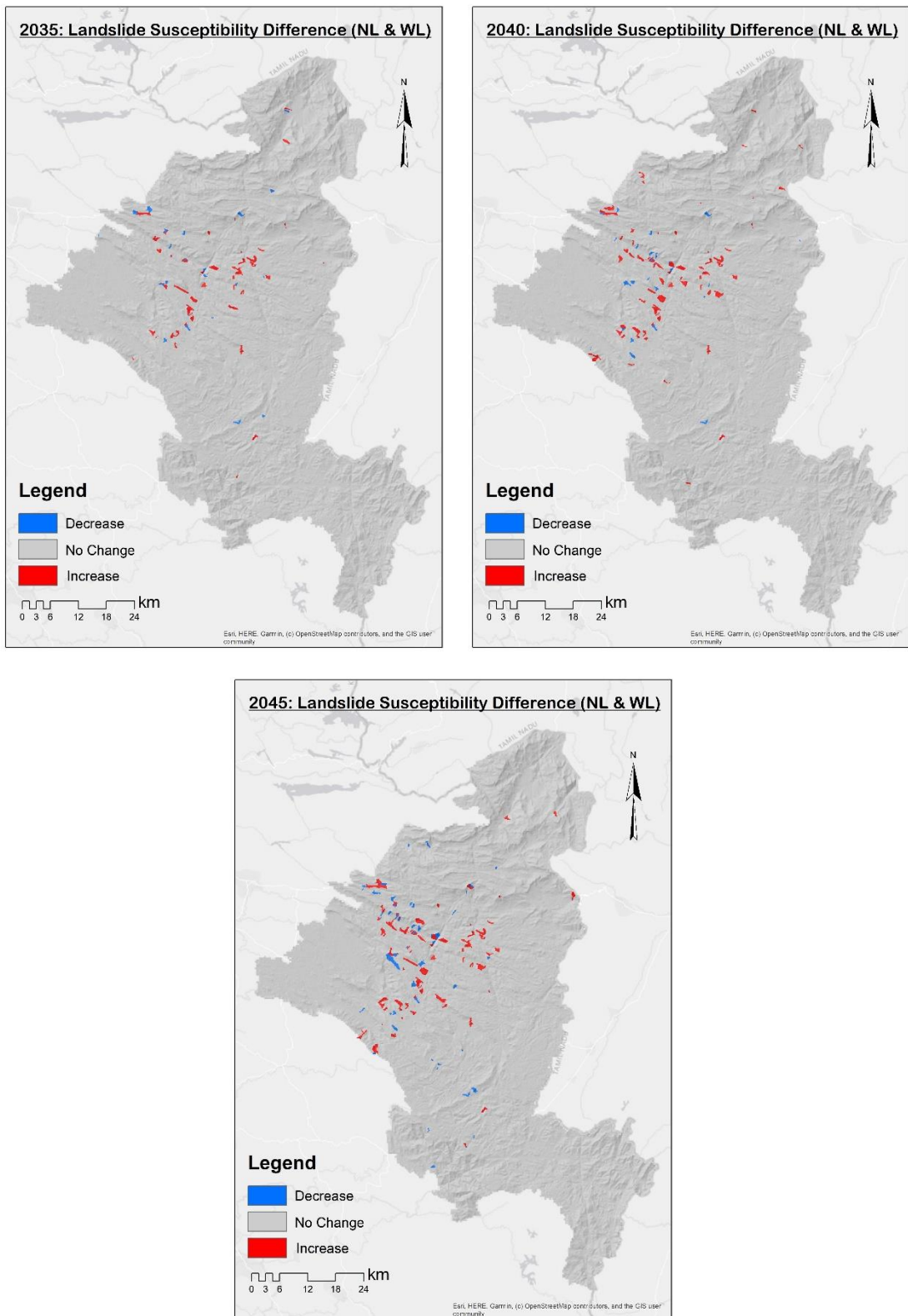


Figure 37: Landslide susceptibility differences (2035, 2040 and 2045)